UNIVERSIDAD DE CHILE
FACULTAD DE CIENCIAS FÍSICAS Y MATEMÁTICAS
DEPARTAMENTO DE GEOLOGÍA

NEOTECTONICS AND SEISMIC HAZARD ON SOUTHERN PATAGONIA

TESIS PARA OPTAR AL GRADO DE MAGÍSTER EN CIENCIAS, MENCIÓN GEOLOGÍA
MEMORIA PARA OPTAR AL TÍTULO DE GEÓLOGA

FRANCISCA BELÉN SANDOVAL SANDOVAL

PROFESOR GUÍA:

GREGORY PAUL DE PASCALE

MIEMBROS DE LA COMISIÓN:

LUISA PINTO LINCOÑIR

FRANCISCO HERVÉ ALLAMAND

FERNANDO POBLETE GÓMEZ

SANTIAGO DE CHILE

2019

ABSTRACT

ABSTRACT TO APPLY FOR: THE DEGREE OF: Geologist and Master of Sciences, mention in Geology

BY: Francisca Belén Sandoval Sandoval

DATE: 01/08/2019

GUIDE PROFESSOR: Gregory G. De Pascale

NEOTECTONICS AND SEISMIC HAZARD ON SOUTHERN PATAGONIA

The southern Patagonian Andes region is crossed by a main crustal-scale neotectonic structure, the Magallanes-Fagnano fault system (MFS), which represent the current boundary between the South American and Scotia Plates. This is also the most important structure accommodating the current separation between the southern tip of South America and the Antarctic Peninsula. The exact location of the main active faults within the MFS in some areas are still poorly unknown and the understanding of how fast these faults slip is restricted only to geodetic data, which in the area cover a limited time period with a limited GPS network. Indeed, the MORVEL model (9.6 ± 1.4 mm/yr to 8.9 ± 1.2 mm/yr) and angular velocities estimated by GPS (6.6 ± 1.3 mm/yr) differs by 2-3 mm/yr, suggesting that field data are necessary to characterize plate motions in this region. Nevertheless, recent earthquakes here demonstrate that structures within the MFS are active earthquake sources (M>7 historical earthquakes) and there is clear tectonic geomorphology evidence of recent motions. To evaluate long term Late-Cenozoic deformation, bedrock geology was compiled and bedrock geologic separations of 40 ± 5, 50 ± 5, 60 ± 5 km were measured, suggesting slip-rates along the MFS of 5.4 ± 3.3 mm/yr (2.1 to 8.7 mm/yr), assuming proposed ages for the beginning of the MFS activity from the Lower Miocene (20 Ma) to the Late Miocene (6 Ma), suggesting that a better age constrain is needed. Afterwards, direct geologic evidence of surface

faulting deformation in the field along the ~130 km long onshore trace of the MFS along the Chilean and Argentine portion of Tierra del Fuego was analyzed. Active fault segments were better characterized by combining remote sensing together with geological observations during fieldwork and Structure from Motion (SfM)-derived high-resolution topographic models' data (7 models). During analysis of these models and during fieldwork, left-lateral offsets were detected, interpreted as the cumulative offsets for the Late-Quaternary events. Then, together with available regional dating the first long- term Late-Quaternary (Late-Pleistocene) slip-rate for these structures was constrained. In addition to the main MF, within the MFS, the Deseado fault (DF) and the Hope fault (HF) were also checked in the field. These results indicate slip-rates of 10.5 ± 1.5 mm/yr (9.1 to 12.0 mm/yr, Chile) and 7.8 ± 1.3 (6.5 to 9.1 mm/yr, Argentina). These geologic data validate previous short-term geodetic-based models. These results provide the first geological parameters to considerate for seismic hazard assessment in Patagonia region, which is currently underestimated as the MFS is a fast slipping, seismogenic, and close to urban areas both in Chile (Punta Arenas, Puerto Natales, Porvenir) and Argentina (Tolhuín, Río Grande, Ushuaia). Geologic and seismological data suggest that the MFS in TdF, along the central and eastern portion of the Scotia-South American plate boundary, consist in a narrow-localized (30-50 km) and well-defined deformation belt composed of the main MF by a straight and relatively smooth and long fault traces bounded by parallel secondary active but slower-slipping faults, such as the HF and DF. The relatively simple geometry (straight) and length (up to at least 1500 km and perhaps up to 3000 km considering the offshore segment) suggest a small ratio between small and high magnitude events and perhaps a recurrence rate for high magnitudes earthquakes. Moreover, as Tierra Del Fuego in both Chile and Argentina is a major zone for hydrocarbon exploration and extraction, understanding the locations and nature of the faults here are critical to perhaps reduce risk of seismic triggering due to hydraulic fracturing operations.

RESUMEN

NEOTECTÓNICA Y PELIGRO SÍSMICO EN PATAGONIA SUR

La región sur de Patagonia es atravesada por una estructura neotectónica de escala cortical, el Sistema de Fallas Magallanes Fagnano (MFS), el cual representa el actual límite de placas entre las Placas Sudamericana y Escocia. Esta estructura es la más importante acomodando actualmente la separación entre el límite sur de Sudamérica y la Península Antártica. La ubicación exacta de las principales fallas activas dentro del MFS en algunas áreas aún es desconocida, y los datos que indican cuando rápido estas estructuras se están desplazando están restringidas sólo a datos geodésicos, los cuales en el área cubren un rango de tiempo limitado al igual que una red GPS limitada. De hecho, el modelo MORVEL (9,6 ± 1.4 mm/a a 8,9 ± 1.2 mm/a) y las velocidades angulares estimadas por GPS (6,6 ± 1.3 mm/a) difieren en 2 a 3 mm/yr, lo cual indica que más datos son necesarios para una mejor estimación del movimiento de placas en esta región. Sin embargo, terremotos históricos recientes con M>7 en la región demuestran que estas estructuras son fuentes activas de terremotos y a la vez hay una evidencia geomorfológica clara que avala esta deformación reciente.

Para evaluar deformación de largo plazo (Cenozoico tardío). Se compiló información sobre la geología regional y se midió la separación de unidades a lo largo de la falla. Estas separaciones desde 40±5 a 60±5 km sugieren tasas de desplazamiento de 5,4 ± 3,3 mm/a (2,1 a 8,7 mm/a), asumiendo un rango de edades propuestas para el inicio de la actividad de la MFS desde el Mioceno temprano (20 Ma) hasta el Mioceno tardío (6 Ma), esto sugiere que aún es necesario contreñir mejor la edad de esta estructura. Posteriormente, se analizó evidencia geológica directa de deformación frágil superficial a lo largo de ~130 km de la traza del MFS tanto en la parte chilena como argentina de Tierra del Fuego. Mediante el uso de teledección para

la ubicación de las trazas de falla y marcadores geomorfológicos desplazados a lo largo de estas, junto con observaciones geológicas en terreno y 7 modelos de elevación de alta resolución derivados de fotogrametría (Structure for Motion, SfM), se pudo realizar una mejor caracterización de la falla. Durante el análisis de los modelos y el trabajo de campo, se detectaron desplazamientos de rumbo sinestrales interpretados como desplazamientos acumulados por terremotos durante el Cuaternario tardío. Luego, junto con las dataciones regionales disponibles, se determinó la primera tasa de desplazamiento a largo plazo del Cuaternario tardío (Pleistosceno tardío) para estas estructuras. Además de la falla principal (MF), la falla Deseado (DF) y la falla Hope (HF) fueron también revisadas en terreno. Los resultados indican tasas de desplazamiento de 10,5 ± 1,5 mm/a (9,1 a 12,0 mm/a, Chile) and 7,8 ± 1,3 (6,5 a 9,1 mm/a, Argentina). Estos datos geológicos validan modelos previos a corto plazo basados en datos geodésicos. Y entregan los primeros parámetros geológicos para considerar en la evaluación del peligro sísmico en Patagonia sur. Este peligro sísmico actualmente subestimado ya que la MFS es una falla con un desplazamiento rápido, sismogénica, y cercana a centros urbanos tanto en Chile (Punta Arenas, Puerto Natales, Porvenir) como Argentina (Tolhuín, Río Grande, Usuhaia). Datos geológicos y sismológicos sugieren que el MFS en TdF y posiblemente en la mayor parte de la longitud dentro límite entre las placas Sudamericana y Escocia, consiste en un cinturón de deformación angosto, localizado y bien definido de no más de 30-50 km, compuesto por una traza principal (MF) recta y relativamente suave y larga (hasta por lo menos 1500 km y quizás hasta 3500 km considerando la sección costa afuera), rodeada por segmentos segundarios paralelos, pero con un desplazamiento más lento cómo la HF y la DF. La geometría relativamente simple y extensa sugiere una razón pequeña entre terremotos de baja y alta. Además, como Tierra del Fuego tanto en Argentina como en Chile es una zona fundamental para exploración y extracción de hidrocarburos, entender la ubicación y naturaleza de las fallas corticales aquí es critico para quizás reducir el riesgo de eventos sísmicos desencadenados por operaciones de fracturamiento hidráulico.

ACKNOWLEDGMENTS

Esta investigación fue financiada la beca Fondecyt del Gobierno de Chile #11160038, una beca de inicio académico de la Facultad de Ciencias Físicas y Matemáticas (FCFM) de la Universidad de Chile, y el programa CIMAR de la Armada de Chile al Dr. Gregory de Pascale. Muchas gracias. Personalmente y sin duda este proceso de tesis ha sido desafiante y complejo en muchos sentidos, y sin el apoyo de mis seres queridos sin duda habría sido más difícil. Primero quiero agradecer a mi mamá por ser el apoyo fundamental durante toda mi vida, todo este proceso fue posible gracias a ti. A mi hermano Agustín, por su amor y alegría infinita. Al Pedro por todo el apoyo durante tantos años. A mi abuela, gracias Yeya por el cariño y por ser tan importante en mi vida. A mi papá, gracias por apoyarme con la universidad y durante estos años juntos. A mis tíos, los adoro. Pablo, gracias por el apañe y el amor durante estos años. Además, quiero agradecer a mis amigos más cercanos: Cau, gracias por siempre estar ahí y por todos los momentos vividos durante tantos años juntas. Vale, Cotito, Ninia, las adoro un montón. A mis amigas de la u, Ara, Coni, Caro, Gabi, gracias por todos los carretes y las risas, la sororidad y el cariño. A todos los cabros de geo, Pelao, Osvaldo, Mati, Mafi, Ale, Mendo, Jasson, Emil, Lucheiro, Poeta, Karen, Frani, Martín, ¡Marcia y muchos más!, por los momentos vividos en terreno, el patio, los carretes, las chelas, los churrasco-palta, definitivamente todos esos momentos hiceron de la u una experiencia inolvidable y mucho más entretenida, los quiero geocabros. Agradecer en especial a todos los cabros de paleomag por la buena onda, el apañe y la buena voluntad para responder cualquier duda, demás está mencionar los break en el patio que eran infaltables: Marío, Joe, Chalo, Seba Herrera, Huber. Gracias infinitas también a todos los funcionarios de la u que fueron fundamentales en todo el proceso, por la buena onda y la sonrisa todos los días y durante los terrenos. Muchas gracias también a la comisión por los comentarios y la buena disposición, Finalmente agradecer a Gregory por la confianza y los años de trabajo, aprendi mucho y vivi buenas experiencias durante el proceso. ¡Gracias a todos!.

This thesis is UChile Neotectonics Group Contribution #48.

TABLE OF CONTENTS

FIGURES INDEX

TABLES INDEX

CHAPTER 1: INTRODUCTION

1.1 Structure of this thesis

This thesis work divides in 6 chapters. The Introduction chapter present the main motivations for carrying out the investigation, the work hypothesis with the assumptions in which it's based and the final objective that guide the process of working and determinate his extend, including the main and specific goals to be achieved. This chapter also resume and includes all the previous works about the main and related topics, including tectonic and geologic setting in Southern Patagonia region, glacial and climate context, and the Magallanes-Fagnano fault system (MFS), including previous slip-rates and displacement estimations, related seismicity and geomorphology, segments locations, among others. The second chapter present the methodology used during the work process to reach the objectives described in the first chapter, which is roughly divided in literature and desktop data review, field data acquisition work, field descriptions, and finally data processing and analysis. The third chapter corresponds to the main results of this thesis work in a paper format which is already submitted. The fourth chapter correspond to the extended results obtained for each study cases, including field photos and figures that were include in Supplemental data for the submitted document. The fifth chapter present the main topics to discuss considering the results and previously available data, while the sixth chapter of conslusions correspond to a summary of the main results and contributions of the investigation. Besides, ideas are suggested for future research about the seismic hazard and neotectonics of Southern Patagonia. The seventh chapter present the reference used during all the work process and finally, and finally the eighth chapter contains additionally attached information and data that complement the obtained results.

1.2 Introduction and motivation

Plate boundary faults are first order tectonic structures which accommodate large proportions of crustal neotectonic deformation (De Mets et a., 2010; Cunningham et al., 2007; McCalpin et al., 2009), hence are important sources of seismic hazard. Thus, the characterization of active faults which are potential seismic source of high magnitude earthquakes (M>7) based on the observation of the recent geological record is an essential aspect in study of paleoseismology, neotectonics and in the seismic hazard assessment (Costa et al., 2006; Bonorino et al., 2012; De Pascale & Landridge, 2012). The detection of geomorphologic markers provides a reference to determinate the magnitude and velocity of deformation of these structures in Late Quaternary times especially in zones with high deposition rates where the interaction between crustal rocks motions by tectonic activity and erosion or deposition by surface processes generate the landscape configuration (Burbank & Anderson, 2012). An important assumption is that the production rate of the geomorphic markers used to determinate the displacement is greater than the recurrence rate of surface-rupturing earthquakes and that clusters of different mean geomorphic offsets identified along a certain fault section represent cumulative slip from different events (McGill & Sieh, 1991; Zielke et al., 2015). Moreover, this data allows to overcome the limitations of the geodetic data in zones with scarce of a good distribution of GPS stations or with a limited span time of observation (Dolan et al., 2017), besides possibly present a better constrain of the slip rate in Late-Quaternary times (millennial-time scale) regardless of when the last earthquake occurred in the study area (Tong et al., 2014).

The southern Patagonian Andes is dominantly transcurrent and an area of transition where the Fuegian belt with N-S trend progressively veering towards E-W in Tierra del Fuego Island (TdF: Diraison et al., 2000; Menichetti et al., 2008; Poblete et a., 2014). The region is crossed by a main crustal-scale

transtensional structure, the MFS, which represent the current on-shore boundary between the South American and Scotia Plate in addition to be the most important single structure accommodating the current separation between the southern tip of South America and the Antarctic Peninsula (Lodolo et al., 2003, 2007; Klepeis et al., 1994, 1997). The exact location of the main faults within the he MFS in some areas are still poorly unknown, especially where tectonic lineaments are hidden by recent deposits, offset and cut by N-S faults (Lodolo et al., 2003), peat bogs and disturbances in the terrain left by current plague of beavers in the area (a.k.a castores; Graells et al., 2015). In the western part of TdF there is not enough geological, geophysical, and geomorphological data to constrain the exact location and the precise partitioning of slip in the different strike slip active faults (Mendoza et al., 2011; Lodolo et al., 2003; Tassone et al., 2005). Moreover, the slip-rate estimations of this regional structure are restricted only to geodetic data (Thomas et al., 2003; Smalley et al., 2003; De Mets, 2010; Mendoza et al., 2011), which in the area cover a deficient time span and with scarce of a good distribution of GPS stations.

Moreover, the seismic hazard in Southern Patagonia is not well characterized because of the short time period and inaccurate records of local seismic events, which perhaps result in an underestimation of the seismic hazard here. Also, the lack of a good number and distribution of seismological stations prevents the asses of focal mechanism and location of medium to low magnitude earthquakes and better constrained estimates for the Scotia and South American Plates still await more data (De Mets, 2010). Indeed, the MORVEL model and angular velocities estimated by Smalley et al, 2003 in nine continuous GPS stations along the South American and Scotia boundary differs in 2-3 mm/yr.

Added to this, the occurrence of this type of events in zones with difficult access, bad climate condition and low or null population contribute to the scarce seismic record and difficult the correct analysis of

seismic hazard and the mapping of seismogenic structures. Nevertheless, there is no doubt that seismic phenomena have been currently presented in southernmost South America during Neogene up to the present as seen by geomorphologic features associated with recent faulting (e.g., Costa et al., 2006; Bonorino et al., 2012; Perucca et al., 2015). In fact, the largest registered seismic event in the southern tip of South America was the Tierra del Fuego 1949, Ms 7.8 earthquake, related to the MFS activity (Pedrera et al., 2014). Then, the population in southern Patagonia was much lower that at present and the industry and infrastructure almost non-existent. Considering the increase in population and hydrocarbon industry in the area, if an event with this magnitude occurred now the consequences would be much more severe without a correct assessment of the seismic hazard and characterization of the possible seismogenic sources. Furthermore, previous studies showed the need to review the seismic zoning for Argentine TdF given by the INPRES on with is based application of seismic resistance standards. The INPRES scheme qualifies Tolhuín it as an area of low seismic risk (2 in a scale of 0 to 4), while the new seismic zoning adapted to a seismotectonic model based on the MFS as a main seismic souce resulted on a seismic zoning parallel and symmetrical to the fault, localizing the city in the zone 4 of seismic seismic hazard (Abascal & Bonorino, 2014). Moreover, the exploration and exploitation of hidrocarburs have a crucial role in the production of energy both in Argentina and Chile. Finally, the occurrence of low to medium size earthquake by the effect of hydraulic fracturing (a.k.a fracking) due to wastewater disposal wells is an important point to considerate due to the influence in the seismic hazard (Holland et al., 2011; Ellsworth, 2013).

In this study, direct geologic evidence of surface faulting activity in geomorphological offsets features as resulted from seismic events are used to constrain the localization of the deformation, displacement and slip rates during Holocene times along the ~160 km long onshore trace of the Magallanes-Fagnano fault

system in Tierra del Fuego Island, by using high resolution 3D elevation models from SfM techniques, ALOSPALSAR 12.5 m. High Terrain Corrected DEM's, satellite imagery and fieldwork observations. With this, it is possible to estimate the long-term surface displacement rate by taking a mean value of individual displacements and considering that all major valleys and lowlands in the area were glaciated in the Late Pleistoscene (~18 calendar ka). Offsets channels flowing into the Atlantic Ocean from the south, moraines and glaciofluvial outwash plains were identified in the elevation models, satellite images and in the field campaign. Displacements were quantified by elevation profiles and contours interpolations both sides the fault. Ages associated with offsets deposits were assigned by correlation with previous dates and age estimations in the area. These results allow us to better constrain of the fault location and slip partitioning of the MFS different segments, besides to obtain the first Late Quaternary geologic slip-rate of one of the longest and fastest slipping active fault in Southern Patagonia and the Southernmost onshore plate boundary on Earth.

1.3 Working hypotheses

1. If the Antarctic Peninsula currently moves eastward with respect to South America, this is represented partly by the displacement of active crustal faults along the boundary between the South American and Scotia Plates (~50-56° S latitude), which onshore in TdF correspond to MFS. Then, this fault system has the potential to produce major crustal earthquakes and there must be evidence of its Late-Quaternary activity in the field that allow to better constrain the seismic hazard there.

2. If offsets geomorphic tectonic features along the MFS are found in the field, these represent evidence of cumulative offsets from recent activity (Late-Quaternary).

3. The seismic potential in Southern Patagonia region is underestimated because of a series of factors. First, the low number and bad distribution of seismological stations haven't allowed a correct instrumental seismic analysis. Second, the geodetic-data-based slip-rates of this system don not represent a good estimation of the seismic potential of the sources, considering the short time span and bad distributions of GPS stations. Despite this, there must be evidence of recent tectonic activity in the field that allows to improve the seismic potential and seismic hazard assessment, since it would be possible to locate and characterize the seismic sources.

4. If slip-rates determined from measurement of offsets in the field demonstrate that the MFS is fast slipping, then the seismic hazard in Southern Patagonia and Magallanes is higher than previously understood with implications for development and regional building codes.

1.4 Objective

1.4.1 General objective

The main goal of this research work is to increase the knowledge about the recent crustal deformation framework of the longest and likely most active fault system in the region, The Magallanes-Fagnano Fault System (MFS). With this, it is intended to improve the understanding about its seismic potential, obtain geologically consistent parameters for this first order structure with the aim to a more accurate seismic hazard assessment in Southern Patagonia region, and relate this recent context with the evolution and development of the tectonic rotations observed in the southern tip of South America.

1.4.2 Specific objective

The specific research goals of this thesis work are to:

- Locate, map, and measure neotectonic offsets based on geomorphologic markers along the MFS traces and, together with previous deposits dated in the area, estimate the first Late Quaternary geologic slip rates for these segments. In addition to make an attempt to quantifying the differents uncertainties in the rates.
- Determinate the precise location of the active fault traces and the general partitioning of slip along them in Chilean territory within the MFS, by using a combination of high-resolution DEM analysis and fieldwork mapping.

- Improve the structural and geomorphological mapping of the MFS area by merging previous works results with field and post-field observations.

1.5. Tectonic setting and Scotia region evolution

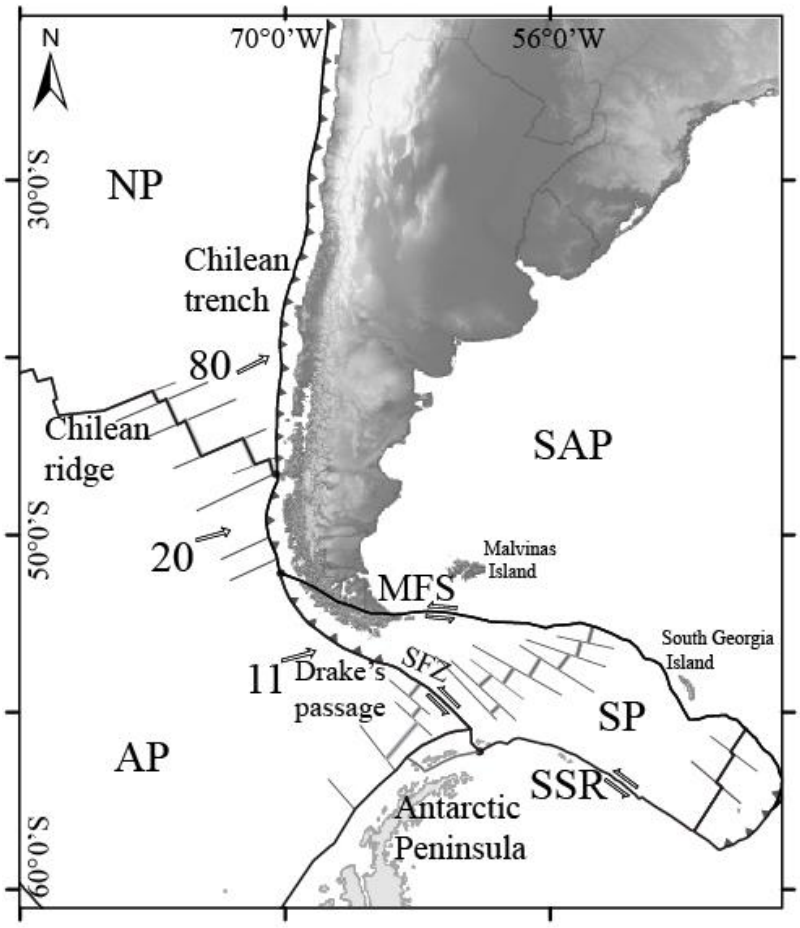

Figure 1.1: Tectonic setting of southern South America and northern Antarctic Peninsula. Base map of South America from ASTER G-DEM 30 m/pix resolution. Paired clear lines indicate ridges. Triangles indicate subduction zones. Circles indicate triple junctions. White arrows indicate current plate velocities in mm/yr (Barker et al., 1991; Diraison et al., 2000). NP: Nazca Plate, SAP: South American Plate, AP: Antarctic Plate, MFS: Magallanes-Fagnano fault system, NSR: North Scotia Ridge, SST: South Scotia Ridge, SFZ: Shackleton Fracture zone.

The southern margin of South American continent is dominantly transcurrent and an area of transition where the Fueguian Andes progressively veers its N-S trend south of the 52°S toward an WNW-ESE trend in TdF (Figure 1.1; Diraison et al., 2000; Ghiglione et al., 2002; Menichetti et al., 2008; Poblete et al., 2014). With this, the amount of crustal thickening decreases and the amount of wrenching increases, giving rise to a continuing bending (Diraison et al., 2000; Poblete et al., 2014). The Patagonian bend is mainly defined by the curved Cretaceous-Paleocene Magallanes Fold and Thrust belt (Figure 1.2; Poblete et al., 2014), related to compressive deformation during since Late Cretaceous times, the coeval onset of the Magellan foreland basin, obduction, crustal loading shortening (Dalziel, 1989; Pelayo & Wiens, 1989) and the closure of Rocas Verdes basin, a deep- marine proto-marginal basin parallel to the continental margin developed within Gondwana during the initial stages of fragmentation as result of a widespread Jurassic extension (Barker & Burrell, 1977; Barker & Dalziel, 1991).

This segment of the Andes range lies in the boundary between the South American and Scotia Plates and divided the Tierra del Fuego Island in two structural domains, a thin-skinned and a thick-skinned domain north and south, respectively (Figure 1.1 Winslow, 1982). The limit is connected offshore at east with a series of active transform left-lateral faults defining the North Scotia Ridge (NSR), which onshore expression is the MFS (Winslow, 1982; Klepeis et al., 1994; Lodolo et al., 2003). This transform system accommodates most of the motion between South America and Scotia plates (Smalley et al., 2003; 2007).

The Scotia Plate is a principal part of the Scotia Arc, composed principally of young oceanic crust developed during the Upper Paleogene (Barker & Burrell 1977; Cunningham et al., 1995). Besides the MFS-NSR system, two others major sinistral transform systems accommodate present day plate motions between South American, Antarctica and Scotia plates. The southern edge of the Scotia Plate with the

Antarctic Plate is left-lateral transform boundary with a sinusoidal geometry defining restraining and releasing structures, the South Scotia Ridge (SSR; Winslow, 1982, Barker & Burrell 1977; Pelayo & Wines, 1989; Cunningham et al., 1995). The western limit of separating Scotia Plate from Antarctic corresponds to the Shackleton Fracture zone (SFZ), a transform boundary with a left-lateral behavior north and south the 57.5° S, respectively (Figure 1.1; Pelayo & Wiens, 1989; Cunningham & Dalziel, 1995). Additionally, the eastern end of the Scotia circuit is composed by the currently active East Scotia ridge, and N-S trending back-arc spreading center opening as result of the convergent boundary between the South- American Plate and the Southern Sandwich microplate (Figure 1.1; Barker & Burrell, 1977). Currently, Antarctic Plate and converge with a rate of 20 mm/yr and 11 mm/yr north and south the triple junction between South American, Scotia and Antarctic Plates, respectively (Figure 1.1; Minster and Jordan, 1978; DeMets et al., 1990), this velocities are considerably lower than the convergence between the Nazca and South American Plate, which produce a considerable decrease of seismicity under the triple point (Adaros et al., 2003).

The northern tip of the Antarctic Peninsula and the southernmost Patagonia probably formed a continuous rectilinear margin at the end of the Early Cretaceous and were very close in the middle to late Cretaceous (Poblete et al., 2015). The relative motion history between Southernmost South America and the Antarctic Peninsula could commenced around 84 Ma, when South American continent had a significantly more rapid westward motion and a non-parallel trajectory with the Antarctic Peninsula relative with fixed African continent. According to Cunningham et al., (1993); this separation and associated wrenching tectonic would trigger the development of the Patagonian bend. Since this time, approximately 1320 km of east-west, left-lateral strike-slip motion has developed and approximately 900 km of the motion occurred after the 50 Ma (Cunningham., 1995).

Other authors suggest that the current plate boundary development is related to an increase in the continental separation rates at 55-40 Ma related during a global Eocene plate reorganization event which led to the onset of seafloor spreading in the western Scotia Sea giving rise to the Scotia Plate and the opening of Drake Passage. According to this model, the strike-slip deformation in TdF occurred after the 60 Ma and dominantly since 30 Ma, superimposing the contractional deformation dominant during Cretaceous times (Winslow, 1982; Klepeis & Austin., 1997; Lodolo et al.,2003; Ghiglione & Ramos, 2005). Between 46 to 20 Ma, the spreading rates in the Western Scotia ridge increase and change to an WNW-ESE direction, possibly related to the onset of the subduction of oceanic seafloor of southern South American beneath the eastern side of the Antarctic Peninsula (Livermore et al., 2005; Lagabrielle et al., 2009). Additionally, some authors proposed that the structural control in the deformation might had migrated further north since the Upper Cretaceous-Oligocene starting in the inherited basement detachment of the Late Cretaceous Andean compressional phase into strike-slip fault along the Beagle Channel fault zone (Winslow, 1981; Cunningham., 1993; Menichetti et al., 2008). Otherwise, paleomagnetic studies indicate that Paleogene rotations observed south Darwin Cordillera are mostly relate to large-scale regional block rotations driven by the shortening in the Magallanes Fold and Thrust belt and no correspond to large amount of in-situ small block rotation related to Cenozoic strike-slip structures (Poblete et al., 2016).

At 20 Ma, a change in the motion to an E-W direction lead to the initiation of spreading at the East Scotia ridge and an important drop in the spreading rates om the western Scotia ridge (Lagabrielle et al., 2009). According to this, the MFS-NSR transform system development may have occurred much later, in the Late Miocene (6.6 to 5.9 Ma; Lodolo et al., 2003; Eagles et al., 2005; Lagabrielle et al., 2009; Betka et al., 2016), coeval to the cessation of western Scotia seafloor spreading and a significant increase in the

Sandwich ridge activity (Lodolo et al., 2003; Eagles et al., 2005; Livermore et al., 2005). This period is also coeval with uplift and exhumation in the eastern domain of Patagonian fold and thrust belt (Fosdick et al., 2013).

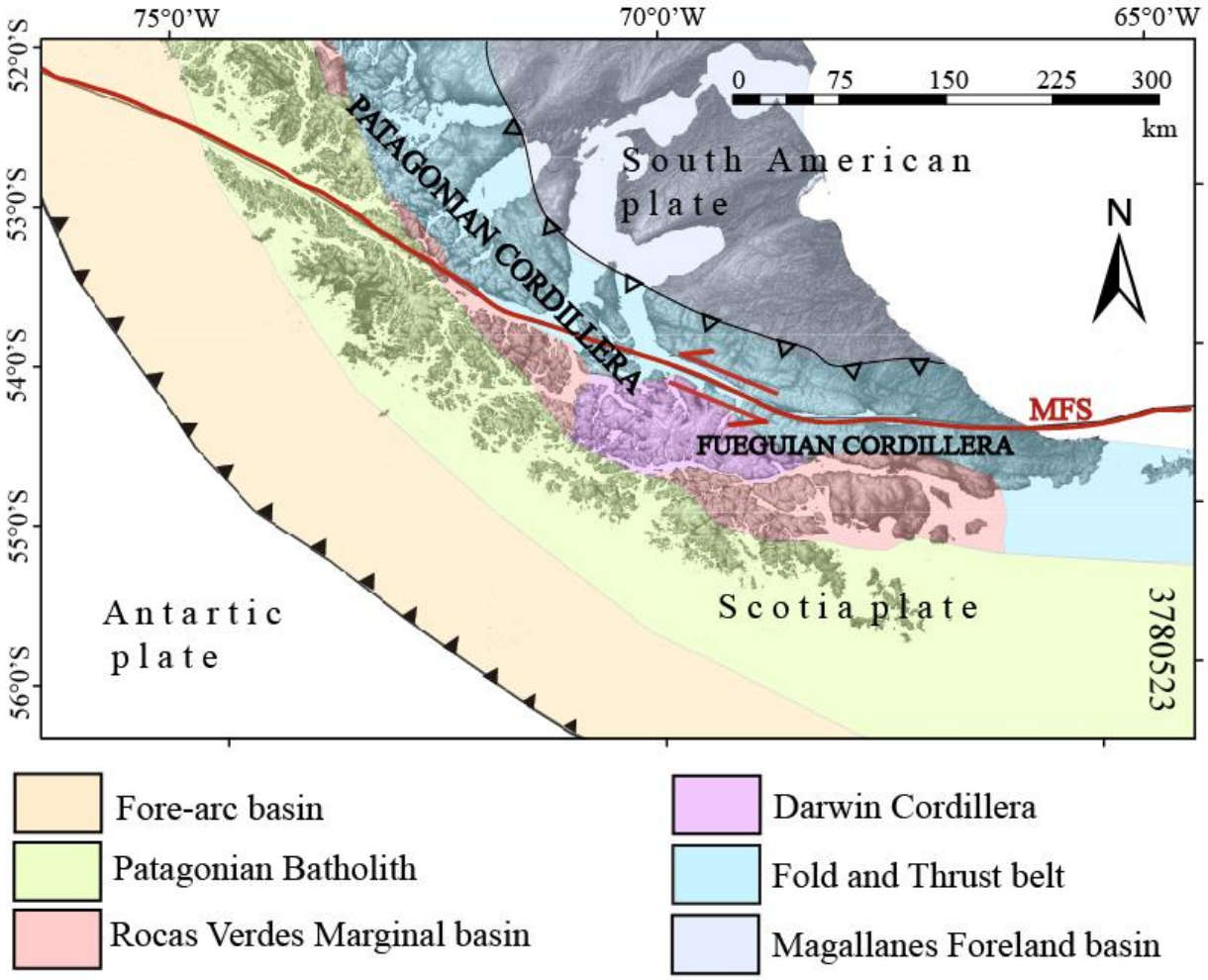

Figure 1.2: Morpho-structural units in Southern Patagonia region. Base map of South America from ASTER G-DEM 30 m/pix resolution. Red solid line indicate location for South American-Scotia plate boundary. Red arrows indicate direction of motion. Filled triangles indicate subduction zones. Hollow triangles indicate locations of deformation front (Extracted from Menichetti et al., 2008).

1.5 Geologic setting

The geological frame in the southern portion of Isla Grande, TdF, comprise a time span from the Upper Paleozoic to Middle Jurassic basement rocks (Metamorfita Lapataia), through the Jurassic-Cretaceous Jurassic infill of the Rocas verdes marginal basin (Lemaire, Yaghán and Beavouir Formations) and the Late Cretaceous-Cenozoic sediments of the Magallanes foreland basin (Cerro Martero, Río Claro, La Despedida and Cabo Peña Formations), to glacial, glacio-fluvial and glaciolacustrine Late-Pleistoscene deposits (Figure 1.3).

The basement rocks of Metamorfita Lapataia, of Late Paleozoic to Mid Jurassic age (Hervé et al., 1981), correspond to highly deformed chlorite-sericite and biotite-garnet schist, greenstones and amphibolites exposed mainly along the Darwin Cordillera, in the southwestern part of the Isla Grande. (Olivero & Martinioni, 2001). This basement rocks are separated from an unconformity from the Lemaire Formation, of Kimmeridgian age (Caminos, 1981; Olivero & Martinioni, 2001), which major outcrops are distributed in a discontinuous belt with NWN orientation including Almirantazgo Fjord, Mount Hope, Sierra de Alvear, Sierra de Sorondo, Sierra de Lucio López, Aguirre Bay and Isla de los Estados (Caminos et al., 1981; Olivero & Martinioni, 2001). The Lemaire Fm corresponds to highly deformed marine acidic volcanic-sedimentary rocks with a sedimentary basal member which grades upwards into acidic complexes of rhyolitic lava, pyroclastic flows, breccias, acidic tuffs and accretionary lapilli (Caminos, 1981). The Yaghan Formation (Tithonian to Lower Cretaceous) overlie Lemaire Fm by a tectonic contact (Caminos et al., 1981) and consists in a volcaniclastic complex with a sedimentary member of coarse conglomerates, mudstones, sandstones, sandy and silty turbidites and tuffs (Dalziel, 1981; Olivero & Martinioni, 2001). The Beauvoir Formation (Lower Cretaceous) is formed by marine sedimentary

succession of black mudstones, sandy mudstones, shales and tuffs result of marine sedimentation in shelf environment in Sierra de Beauvoir north and east of Lake Fagnano, northern Península Mitre and Isla de los Estados (Caminos et al., 1981; Olivero & Martinioni, 2001). West of Sierra de Beauvoir, this formation correlates with La Paciencia or Vicuña Formation in Chilean side (Klepeis, 1994). Most of the strata here are involved in thrust-sheets and form asymmetrical folds with sub-vertical east-west striking axial planar cleavage, while in the central core of Sierra de Beauvoir, where the formation reaches its maximum thickness, presents east striking beds with variable dips (Olivero and Martinioni, 2001).

The Upper Cretaceous Cerro Martero - Policarpo Formation, equivalent to Camacho Formation along the Atlantic coast of Península Mirtre (Olivero & Malumián, 2003), consists in a marine shelf environment sequence with a thick basal unit of mudstone overlying by a unit of mudstones and sandstones intercalations (Martinioni et al., 1997; Olivero & Martinioni, 2001). The lower Upper Cretaceous section present mostly massive mudstones and siltstone, which are predominant in southern coast of Península Mirtre. The uppermost Cretaceous part located 700 km north of Sierra de Beauvoir consist in bioturbated silty-sandy mudstone, siltstone and fine sandstone exposed along the Atlantic coast. (Olivero & Martinioni, 2001). All these sedimentary packages are folded and form thrust-sheets (Klepeis, 1994; Olivero & Malumián 1999).

The Paleocene Río Claro Formation correlates with the Cerro Cuchilla formation in Chilean side of Tierra del Fuego Island (Klepeis, 1994) and correspond to sandstones succession with high variation of facies and exposures north of Sierra de Beauvoir, in the Rio Claro valley; in Sierra Las Pinturas, northeast shore of Lake Fagnano; and along the Atlantic coast, forming a discontinuous east-west striking mountain belt (Caminos et al., 1981; Olivero and Martinioni 2001). La Despedida group of Eocene age, consist in a

fossil rich marine sedimentary clastic wedge with its southern part thicker exposed near Estancia La Despedida and along the Atlantic shore south of Cabo San Pablo (Olivero & Martinioni, 2001; Olivero & Malumián, 2003). Its upper unit is separated by an angular unconformity with the strata of the Uppermost Eocene to Lower Oligocene Cabo Peña – Río Leona formation (Olivero & Malumián, 2003), conformed by an extensive sub-horizontal marine-non marine complex outcrop of bedded mudstones with sandstones intercalations north of folded strata of La Despedida group and along the Atlantic shore (Olivero & Malumián, 2003).

East and south Lake Fagnano, Holocene glacial, fluvial and fluvio-glacial deposits cover the lowlands. In the cliffs south of Lake Fagnano, the sedimentary profile is composed by glaciofluvial deposits of basal till, intercalated with till levels and small lacustrine basins infill by layers of clay and fine and laminated sand (Onorato et al., 2015). South of Udaeta bog, 30 km east of Lake Fagnano, the Holocene sedimentary sequence is constituted in its base by levels of clay intercalated light and grey color massive sand superimposed by fine gravel levels with abundant roots of trees.

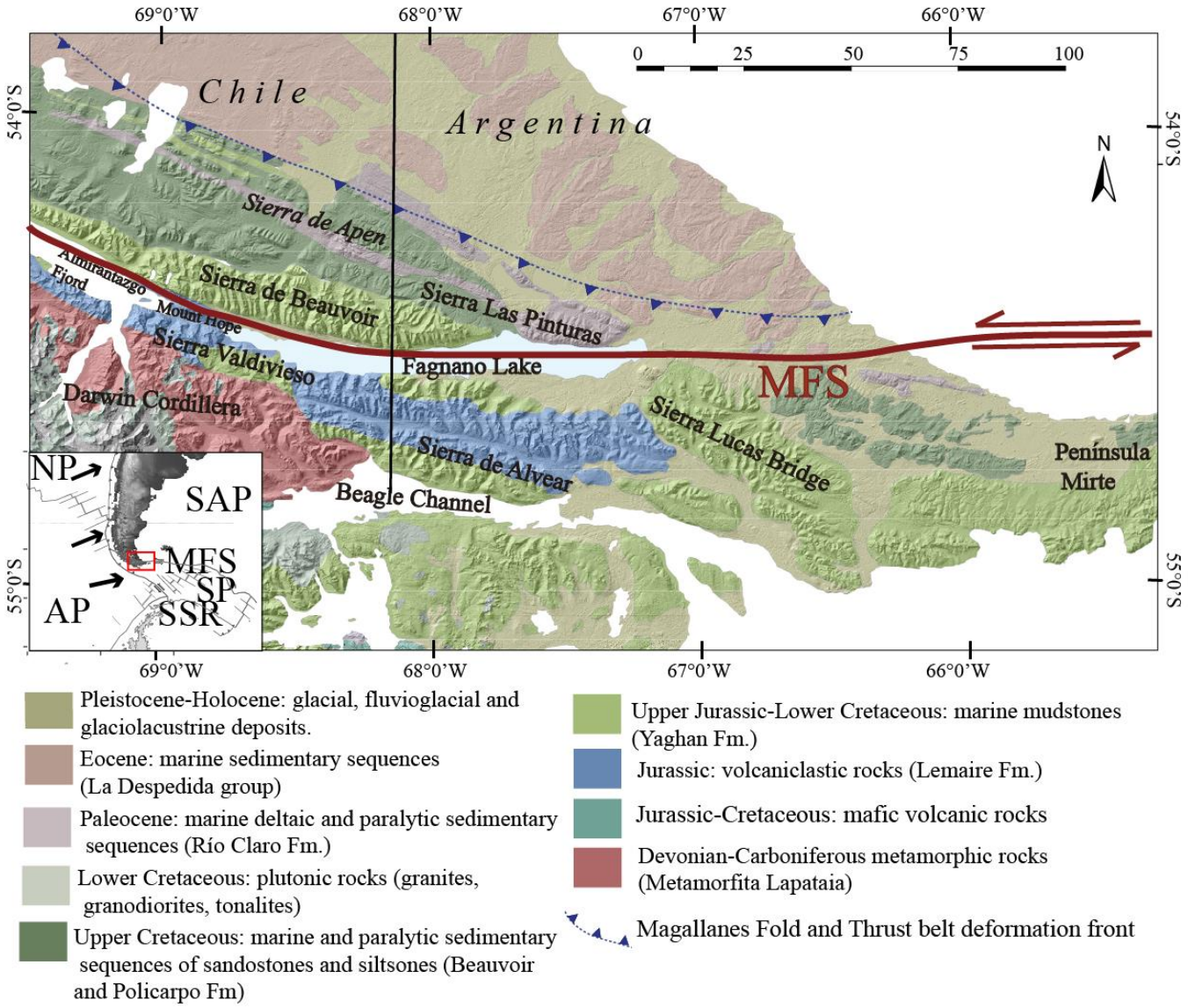

Figure 1.3: a) Geologic setting of southern of southern-central portion of Tierra del Fuego. Base map of South America from ASTER G-DEM 30 m/pix resolution. Triangles indicate location for Magallanes fold and thrust belt deformation front. Extracted from Klepeis, 1994; Caminos, 1981; Olivero & Martinioni, 2001; SERNAGEOMIN, 2003.

1.7 Glacial history and Quaternary geomorphology

Numerous glacial advances and retreats occurred in Southernmost Patagonia and at least five major glaciations were identified in Tierra del Fuego region since the Pleistocene, based on the glacial deposits located along the Magellan Strait and from Inútil Bay to San Sebastián Bay (1 Ma to 23 ka; Caldenius, 1932; McCullogh, 2005; Rabassa & Coronato, 2011). Glacial sediment accumulation covers the entire Holocene and dated back to the Last Glacier Maximum (LGM; Bujalesky et al., 1997). Particularly, the Lake Fagnano in the central southern portion of Tierra del Fuego is considered as one of the most extensie glacier areas in southern Patagonia, and the ice network in this region was developed due mostly to the topography given by the Fueguian Andes (Coronato et al., 2009: Rabassa et al., 2000; 2011). The main ice body was defined as an outlet glacier flowing eastwards from the Darwin Cordillera through different lobes (Figure 1.4; Magellan, Bahía Inútil, Beagle and Fagnano lobes; Caldenius, 1932, Coronato et al., 2009) leaving an extensive cover of glacial, fluvio-glacial, and glacio-lacustrine Pleistocene deposits, (Coronato et al., 2009). A dominant alpine-type landscape in the western portion of Lake Fagnano valley fed by almost 50 alpine-type glaciers flowing from the northern and southern mountain ranges was developed, while a piedmont-type landscape in the eastern region developed with abundant glaciofluvial and glaciolacustrine deposits and an ice-disintegration landscape leaved by outwash paleo-streams flowing into the Atlantic Ocean through four main outwash plains (Figure 1.4; Coronato et al., 2009; Rabassa et al., 2011).

When descending from these mountains, these Late Cenozoic glaciers left wide glacier valleys by carving in weak zones which are now mostly occupied by water, glacial deposits or peat, which difficult to determinate the relative contribution between this glacier erosion and the transtensional tectonic input to

the formation of this valleys, fjords and basins (Rabassa et al., 2000; Coronato et al., 2009). The Lake Fagnano is one of the main glacier valleys whose formation was controlled by both tectonic and glacier activity (Bujalesky et al., 1997; Tassone et al., 2005; Lodolo et al., 2003), while the Fuego and San Pablo valleys were the drainage channels of meltwaters during the different glacial and deglaciation stages of the ice bodies of the present Lake Fagnano basin (Figure 1.5, Caldenius, 1932). Other expressions of this valleys are now occupied by the Strait of Magellan, Beagle Channel, Seno Almirantazgo and bays as San Sebastián or Bahía Inútil.

The southern-central Tierra del Fuego Island experienced several stages of glacier growth and retreat since the Last Glacial Maximum (LGM; Caldenius, 1932; Rabassa et al., 2000; Coronato et al., 2009; Waldmann et al., 2010). The glacial boundaries, pre-LGM, LGM and Late Glacial were determined in this region by previous works (Figure 1.4, 1.5; Caldenius, 1932; McCullogh et al., 2005; Coronato et al., 2009). Minimum ages for the ice recession were estimated by basal radiocarbon dating in interbedded peat in the glacial deposits. In total, the ice would occupied a total area of 4000 km^2, with an eastward slope of 8° and a total ice volume of ~54 x 10^5 m^3 (Coronato et al., 2004b; Coronato et al., 2009).

The easternmost glacial terminal positions correspond to the LGM maximum extension in Argentina at 66°45'W along the San Pablo, Ewan and Fuego valleys. This stage is correlated with the limit "B" in the Magellan Strait-Bahía Inútil model of McChulloch et al., (2005), which beginning was proposed between 25.2 to 23.1 cal. ka B.P. In this stage the till remnants of basal moraines in the southern shore of the lake and in San Pablo valley, the lateral moraines eastward Jeu-Jepen Mount and basal moraines on the easternmost part of the island would have deposited (Figure 1.5; Coronato et al., 2009 (Coronato et al., 2009; Rabassa et al., 2011). A maximum age for the beginning of the ice advance of the glaciers in TdF

between 53.2–43.4 and 37.0–35.2 cal. ka B.P was proposed in Lago Fagnano area for Coronato et al., (2009) by radiocarbon dating of the fossil peat found in basal till in the southern coast of Lake Fagnano. A thermoluminescence age of 25.7 ka was obtained in the latero-frontal LGM moraine in the Río Fuego valley (Coronato *et al*., 2009). Moreover, the basal ages of the peat bog dated by Coronato et al., (2009) near Río San Pablo and La Correntina indicated a minimum age range for ice recession between 14.4 and 13.4 cal. ka B.P. (Figure 1.5). The Beagle Channel and its tributary valleys along the north coast were covered by ice during the LGM, basal and radiocarbon ages in coastal and lowlands peat suggest a minimum ice recession from the study area of 14.3 and 10.0 ka (Heusser, 2003).

The glacial boundaries recognized at west of the LGM maximum extension correspond to recessional stages occurred during the ice stabilization and glacial westward recession in Late-Glacial times (Recessional Phase 1 to 3) (Figure 1.4, 1.5, Coronato et al., 2009) which would have occurred approximately between 18 kya and 10.2 ka uncalibrated C^{14} years according to the Bahía Inútil and Magellan Strait model (McCulloch et al., 2005). The earliest Late Glacial or Recessional Phase 1, represented by the Tolhuín frontal moraine, developed on the eastern end of Lake Fagnano during the first re-advance as in the Bahía Inútil lobe (McCulloch et al., 2005a; Coronato et al., 2009, Rabassa et al., 2011). Also, in this area was reported a proglacial environment, with an extensive glacio-fluvial or outwash plain formed by melting of the Fagnano paleoglacier (Figure 1.5; Coronato et al., 2009). The basal ages of peat bog obtained in this area by Coronato et al., (2009) would not indicate the minimum absolute age of the ice recession in this area (Figure 1.5; Río Turbio and Lago Fagnano peat with 8990-9300 and 9860-10230 cal. years B.P. respectively), due to the ice would remain as ice blocks debris-covered delaying the peat formation several thousand years. However, comparing this stage of major advance or stillstand with the "Stage C" in the Bahía Inútil model by McCulloch et al., (2005), the ice

would have advanced and retreated before 21.7-20.4 cal. years B.P. The deposits from this stage include the glaciofluvial outwash deposits resulting from the melting of the Fagnano paleoglacier founding from this point through east through the San Pablo, Lainez and Irigoyen valleys (Coronato et al., 2009). Morever, Abascal & Bonorino, (2014) made a surficial geological survey of 120 meters depth in the 1 km long area between the eastern coast of Fagnano lake and the city of Tolhuín, identifying below the urbanization zone clay layers of glacio-lacustrine origin covered by a thin layer of debris flow. Under this, sandy levels predominant up to 60 meters deep under which follows a glacial diamictite matrix-supported with sand intercalations separated by the Río Claro Fm. by an erosive discordance at 200 meters depth. This layer is covered by modern gravel along the coast of the lake.

The Late glacial advances or 2nd Recessional phase was recognized in the Lake Fagnano by bathymetric, seismic and coring studies (Figure 1.4; Waldmann et al., 2010). A lateral morainic arc characterized by the Valdéz moraine complex formed by merge of the Fagnano paleoglacier with other tributary lobes from the southern range during this stage (Coronato et al., 2009; Rabassa et al., 2011). The basal ages of the peat bogs dated in this area indicated that the area was free of ice during the Late Glacial between 14.8 and 12.7 cal. ka B.P. (Figure 1.6; Coronato et al., 2009), and is comparable with the "Stage D" of the Bahía Inútil model, which occurred before 17.5 – 16.6 cal. Ka B.P (McCulloch et al., 2005).

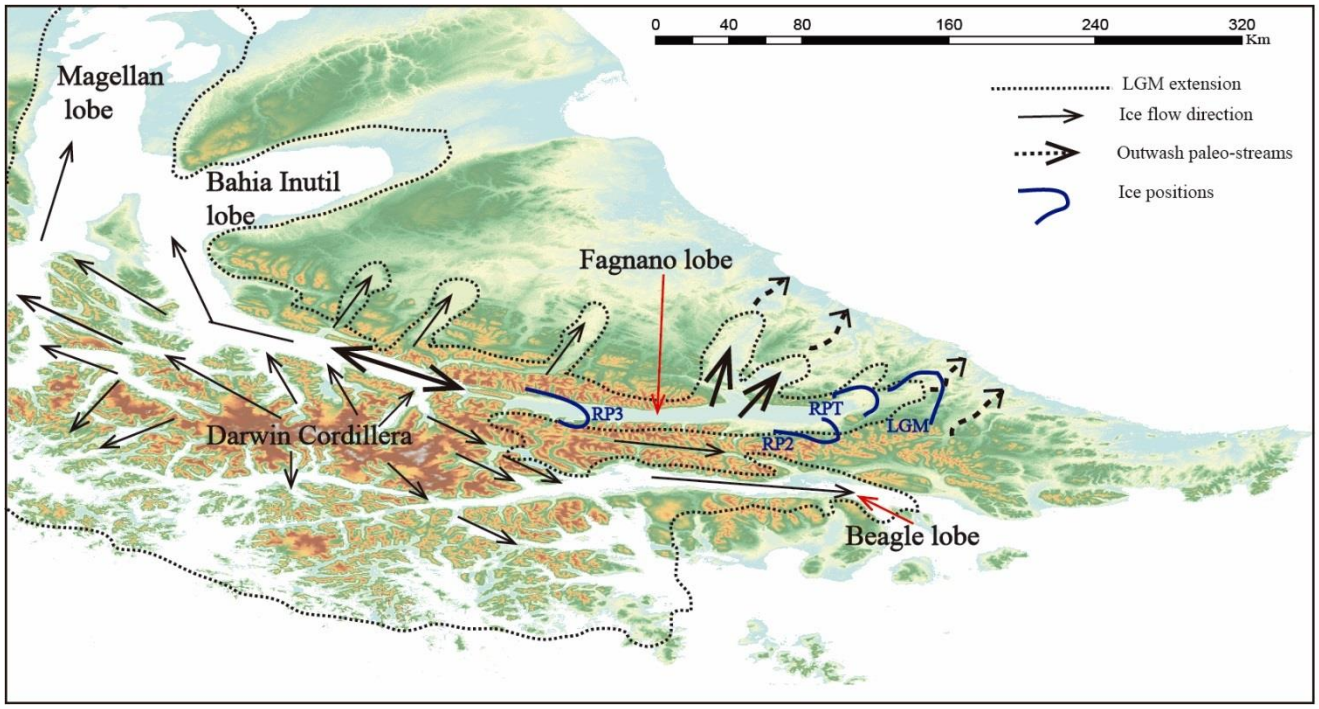

Figure 1.4: Glacial boundary maps of Southern Patagonia. Base map of South America from ASTER G-DEM 30 m/pix resolution a). Dark blue lines indicated the maximum extension for the ice stillstands and retrea (LGM maximum extension at east and recessional phases). Dotted line indicated the extension for the Last Glacial Maximum in Southern South America. LGM: Last Glacial Maximum, RPT: First Recessional Phase or earliest Late glacial (a.k.a. Tolhuin Recessional Phase), RP2: Second Recessional Phase or Late Glacial, RP3: Third Recessional Phase or Latest Late Glacial (Modified from Coronato et al., (2009) and Caldenius, (1932)).

The deposits associated to the 3^{rth} recessional phase, also known as the Latest Late Glacial after the LGM, is represented by the Martínez and Chilena moraines located in the western mountainous portion of the study area. This stage is suggested as the last depositional and standstills stage of the Fagnano paleo-glacier in its accumulation zone before its definitive recession to the highest mountains of Darwin Cordillera, once its edge reached the present Azopardo river threshold (Coronato et al., 2009). Lateral moraines of the Fagnano paleoglacier were interpreted in the southern lake shore in elongated hills of E-W orientation, together with ground moraines of 20 meters thick basal till. The till in the slopes can be

observed in this area reach the 700 m a.s.l. on the slopes of tributary valleys (Coronato et al., 2009). Furthermore, in the western portion of the lake both in the southern and northern shore, undifferentiated till has been described in elongated morphologies in the narrow northwestern and southwestern shores of the Fagnano Lake, east Mount Hope. (Figure 1.5). Although no absolutes ages exist for this deposit, a maximum age of 12.5 to 11.7 ka age have been proposed in the area comparing this phase with "Stage E" in the InútilBay model after McCulloch et al., (2005). During the final stage of the deglaciation, the Fagnano glacier retreated westward from the western Fagnano sub-basin, clearing a drainage pathway from the lake to the Almirantazgo Fjord and to the Magellan Strait, accompanied by a lake level lowering (Waldmann et al., 2010a).

West of TdF, the age obtained in a sediment core in Seno Almirantazgo indicated that the deglaciation here occurred prior to 14,300 cal yr BP, and became a predominantly saline fjord environment with near-modern oceanographic conditions by 9800 cal yr BP, as indicated by an increase in the alkenone and organic carbon of margin origin content, which is well correlated with the Holocene sea level rise (Bertrand et al., 2017). Otherwise, Boyd et al., (2009) indicate that ice retreated from most of the fjord by ~15.5 ka. There is no evidence of a glacial re-advance on Seno Almirantazgo after 16 ka, but neither are studies on the Late Pleistoscene marine record nor the sea floor morphology in the Fjord.

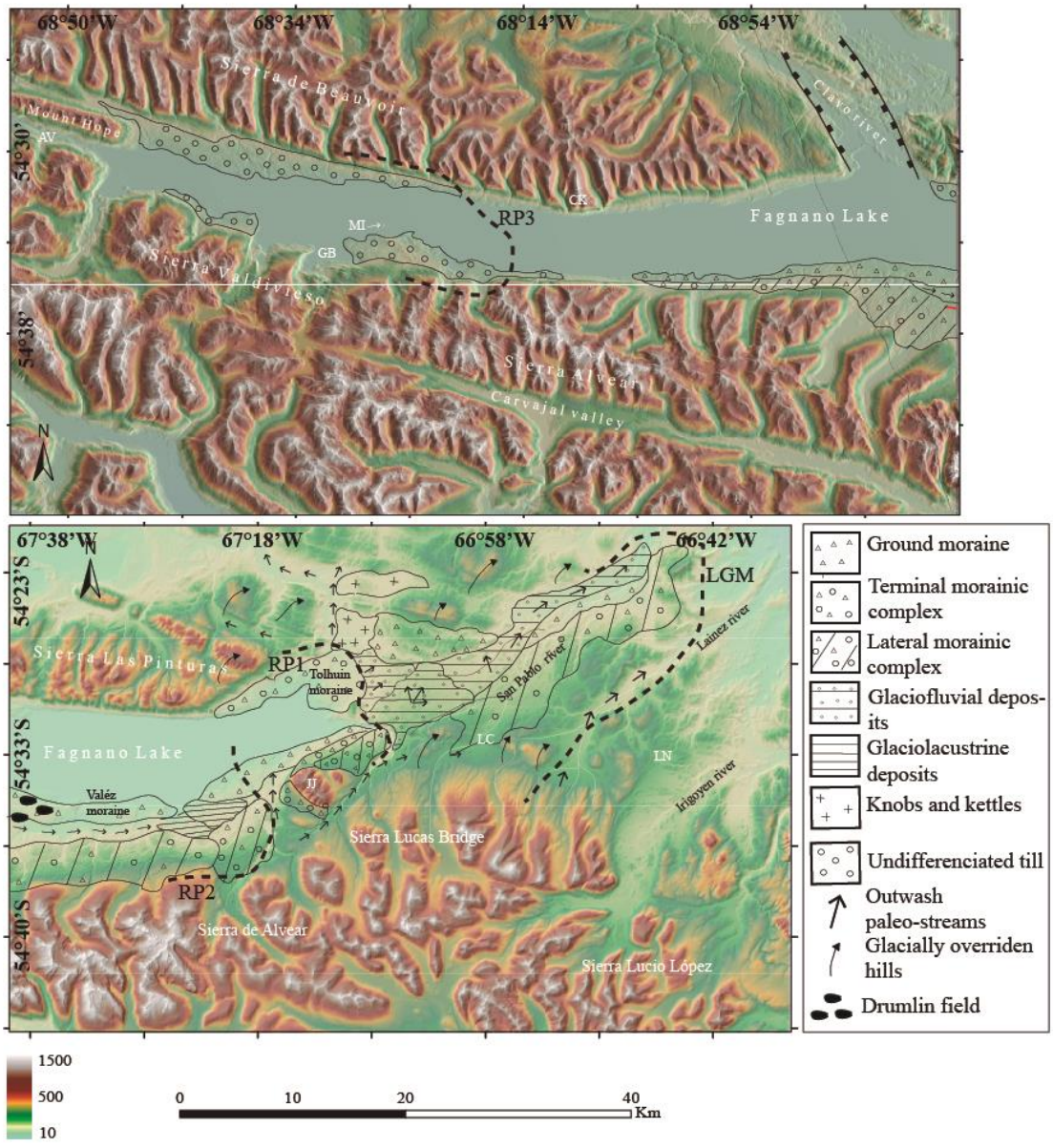

Figure 1.5: a) Glacial landforms and deposits in Lake Fagnano area. The base map corresponds to the high-resolution terrain corrected ALOSPALSAR Global Radar Imagery with 12.5 m resolution illuminated DEM (Acquisition date: 2010-12-30, 2011-01-11). Doted black lineas indicate glacial boundary for the LGM maximum extension and Recessional Phases. The topography height is in meters. RP1-3: Recessional Phases 1 to 3 boundaries (after Coronato et al., 2009). LN: Laguna Negra bog, LC: La Correntina camping, JJ: Jeu-Jepen hill, MI: Martínez Island, GB: Grande Bay, CK: Kranck hill, AV: Azopardo valley (Modified from Coronato et al., (2009)).

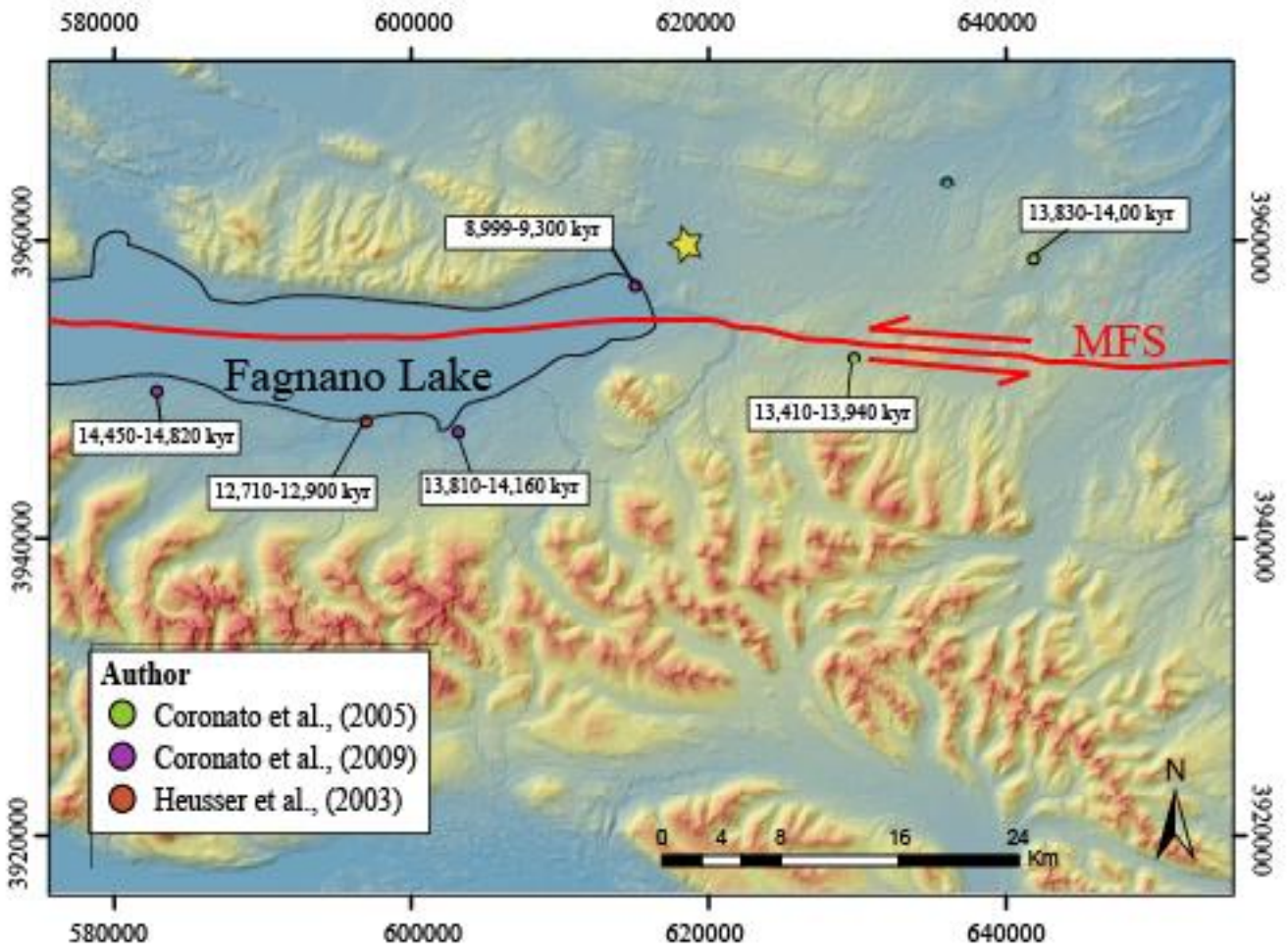

Figure 1.6: Peat bog ages sites obtained by radiocarbon dating by previous authors in the Argentina portion of Lake Fagnano area (Coronato et al., 2005; Coronato et al., 2009; Heusser et al., 2003) Yellow start indicate location for Tolhuín. The base map is high-resolution terrain corrected ALOSPALSAR Global Radar Imagery with 12.5 m resolution illuminated DEM (Acquisition date: 2010-12-30, 2011-01-11). Red solid lineas indicate locations for main MFS trace in Argentina and secondary lineaments.

1.8 The Magallanes-Fagnano fault system

The MFS in Tierra del Fuego Island represents the onshore boundary between the South America and Scotia Plates according to its clear morphologic expression and its evidence of recent activity (Klepeis., 1994; Lodolo et al., 2003). This continental fault system connects to the east towards onshore with the North Scotia Ridge (NSR) (Figure 1.1; Winslow., 1982), and presents a transtensional overall regime in TdF and the Magellan Strait (Lodolo et al., 2003; Betka et al., 2016). The MFS presents a sinistral kinematics and accommodates part of the overall motion between South America and the Antarctic Peninsula (Winslow, 1982; Dalziel 1989; Pelayo y Wiens, 1989; Barker & Dalziel 1991; Lodolo et al., 2003; Smalley et al., 2003; Smalley et al., 2007)

The amount of the long-term strike slip along the MFS was estimated by the correlation of stratigraphic limits and regional structures (Table 1.3; Klepeis, 1994; Olivero & Martinioni, 2001; Torres-Carbonell et al., 2008; Rosello et al., 2005). Some authors suggest that wrenching deformation occurred since the Andean orogeny during Cretaceous times until now, which also gives rise to the oroclinal bending of the Magallanes Fold and Thrust belt (Cunningham, 1993, 1995; Menichetti et al., 2008). According to this, the MFS may have accumulated a deformation of about 900-1500 km of transcurrent offset since the beginning of the regime in the region during the Upper Cretaceous (Cunningham., 1993, Cunningham.,1995). Klepeis et al., (1994), according to the 20-25 km of cumulative left-lateral separation on a thrust contact in the Chilean portion of TdF, suggested that strike-slip motion is partitioned since the onset of the transcurrent regime along the boundary plate or that this segment represent the younger structure of the modern plate boundary that migrated to its present location during the last million years. Otherwise, recent studies indicate that strike-slip deformation overprinted the Cretaceous-Eocene

contractional structures of the Magellan Fold and Thrust belt since the opening of the Drake Passage and onset of the development of the Scotia place from the Oligocene to the Middle-Upper Miocene (Lodolo et al., 2003; Ghiglione & Ramos, 2005; Menichetti et al., 2008; Lagabrielle et al., 2009).

Table 1.1: Lateral and vertical long-term cumulative offset with its respectively kinematics of the MFS obtained in previous works.

Site	Lateral offset	Vertical Offset	Kinematics	Reference
Contact between Upper Cretaceous-Paleocene rock units in an area southeast TdF	48 km ± 20	none	Sinistral	Torres-Carbonell et al, 2008
Near Argentina-Chile limit in Mount Hope area, in a contact between Upper Jurasic and Lower Cretacic	25 km of cumulative offset of each recognized fault, and only 15 km considering regional offset.	none	Sinistral with an extensional component	Klepeis, 1994
Offset in a previous fault zone both sides of the MFFS (lineamientos Río Candelaria Río Claro y Estancia La Correntina-Bahía Sloggett)	55 km	none	Sinistral	Rosello et al, 2005
In Argentinean side of the Isla Grande, from the contact between stratigraphic units both sides of the fault.	20- 30 km	none	Sinistral	Olivero & Martinioni, 2001
Apparent offset in the western margin of the Patagonian Batholith	80 km	none	Sinistral	Winslow, 1982

The main fault system trace is mostly recognized at regional scale and trace can be traced onshore from the Atlantic coast across Isla Grande, TdF (Lodolo et al., 2003; Sue & Ghiglione., 2016). Broadly east-

west trending fault segments were identified mostly by remote sensing and geomorphic expression along the valleys of Irigoyen River, Turbio River and Lake Fagnano (Lodolo et al., 2003; Tassone et al., 2005; Menichetti et al., 2008). To the west, the main regional fault trace pass through to Seno Almirantazgo and the west arm of the Magellan Strait until to the intersection with the Chilean Trench (52ºS, 76ºW), defining a triple point between the South American, Antarctic and Scotia Plates. (Figure 1.1; Winslow 1982, Dalziel 1989, Klepeis 1994, Lodolo et al., 2003).

On a more local scale, the MFS was previously mapped by some authors onshore both in Chile (Klepeis, 1994; Menichetti et al., 2008; Esteban, 2014; Betka et al., 2016) and Argentina (Costa et al., 2006; Torres-Carbonell, 2008). Nevertheless, the exact location of the onshore faults in some areas is still poorly unknown, especially where tectonic lineaments are hidden by recent deposits, offset and cut by N-S faults, peat bogs and disturbances in the terrain left by beavers in the area, mostly in western part of Lake Fagnano and near the Atlantic coast (Lodolo et al., 2003; Tassone et al., 2005). In this area, does not exist enough geological, geophysical and geomorphological evidence to constrain the exact location and the precise partitioning of slip in the different strike slip active faults (Lodolo et al., 2003; Tassone et al., 2005, Menichetti et al., 2008; Mendoza et al., 2011). West TdF, according to fault slip data along the Magallanes retroact fold and thrust belt near Peninsula Brunswick and Seno Otway, strike slip and oblique-slip normal faults sets reflects a regional bulk transtension and the MFS in its western portion would form a plate-bounding strike slip fault zone diffusely distributed and partitioned onto splays reverse reactivated faults within a pre-existing fold and thrust belt and localized along mechanical anisotropies defined by the structural trend of the orogen (Betka et al 2016).

Seismic images and gravimetric data identified a half-graben like structure offshore and onshore Tierra del Fuego, interpreting the fault zone to be composed by a main segment with vertical and sub-vertical faults and a series of tectonic lineaments with an *in échelon* geometry, each from 5 to 15 km long, along which pull-apart depocenters have formed (Lodolo et al., 2003; Tassone et al., 2005; Lodolo et al., 2007). Onshore the principal of this depocenters corresponds to the Lake Fagnano, formed by at least two subparallel, disconnected and *in échelon* segments (Lodolo et al., 2003). The sedimentary architecture of this asymmetric basins suggests a simultaneous strike-slip and extensional motion resulting in a transtensional tectonic regime (Klepeis, 1994; Lodolo et al., 2003, Betka et al., 2016). Another similar pull-apart basin related to the transtensional nature are known in the Magallanes Strait, the Seno Almirantazgo, and to the Atlantic off-shore (Fuenzalida, 1976; Dalziel, 1989; Lodolo et al., 2003; Menichetti et al., 2008; Tassone et al., 2011).

The crustal deformation in the area or slip-rate is also poorly known and is restricted to GPS measurements, most of them with limited spatial resolution and restricted observation time-span or structural limitations (Table 1.2; Smalley et al., 2003; Mendoza et al., 2011). A network of GPS stations in the Scotia-South America onshore plate boundary in Tierra del Fuego was implemented for this purpose (Smalley et al., 2003; 2007). A slip-rate of 6.6 to 6.8 ± 1 mm/yr was proposed for the MFS in TdF based on a set of 20 GPS stations (Smalley et al., 2003). The results and strain analysis suggest that main crustal deformation zone in TdF is concentrated in the MF along a belt which extends approximately 40 km to the north and south of its trace which present an area of maximum extensional rates along Lake Fagnano basin (Mendoza et al., 2011, 2015). Moreover, this active zone would present a slip motion partitioned by the different segments of the MFS and other structures such as the Deseado fault zone (Klepeis et al., 1994) and would be surrounded to the north by a much less active area with slower deformation (Smalley

et al., 2003). Moreover, the MORVEL plate boundary displacement rates model along the NSR gives rates that decrease from 9.6 ± 1.4 mm/yr (1 σ) at the western (65°W) to 8.9 ± 1.2 mm/yr at the eastern MFS (35°W) (DeMets et al., 2010). The several millimeters/ years of difference is suggested to be caused by the different closure constraints that are imposed for the Antarctic-South America plates motion (De Mets et al., 2010)

Table 1.2: Slip rates estimated along the MFS published in literature.

Slip rate	Reference	How the slip-rate was estimated
6.6 ± 1.3 mm/yr	Smalley et al 2003	Independents set of 20 GPS stations in the central portion of the MFS, assuming a vertical slip fault model with 15 km locking depth.
5 mm /yr	Pelayo & Wiens, 1989	Slip vectors from source parameter inversion of waveforms and amplitudes for eight strike-slip and thrust faulting events along the Scotia plate. According to the author, the results are poorly constrained.
4.4 ± 0.6 mm/yr	Mendoza et al., 2011	Repeated geodetic observations since 1993 of a GPS regional network of 29 sites in central and southern Tierra del Fuego Island in Argentina.
5.9 ±0.2 mm/yr	Mendoza et al., 2015	Block model of the MFS fault trace using interseismic velocities from 48 sites, obtained from field measurements spanning 20 years, considering two blocks (SAM and SCO Plates) and three main fault traces (Irigoyen, Turbio and Lake Fagnano valleys)
9.6 ± 1.4 mm/yr to 8.9 ± 1.2	De Mets et al., 2010	MORVEL model from the western to the eastern NSR based on geodetic observations and spreading rates
7.0 ± 3.5 mm/yr	Thomas et al., 2003	Using a combination of slip vectors, spreading rates and azimuths presented a solution for the Scotia plate motion. Slip rates for the NSR and the SSR were obtained by closure.

Mendoza et al., (2015) used a block modeling which relates block motions and fault slip and infer slip rates, locking depths and inclination of the MFS's active fault traces by the inversion of observed interseismic velocities. The resulting model present a locking depth of 11 ± 5 km, with a small ratio between this depth and the lithospheric thickness considering a pure elastic model and a fault's inclination of 66° ± 6° southward, which differs with other results which suggest a two dimension fault with a dip of 90°±40° and locking depth of 15 km, accordgin to the inversion of an independent ser of geodetic observations (Smalley et al., 2003). Other fault's dip estimations have been made by Tassone et al., (2005), which was based on interpretation of gravimetric data and structural observations and estimated a dip of 75°. Adittionally, the model indicated normal faulting along central eastern MFS, the same as other investigations in the area (Tassone et al., 2005; Menichetti et al., 2008) Otherwise, neither Mendoza or Tassone's results could resolve the slip portioning between the several segments that make up the main fault trace.

1.9 MFS main fault trace and secondary structures

Fault mapping of the onshore MFS was reported by previous authors based on kinematic data, bathymetric mapping and seismic profiling interpretation and geological offsets both in Chile and Argentina MFS (Klepeis, 1994; Menichetti et al., 2008; Esteban et al., 2014; Betka et al., 2016). The faults location in Chile and Lake Fagnano area is imprecise and the kinematic data-based mapping could may also correspond to shear motion along secondary fracture planes with no reports of significant amount of slip. Moreover, no evidence of fault rocks as gouche, cataclasite and fault breccia have been reported in these structures, and there is no geomorphic or structural data to affirm that the faulting reported in Lago Fagnano area accommodated remarkable amount of slip or are currently active. The most reliable and

clear expression of a fault zone in Lake Fagnano stratigraphy was reported by Waldman et al., (2011) located at the center of a seismic profile in the central sub-basin from NE to SW.

Klepeis, (1994) carried out the first MFS mapping in Chilean territory between the eastern portion of Fagnano Lake and the Almirantazgo Fjord encompassing all the Mount Hope area (Figure 1.7.a). He described the principal MFS fault in the Azopardo valley going through the norther slope of Alvear range from Caleta María bay to west crossing the lake parallel its main axis. Three MFS segments cumulative, stepwise and sinistral offset the thrust contact between Upper Jurassic volcaniclastic rocks of the Lemaire Fm. and Upper Jurassic to Lower Cretaceous tuffs in 20-25km. The kinematics analysis made in the minor faults subordinated to the main trace in the southern valley suggest a Riedel shear geometry like that observed in Lago Deseado to the north, indicating a sinistral shear in the Mount Hope segment of the MFS with and extensional component. In addition to this, a series of secondary fault zones with NNW-SSE strike in Río Claro area and in the SW shore of Lake Fagnano were described as part of a single anti-Riedel fault with a 20 km of right-lateral offset (Rosello, 2005).

Menichetti et al., (2008) and the further Esteban et al., (2015) mapped the Lake Fagnano area both in Chile and western Argentina based on seismic profiles interpretation and bathymetric data, where the main structures are represented by the Hope-Catamarca-Knokeke fault, the Río Turbio-Las Pinturas fault, and San Rafael fault (Figure 1.7.b). Subsidiary to these structures are several transversal transtensional or extensional faults that subdivide the main segments in shorter arrays. The Hope-Catamarca-Knokeke fault is described as a sub-vertical main array of the principal deformation zone crossing obliquely the Lake Fagnano (Figure 1.7.c; Esteban, 2014) until the southeastern shore to then connect with the array southeast Lake Fagnano in the Sierra Lucas Bridge (Figure 1.7.b, 1.6.c). The San Rafael fault goes along the

southwestern shore of the lake north of Sierra Valdivieso and would be composed by a steeply and north dipping WNW-ESE striking fault array (Esteban et al., 2014). Las Pinturas fault, like the San Rafael fault, goes parallel to the lake shores forming a releasing step-over and would be related to transversal extensional structures. It connects with the Rio Turbio fault east of Lake Fagnano, and both would present a sub-vertical fault plane striking E-W. Subordinately, minor sub-parallel lineaments were recognized in the eastern portion of Tierra del Fuego in Argentina by Torres-Carbonell et al., (2008), conforming with the master fault that has a ~10 km wide shear zone.

West TdF across Peninsula Brunswick in southern Chilean Patagonia, Betka et al., (2016) mapped a left-lateral fault segment named Bahía del Indio, which would belong to the MFS and strikes NW between the Estrecho de Magallanes and Seno Otway. According to this author, the southwestern end of Península Brunswick ocurrs in a left-lateral left-stepping releasing zone between Bahia del Indio fault and the MFS main fault trace along the Magellan Strait.

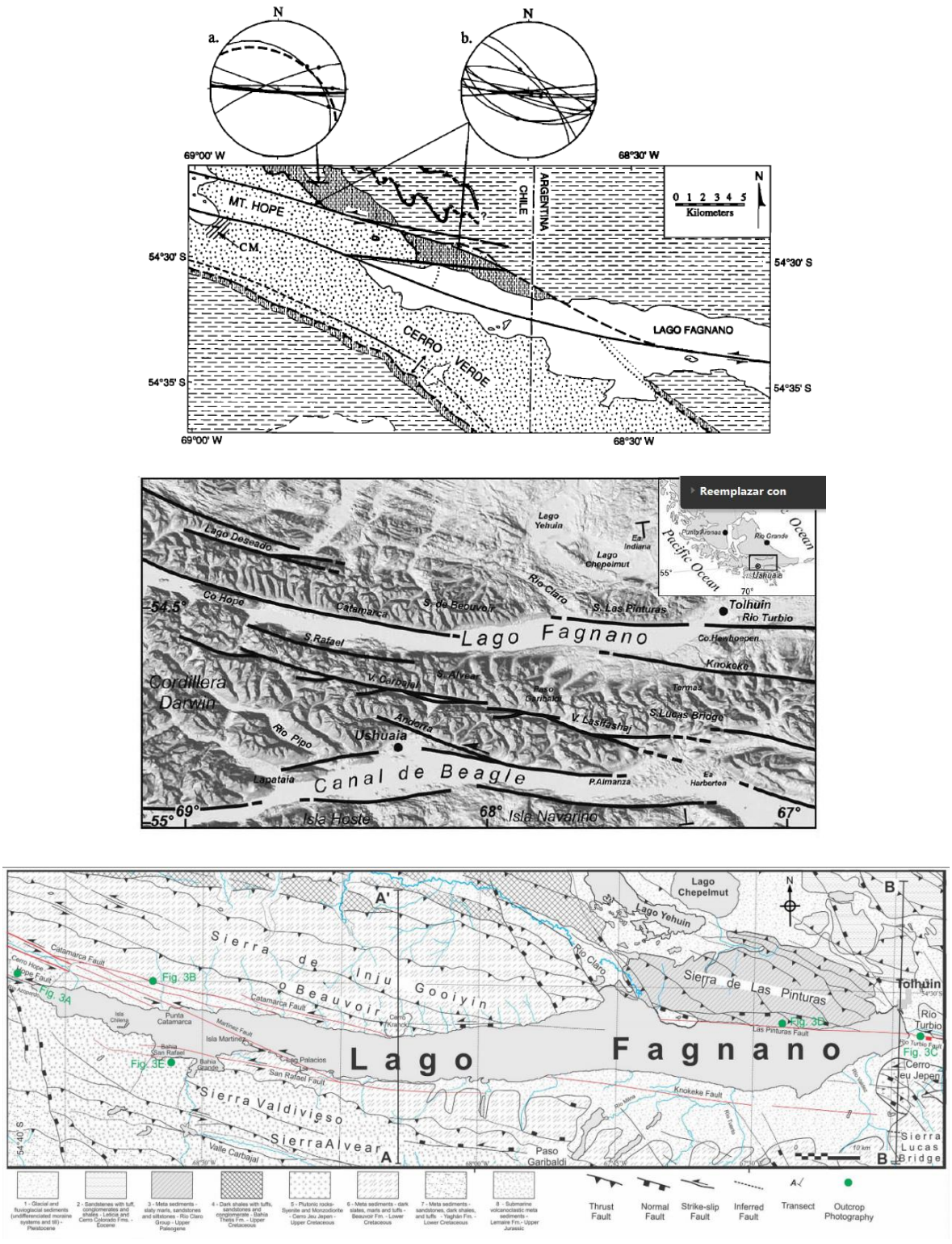

Figure 1.7: Magallanes-Fagnano faults mapping by previous authors. Extracted from a) Klepeis, (1994) b) Menichetti et al., (2008), c) Esteban et al., (2014)).

1.10 Seismicity in Southern Patagonia region

The southern Patagonia region was described as zone with a moderate to low seismicity (Adaros et al., 2003). According to the INPRES scheme the seismic threat for Tolhuín, the city is in the zone 2, which correspond to a low threat with NNW-SSE orientation of the seismic zones, this is based on tectonic model where the main seismic source is located along the South American and Pacific margin, with a low convergence rate, instead of consider a seismotectonic model based on the MFS ,which resulted on a seismic zoning parallel and symmetrical to the fault, localizing the city in the zone 4 of seismic seismic hazard (Abascal & Bonorino, 2014). Part of this low seismicity statement is also due to the lower slip rates in the Antarctic-Scotia (1.1 cm/yr, Pelayo and Wiens 1989), compared with the subduction rate of the Antarctic Plate under the South American Plate north of the 52°S (2.4 cm/year, DeMets et al., 1990). Nevertheless, a significant number of seismogenic structures have been recognized both onshore and offshore in the Southern Patagonia region arguing for high-magnitude earthquake activity during the Holocene (Bonorino et al., 2012, Costa et al., 2006). Indeed, the occurrence of high magnitude earthquakes in historical times (Lomnitz, 1970; Febrer et al., 2000); and the geomorphologic evidence of recent activity (Costa et al., 2006; Bonorino et al., 2012; Shwartz et al., 2012; Perucca et al., 2015) suggest a high current tectonic activity for this structure and associated seismic hazard.

1.10.1 Historical and instrumental seismicity

The instrumental seismicity in Southern Patagonia cover a short time span from 1999 to present with scarce of permanent seismic stations (Buffoni et al., 2009; Perucca et al., 2015). This, in addition to the low population density in the region in XX century, have caused a virtual scarce of historical records,

which results in an underestimation of the seismic activity rates and their impact in the seismic hazard. Despite of this, historical events were recorded in the international catalogues in the years 1907, 1929, 1930, 1944, 1949, 1950 and 1970 (Table 1.3; ISS – ISC: Catalogue of the International Seismological Centre, Berkshire, Great Britain. (http://www.isc.ac.uk), UNLP (Universidad Nacional de La Plata, Jaschek et al., 1982) and nearly 30 moderate (M~5) earthquakes were registered between 1960 and 1977 (Figure 1.7; Sabbione et al., 2007; IRIS database, NEIC catalogue, International Seismological Centre ISC catalogue, Universidad Nacional de la Plata UNLP).

The earliest reports of seismicity were made in 2 February of 1879, with an MSK intensity of VIII in Ushuaia zone and estimated magnitude of M7.0-M7.5 (Lomnitz, 1970; Febrer et al., 2000). Perucca & Moreiras., (2009) reported another earlier event before the European colonization according to an Ona legend (a.k.a. Yaghán). The biggest recorded event is the Ms7.8 December 17, 1949, at 00:12 local time as reported by the Observatorio de La Plata (Lomnitz, 1970; Pelayo & Weins., 1989 Febrer, 2000). The event felt stronger in eastern TdF. A foreshock of Ms7.5 (Lomnitz, 1970; Jaschek et al., 1982; Pelayo & Weins., 1989; Febrer, 2000) started before at 15:52 local time and was felt with higher intensity in Punta Arenas. The effects of this events in the geomorphology of the region were multiple, as landslides along the west Coast of TdF, particularly at San Nicolás, Almirantazgo Bay, and along the banks of Lake Fagnano and the Belverde River (Lomnitz, 1970; Menichetti et al., 2001; Lodolo et al., 2003). Drowned forest occurred in the eastern coast of Lake Fagnano (Costa et al., 2006; Pedrera et al., 2014), while scarps and tsunamis were registered in the Peninsula Brunswick area (Jaschek et al., 1982). Geomorphic evidence of the 1949 ruptures is still preserved in the Quaternary deposits east of Lake Fagnano (Costa et al. 2006).

Table 1.3: Historical seismicity of Tierra del Fuego (ISS – ISC: Catalogue of the International Seismological Centre, Berkshire, Great Britain. (http://www.isc.ac.uk), UNLP (Universidad Nacional de La Plata, Jaschek et al., 1982)

Date	Reference	Time	Lat	Long	Depth	Magnitude
02/02/1879	Lomnitz, 1970	03:30 (local)	-	-	-	M7.0-7.5
17/12/1949	Jaschek et al., 1982	00:12 (local)	54.24°S	69.03°W	10 km	Ms7.8
17/12/1949	Jaschek et al., 1982	15:52 (local)	53.89°S	69.67°W	10 km	Ms7.5
30/01/1950	Jaschek et al., 1982	00:56 (UTC)	53.5°S	71.5°W	10 km	M7.0
15/06/1970	ISC	11:14 (UTC)	54.467°S	64.499°W	10 km	M7.2

Jaschek et al., (1982) relocated the 1949 events in 54.24°S, 69.03°W and 53.89°S, 69.67°W for the first and second event respectively. Preliminary modeling of the focal mechanism of these earthquakes indicated a strike-slip regime (Costa et al., 2006, by a personal communicator), although no published data is available. A significant number of aftershocks occurred in TdF for several months after the mainshock, the stronger was the Ms7.0 1950 event, which epicenter was located in the coordinates 71.5°W/ 53.5°S (Jaschek et al., 1982). Another recent historical event is the Ms7.0 1970 earthquake along the NSR trace at east, with a body-wave inversion for the focal mechanism indicating left-lateral slip on a sub-vertical E-W plane (Pelayo & Weins 1989).

Pedrera et al., (2014), using dendrocronology in Lenga trees (N*othofagus pumilio*) along coesismic surfaces ruptures in Argentina located in the eastern shore of Fagnano Lake and in Irigoyen river area, dated abrupt changes in tree rings from concentric to asymmetric in 1883 ± 5 yrs and 1941 ±1 yr. These results coincide with the 1879 and 1949 TdF earthquakes, indicating that the MFS was the source of this events. Additionally, the surface rupture seen immediately after the first event would have occurred in the MFS trace and left-lateral displacement of 0.4 up to 6 meters were reported (Smalley et al., 2003; Costa et al., 2006) according to personal communicatos. Adittionally, estimations were made previously based on low reliable back-slipped fences estimations of 0-4 meters in San Pablo area and about less than 1 meter east the western branch of Lainez River (Costa et al., 2006).

Despite of the limitations in terms of spatial distribution and number of seismic stations in TdF, some authors recorded the instrumental seismicity in time spans over periods no longer than 2 years, nonetheless the uncertainty for locations are high (Figure 1.8; Febrer et al., 2000; Sabbione et al., 2007; Buffoni et al., 2009). Since 1999 the Astronomic and Geophysics Faculty of the Universidad de La Plata (UNLP, Argentina) and the Nazionale di Oceaografia e di Geofisica Sperimentale Faculty (OGS, Italy) installed a seismological network of 5 statiojns in the Argentine portion of TdF and more than 300 low magnitude earthquakes spatially related with the MFS were registered in the last 10 years (Buffoni et al., 2009). Moreover, several 3 and 4 magnitude events were felt by the TdF inhabitants in the last years. A group of events with hypocenters in the first 30 km depth (most under 10 km) are located along or adjacent to the MFS trace, consistent with the location of historical earthquakes. The hypocenters of the events related to the MFS are located between 5 and 10 km depth, with a locking depth of 15 km (Smalley et al., 2003), while the cortical depth is 28 to 34 km for TdF according to Buffoni et al., (2009). The magnitudes of these events are in general low to moderate ($2<M<5$) (Figure 1.8; Winslow 1982, Pelayo & Wiens 1989;

Febrer et al., 2000; Sabbione et al., 2007, Buffoni et al., 2009). Other cluster of events is near the Beagle channel and in the southernmost Fueguian archipelago. Offshore, toward the east some epicenters are related to the North Scotia ridge, while to the south are associated to the subduction in southern limit of the Chilean trench and in the Shackleton fracture zone.

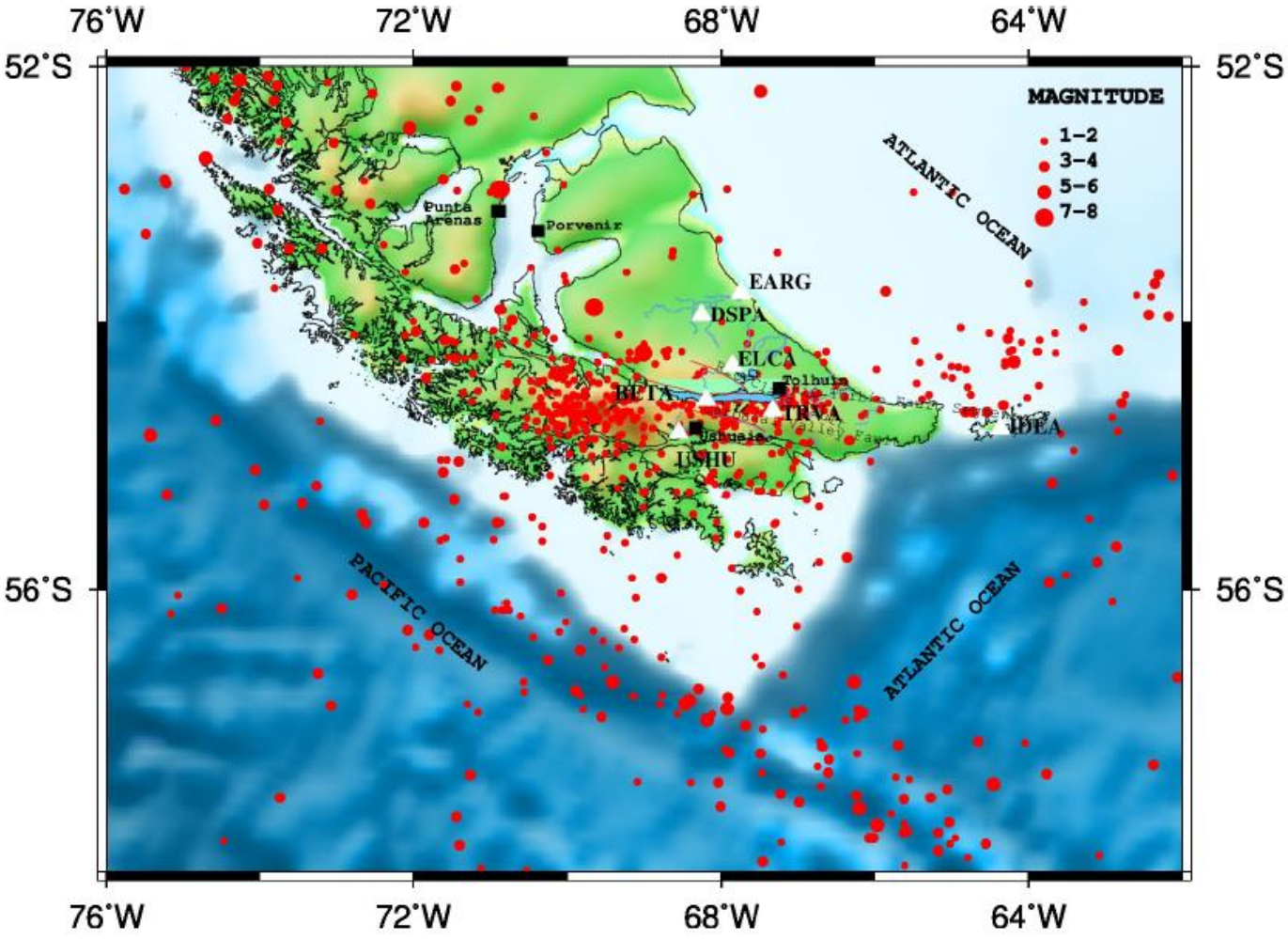

Figure 1.8: Instrumental seismicity in Southern Patagonia region. (ISS – ISC: Catalogue of the International Seismological Centre, Berkshire, Great Britain. (http://www.isc.ac.uk).

1.10.2 Paleosesimicity and geomorphologic evidence of the MFS activity

Different methods have been done with the aim of date paleo-events related to the MFS activity and to stablish recurrence rates of high magnitude events (Table 1.4). Costa et al., (2006) used radiocarbon dating methods east where Río San Pablo crosses a secondary fault trace, recognizing at least 3 paleo-events in the last 9 kyrs, resulting in a recurrence interval of 2 ka. Waldmann et al., (2011) by high-resolution seismic imaging analysis dated slope failure and mega-turbidities in the eastern sub-basin of Lake Fagnano, since considering the proximity of the source the sedimentary infilling of the Fagnano basin is a potential archive of paleo-seismic activity along the MFS. Its result indicates at least 19 underwater landslides in the last 12 kyrs, additionally he observed recent faulting of the youngest sedimentary infill of the lake which could be correlated with historic seismicity. Bonorino et al., (2012) using ground-probing radar, vertical sounding and seismic refraction identified normal co-seismic faults in two strand-plains north of the Strait of Magellan, reported ages of 0.9, 1.3, 2.4, 3.0, 3.9 and 6.4 ka BP and a recurrence rate of 0,9 ka for damaging earthquakes. Besides, the same author dated the co-seismic uplift in restricted littoral deposits along the Beagle Channel in 1-2 meters height steps, giving a recurrence interval of 1,2 ka on average for M>8 events.

Table 1.4: Recurrence intervals determined on the MFS in previous works

Reference	What was dated	Recurrence interval
Costa et al., 2006	Fault slip by the changes in trench sediments on a secondary fault trace	2 ka
Waldmann et al., 2011	Slope failure and megaturbidite formation in the eastern sub-basin of Lake Fagnano	0.35-0.85 ka
Bonorino et al., 2012	Coesismic faults in two strandplains north of the Strait of Magellan in response to dee-seated faulting	0.9 ka
Bonorino et al., 2012	Coseismic uplift of marine littoral deposits along the Beagle Channel, in steps 1–2 m in height, an offset that could be accounted for by earthquakes of ca M = 8.	1.2 ka
Smalley et al., 2003	Based on the slip rate of the fault and a 5 m of offset for the 1949 earthquakes.	0.75 ka

Moreover, different morphologic analysis reported neotectonic and paleoseismological evidence related to Holocene tectonic activity, mostly in Argentinean side of TdF Island (Winslow 1982, Lodolo *et al.* 2003, Schwartz *et al.* 2001, Olivero & Martinioni 2001, Costa et al., 2006; Perucca et al., 2015). Perucca et al., (2015) suggested that tectonic uplift rates of the MFS activity rates must be faster than the stream erosion rate after identified abandoned fluvial valleys along the fault trace between the Lainez River and its tributaries, since a quick uplift may disconnect a stream from its headwaters. This author also discusses about the time span between major earthquakes which must be much higher (10 ka), considering the slip-rates, fault models and left-lateral maximum displacement proposed in previous works, suggesting a complex earthquake type recurrence of the MFS. According to Coronato et al., (2002), the Turbio River was diverted into Lake Fagnano after 12 kyr due to the fault activity, since previously it flowed towards the Atlantic Ocean. More drainage anomalies were reported by the same author as changes in the incision

depth or in the river pattern from anastomosing to meandering. Other evidence of this quick uplift in this segment is the presence of truncated meanders and wind gaps (Perucca et al., 2015).

Along the E-W trending main fault in Argentina, several authors reported geomorphic indicators as truncation of the vegetation in fresh and aligned fault scarps and depressions or sag ponds E-W orientated along the fault trace (Dalziel, 1989; Costa et al., 2006; Perucca et al., 2015). Laguna negra bog for instance, form part of series of small depression in the left-stepping extensional in echelon zone (Menichetti et al., 2001). Moreover, liquefaction in sandy irregular injections were observed in two sites affected by the MFS, one in sediments naturally exposed in the cliffs south of Lake Fagnano and other in outcrops without vegetal cover in the south coast of Laguna Udaeta (Onorato et al., 2015). Other coesismic off-fault features as *in échelon* open cracks and shear fractures with less than 6 meters of lateral offset were reported closer to the Irigoyen River near the Atlantic coast (Costa et al., 2006). Coaxial grabens, tension gashes with *in échelon* geometry and mole tracks have also been reported (Shwartz et al., 2002, Perucca et al., 2015).

Shwartz et al., (2002), Costa et al., (2006) and Pedrera et al., (2014) described the linear and quite degraded scarp of 0.5 to 1.0-meter-high related to the 1949 earthquakes in the eastern coast of Lake Fagnano, near the mouth of Turbio river. The scarp cuts unconsolidated gravels of the actual and paleo-shorelines of the Lake. In this portion, the dropped southern side of the fault entrench the river and Lenga trees are bent or in upright position in a floodplain caused by the earthquake (Pedrera et al., 2014). In San Pablo River, about 30 km from Tolhuín, the scarp reaches 5 to 11 meters high developed through cumulative seismic events related to the MFS and exposes successive terraces of Quaternary glaciofluvial (Costa et al.,2006). The trace is also clearly marked by a sudden change in vegetation cover with Nothofagus woods in the up thrown side and peat in the southern block. Fieldwork in two section of the MFS that suffered rupture in

one of both 1949 earthquakes suggest a maximum vertical slip of 1 m and a horizontal component of no longer than 4 m and probably lower than 0.4 m, which is consistent with the kinematics of a local releasing bend, or at the end of a strike-slip rupture zone (Costa et al., 2006). Furthermore, Smalley et al., (2003) indicated, according to a personal communicator testimony, that after the first 1949 earthquake horizontal offsets of fences of up to 5 meters were resported along the Atlantic coast where the MFS goes out to the sea.

1.12 Geophysics framework

A review of the geophysical framework and previous work here provides insight into the MFS. The analysis of gravity data collected in the region can be used to determinate the subsurface characteristics of geological bodies or structures in absence of clear outcrops or structural indicators. Tassone et al (2005) used gravimetric and magnetic data to determinate the morphological characteristics of the fault segments and pull-apart basins formed within the MFS' principal displacement zone, besides suggesting the existence of intrusive bodies in the subsurface, which emplacement could be favored by the existence of a releasing bend associated with the MFS. Lodolo et al., (2007) realized a complete Bouguer gravity map in the eastern and center part of TdF. His results showed a regional anomaly trend range from about -10mGals to -60mGals and a progressive negative gradient from N to S superimposed by a positive gradient from E to W associated to the presence of elongated basins in the zone of the Magallanes-Fagnano fault system trace. Klepeis & Austin, 1997 showed the sedimentary of the basins associated with the master segments of the fault system in the central part of the Magallanes Strait by seismic records.

Three main gravimetric minima are interpreted as pull-apart basins within the MFS's principal displacement zone developed during a transtensional tectonic regime, corresponding to the morphological expression of diverse segments of this fault system (Lodolo et al., 2003, 2007; Tassone et al., 2005). The Lake Fagnano correspond to the surface expression of the largest pull-apart basin formed by at least two parallel segments of the MFS in *an échelon* geometry (Lodolo et al., 2003). Others localized gravity minimum are in correspondence with the E-W trending Rio Irigoyen and Rio Turbio valleys in Argentinean side of TdF island (Tassone et al., 2005). Other similar extensional depocenters have been recognized in the Carbajal valley and in the northern shoreline of the Beagle channel (Caminos et al., 1981). The sedimentary architecture of this depocenters are in direct relation with the transform activity of the boundary plate, which combines normal extension and strike-slip motion (Lodolo et al., 2003; Yapusky et al., 2004; Tassone et al., 2005). Offshore east of Isla Grande of TdF, other asymmetric basins has been recognized (Lodolo et al., 2003), the elongated fan shaped geometry and changes in dip and thickness of the depocenters are evidence of their syntectonic character.

The gravity maximum is due to the presence of crystalline bodies, as the monzodioritic Hewhoepen body, which intrude the Yaghan formation ESE Lake Fagnano (Tassone et al., 2005). Its morphological expression with NW-SE major axis orientations suggest a post late Cretaceous counterclockwise rotation of about 30° and a northward tilting, which may be caused by the MFS transtensional activity (Tassone et al., 2005). Additionally, its emplacement may be favored by a releasing bend as result of the transtensional activity along the MFS.

1.13 Lake Fagnano

The Lake Fagnano correspond to the 110 x 2-11 km surface and 609 km^2 total area expression of a large pull-apart basin formed by at least two parallel segment of the MFS in *an échelon* geometry (Lodolo et al., 2003), the basin formed a fjord-like environment due to the former glacier advance from the west during the LGM and subsequent glacier advances (Coronato et al., 2009). Besides glacier activity, tectonic activity is other first control order in its morphologic features), delineated mostly by bathymetric, gravimetric and seismic methods (Bujalesky et al., 1997; Tassone et al., 2005; Lodolo et al., 2003; Lodolo et al., 2007; Wallman et al., 2010). The result shows a high asymmetric shape between the western and eastern portion, separated by an elevated area in the central part of about 35 m below the lake level in the outlet of the Claro river, interpreted as a small pressure ridge. Lodolo et al., (2007) propose that this elevated area may correspond to a pressure ridge within the principal displacement zone of the MFS. Three basins were recognized, all of them are limited on one side by a sub-vertical master fault and are characterized by an asymmetric sedimentary fan which thickens towards the main fault (Lodolo et al., 2007; Esteban et al., 2014). The eastern end of the lake is also the deepest and asymmetric main sub-basin (206 m of water depth), and the northern slope have highest topographic gradient, greater depth and trend that parallels the strike of the Río Turbio- Las Pinturas fault (Esteban et al., 2014). From the Río Claro to Punta Catamarca, the western sub-basin is mostly symmetric in shape, and, like the eastern part, shows a flat depocentral area, probably related to the Hope-Catamarca- Knokeke fault (Figure 3.3). In the western portion of Lake Fagnano, a smaller basin was developed, and according to Esteban et al., (2014), would be related to a negative flower structure due to the transtensional activity of the Hope fault. According to the bathymetric tracks in Lake Fagnano acquired by Lodolo et al., (2007), two sub-parallel tectonic lineaments, the Catamarca fault at north and the Hope fault at south, control the ground morphology of

the lake and onshore are represented by two graben structures which bound both sides of Mount Hope (Lodolo et al., 2003; Lodolo et al., 2007). Acoustic penetration by a multichannel seismic system allowed the identification of a complex bedrock morphology overlaying by a thick sedimentary infill succession of more than 100 and 60 meters thick glacially derived and lacustrine sediments in the western and eastern basin, respectively, which occasionally intercalated with deposits resulting from mass wasting event such as turbidities (Waldmann et al., 2008) and tephra intercalations from the Hudson volcano during the entie Neoglacial period marking the onset of distinctive climate fluctuations and moisture changes during the Holocene recognized by the iron content records of the sediments at the bottom of the lake (Waldmann et al., 2019).

On the Atlantic coast another basin of 5 km wide, the Irigoyen pull apart basin, is emplaced along the plate boundary in the Irigoyen river mouth and Irigoyen valley (Ghiglione & Ramos, 2005), its infill is composed by sub-horizontal Late Miocene-Late Pliocene rocks (Irigoyen formation). On a smaller scale, the Laguna Negra bog form part of series of small depression in the left-stepping extensional in echelon zone in the fault trace area (Menichetti et al., 2001).

There is still a lot to know about the Southern Patagonia region associated with the MFS, specially related to its Late Quaternary activity and the implication in the seismic hazard. Indeed, the MORVEL and Smalley et al., (2003) Scotia-South America boundary slip-rates estimates differ more than for the other plate pairs in the Scotia Sea region (De Mets et al., 2010), being the MORVEL models 3-4 mm/yr higher than the rates measured in the GPS sites in the Scotia plate and the Smalley et al., (2003) results suggesting that more data are necessary for better constrained estimations for active plate motions in this region. Although determinate discrete offsets for the last Holocene events independently is difficult considering

the the characteristics of the terrain in the study area including peat deposits, beaver damns and vegetation, cumulative offsets for the Late-Quaternary events are possible to determinate using the photogrammetric method together with field observations, with the aim to determinate the first geological Late Quaternary slip-rates for the one of the main plate boundary in the Southern Hemisphere and the main active first order structure in Southern Patagonia region.

CHAPTER 2: METHODOLOGY

2.1 Literature review and desktop work

The first part of the thesis consisted in desktop work and literature review about Southern Patagonia region, carried out in the Neotectonic Laboratory, Department of Geology in Universidad de Chile. This included compilation of previous works related to the regional tectonic and geological setting, climate, and main geomorphologic features in Southern Patagonia region.

Emphasis was also placed on the glacial history in the TdF region, for which was compiled and digitalized the glacial boundaries identified, mapping of glacial landforms and the available ages of these deposits. In addition, information and previous works related to the Magallanes-Fagnano fault system (MFS) was considered, including previous slip-rate estimations, slip partitioning, related seismic hazard, associated seismicity, and previous structural mapping on the study area, with the aim to obtain a baseline for where to target the field investigation. The references used here, consisted mainly in available academic publications on scientific journals, reports and literature. Also, by using the ArcMap 10.3 GIS software and Adobe Illustrator CS6 graphic design software, different maps and figures were developed by compiling the regional tectonic features, geologic setting, seismic record of the region and geomorphologic evidence related to past seismic events available on previous work. As base map for the digital mapping World map satellite imagery and high-resolution terrain corrected ALOSPALSAR Global Radar Imagery with 12.5 m resolution (2006-2011) illuminated digital elevation models (DEM) were used (Acquisition date: 2010-12-30, 2011-01-11). Additionally, preliminary geomorphological mapping was

done in the fault area both in Chilean and Argentine territory, with focus in the location of lineaments, fault scarps among other tectonic evidence of seismic activity, which was complemented with previous geomorphic maps published. The objective of this was to determinate the best locations for the fieldwork analysis, and a preliminary localization of the different fault traces and landforms modified by the fault ruptures as offset Quaternary deposits, river channels, landslides and shutter ridges.

2.2 Fieldwork and characterization of the study area

An eight days field campaign was realized between 22th and 28th February 2018 in Isla Grande, TdF, Southern Patagonia. Fieldwork focused on the collection of high-resolution survey images, field characterization, and documentation of field conditions along the MFS. The observation sites were in both Chilean and Argentinean territory, in the western and eastern portion of the Island, respectively (Figure 2.1). The area in Chile comprise the segment in the northwestern shore of Lake Fagnano until Mount Hope at the western portion of TdF, including the valley Azopardo at south. In Argentina the study area comprised the ~20 km fault segment from the eastern shore of Lake Fagnano south Tolhuín until Lainez river area, in the central-eastern portion of TdF.

2.2.1 – Digital air photo acquisition

After a ground reconnaissance and examining the available aerial and topographic data, together with previous markers prospects examination, the optimum sites were chosen where reliable geomorphic features were offset by the MFS. Thousands of pictures were taken in 10 flights in Chilean portion of TdF Island (Figure 2.2) made by using the DJI Phantom 4 Quadcopter (a.k.a Unmanned Aerial Vehicle (UAV)

or Drone). Stops were made along the route from the northwestern shore of Lago Fagnano, until Caleta María Bay by the Azopardo river valley. In Argentina, 11 flights were made in Argentinean territory using the Drone along the ~E-W path of the fault trace from the eastern shore of Lago Fagnano until about 20 km at east, near Estancia La Correntina (Figure 2.1).

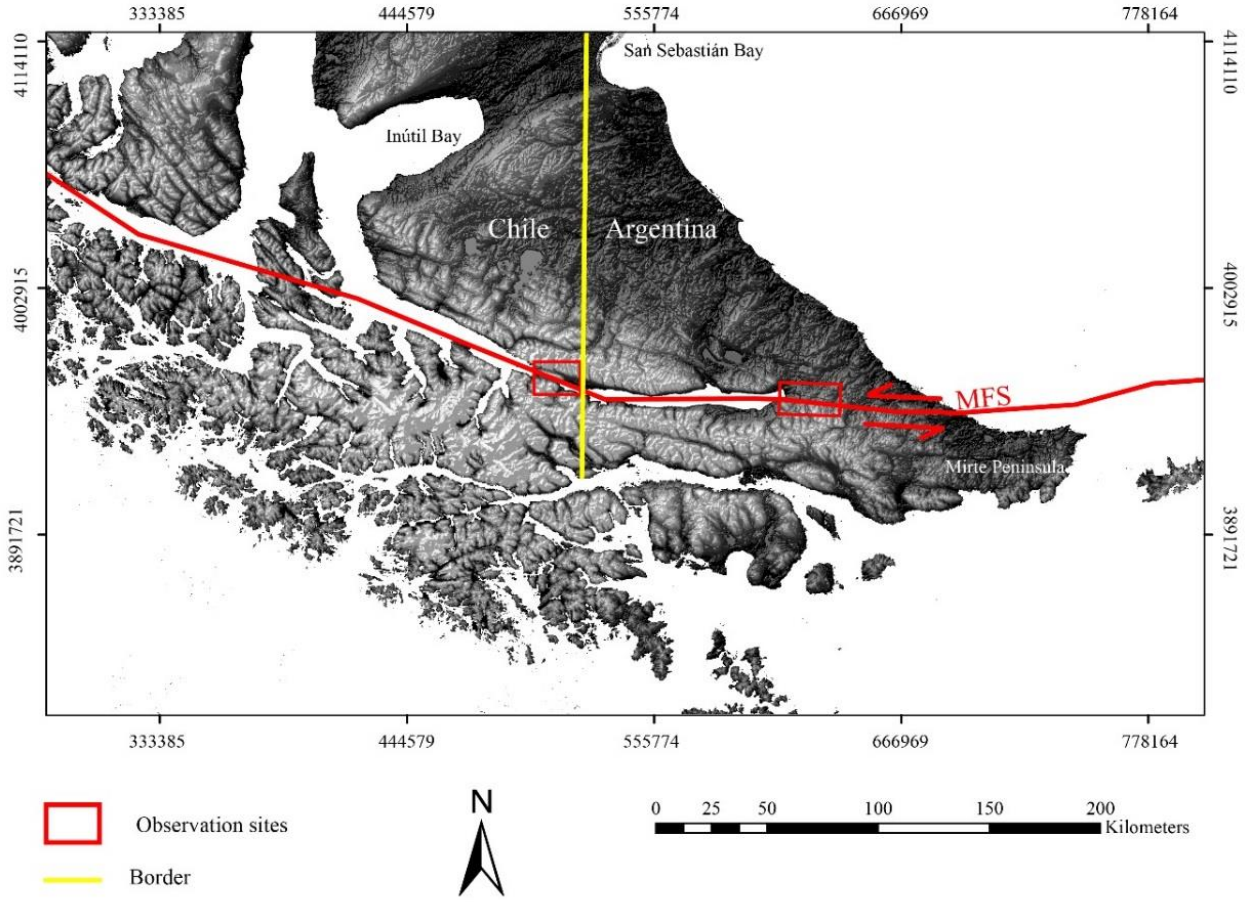

Figure 2.1: Study sites in Southern Patagonia region, Tierra del Fuego. Base map of South America from ASTER G-DEM 30 m/pix resolution. Red solid line indicate location of the MFStrace. Yellow line indicates Chile and Argentina boundary. Red boxes indicate study areas in Chile and Argentina.

2.2.2 – Field mapping of geomorphic features and description of deposits

In addition to the above, field mapping and characterization of deposits and other landforms were done in the observation sites with the aim of improve the geomorphologic and structural mapping in the area. For this, the focus was put on mainly in the localization and characterization of geomorphological markers as landforms, displaced streams and offset linear and non-linear deposits that allowed identification of displacements along the fault traces. Additionally, geomorphological tectonic features as fault scarps, shutter ridges and sag ponds were validated in the field. The description of unconsolidated Quaternary deposits was done with the aim of understanding the Quaternary history and for correlation with previous geomorphological mapping and dating. Besides, in the scarce areas with consolidated rocks cut by structures, these were described in base to structural measurement of the principal fault planes, subsidiary planes and slickensides. The notation method used for the fault planes was azimuth/dip, measured with a Silva Ranger mapping compass, while the locations of field observations were recorded by means of a Garmin eTrex® 10 GPS. Finally, the description of the fault zones and damaged areas was done based on the presence of fault rock in natural outcrops such as plastic gouge, cataclasite, and fault breccia in the fault core (Sibson, 1977; Ben-Zion., 2003) and of multiple fractures, folds and veins in the surrounding damaged rock (Sibson, 1977).

Finally, ground control points were acquired using the GPS inside of each of the flight areas to model, to improve the global accuracy of the photogrammetric models. The points in each area were not collinear and were easily visible in the images taken in the field, among which the most common were bridges corners and fences.

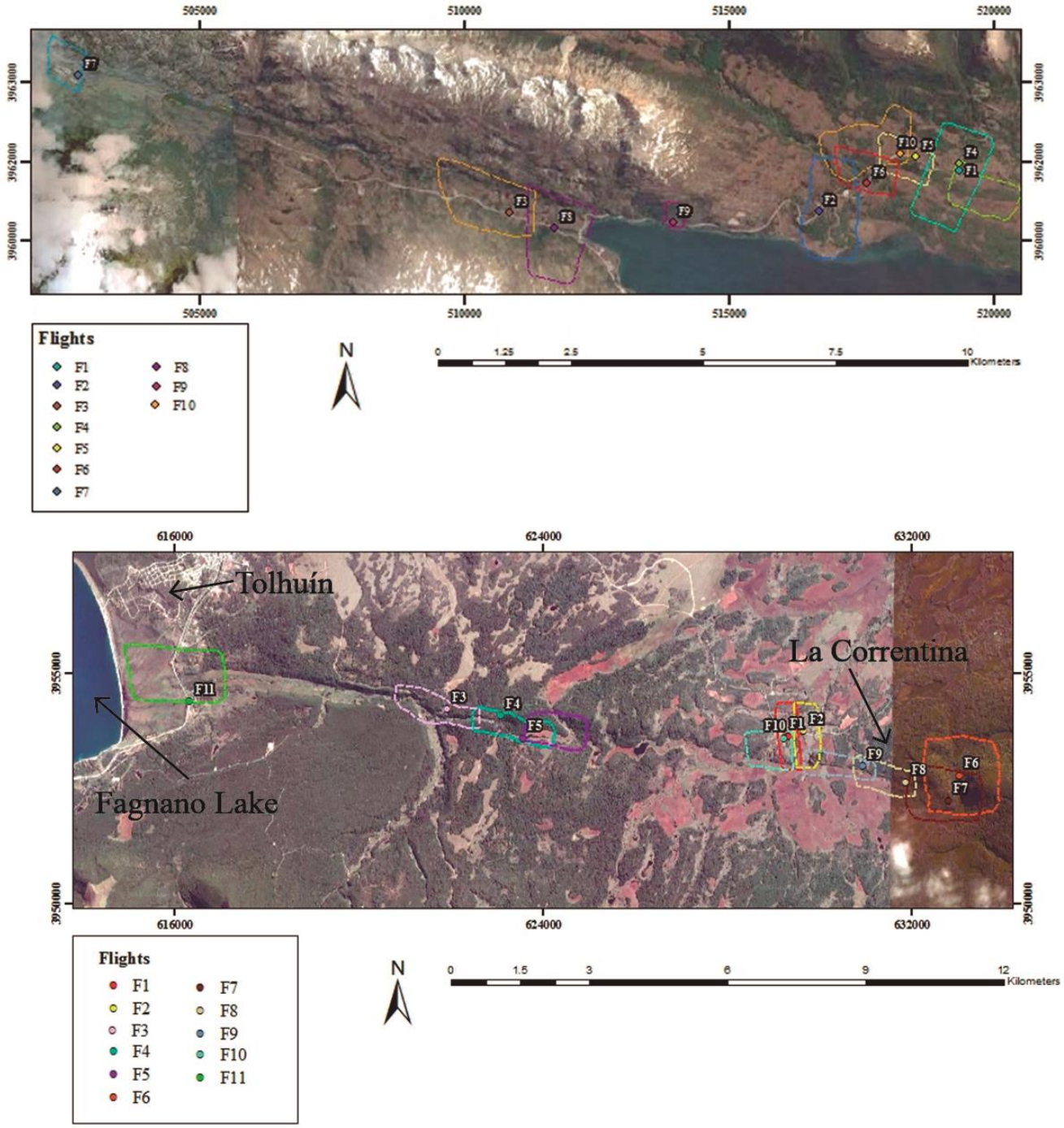

Figure 2.2: a) Locations of the 10 drone flights made in Chilean study area. b) Locations of the 11 drone flights made in Argentine study area. The colored point indicates the location of the drone manager, while the dashed lines indicate the maximum extension of the flight area.

2.3 Drone-acquired Structure from Motion (SfM) photogrammetry and geomorphic models.

Digital photogrammetry is a discipline which allows to construct a 3D digital elevation model with high spatial resolution of from 2 m to <1 m (Figure 1.5) from several of 2D images acquired through an Unnamed Aerial Vehicle (UAV)-based aerial remote sensing (Zuñiga et al., 2015; Duelis, 2015; Kurz et al., 2011) with no need of knowing the location and orientation of the cameras or control points inside of the model, simplifying the data acquisition in the fieldwork, besides being a low-cost alternative to the classical manned aerial photography (Zuñiga, 2016). This is due to the stereoscopic phenomenon which requires the superimposition between pairs of images of 60% laterally and 30% longitudinally (Figure 2.3; Duelis, 2015). Structure for motion (SfM), inside of the field of the photogrammetry, is a technique which uses movement sensor to obtain the 3D images with no need of knowing the location and orientation of the cameras or point control inside of the model, the topography and field geometry are automatically solved by an iterative process (Zuñiga, 2016). Subsequently, the recorded scene is analyzed with a SfM algorithm, which estimates the camera motion and reconstruct a 3D point cloud of the static image (Kurz et al., 2011).

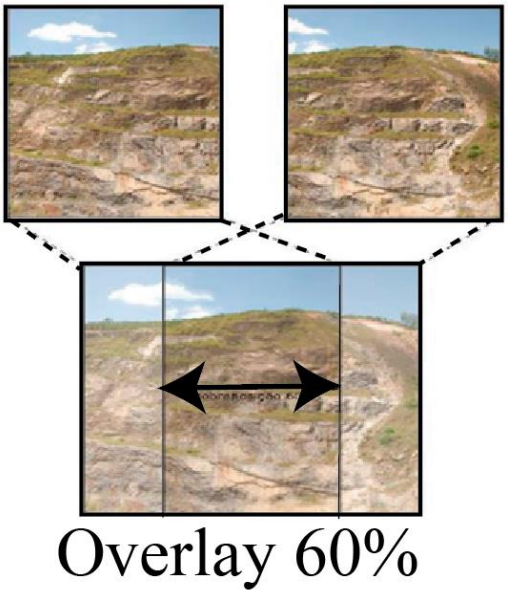

Figure 2.3: Stereoscopic phenomenon in SfM technique, which requires the superimposition between pairs of images of 60% laterally and 30% longitudinally, extracted from Duelis (2015).

Using a DJI Phantom 4 Quadcopter (i.e. UAV or Drone) and a camera model FC330, an average of 200 to 300 photos per flight were taken during the fieldtrip to MFS in Argentina (11 flights) and Chile (10 flights), with a resolution of 4000 x 3000, a focal length of 3.61 mm and pixel size of 1.56 x 1.56 μm (For details see Annexed II). To minimize the loss of resolution by surfaces non-captured, it was tried to capture the target or area from as many perspectives as possible by making an air sweep in the area to model. In addition, attempted to take the photographs with the same light conditions, so these for each flight were taken in the shortest time possible, and avoiding intense rain and wind conditions, which is common in the study area.

The tridimensional reconstruction is based on the SfM algorithm, and the pictures were loaded into the photogrammetric software Agisoft Standard Photoscan Pro 1.3.2 version build 4205, in a Mac OS 64

platform. This software, without any other input but the pictures, recognizes matching points between the images and through a comparative recursive process determines the geometry of the surface and the relative location of the cameras (Zuñiga et al., 2016). This base algorithm can be divided in two stages: the first approximation of the image's analysis and a resolution of the 3D space by a least square regression in no linear models. The first stage consists in apply the method only in some specific key pairs of points with similar parameters of interest (different between pair of points, invariance, metrics, interpretability of changes of tonality, edges, etc.) in the different images by separate to obtain a general geometry of the scene, approaching by the least square regression method the relative position of the camera. Subsequently, the technique is applied in all points of the image in an iterative process to determinate them relative position inside of the scene. Based on the estimated camera position, the software calculates depth information for each point to be combined into a single dense point cloud. After dense point cloud is built it is possible to generate a surface model or polygonal mesh obtaining the 3D model, on which is possible to make a texturizing process to capture the textural features on the smooth surface. For this, an orthophoto of the model is projected on the mesh surface from a specific view to obtain the result (Zuñiga et al., 2016). Finally, for the georeferencing of the model the method used was the proposed by Zuñiga et al., (2016). For this, the ground control points taken in the fieldwork were entered into the model, for what it was necessary to know one control point inside of the area to model, besides the relative location to this of other two points, so that these three were not collinear.

The result was a total of 4 models in Chile and 3 models in Argentina (See Annexed II for details). The corresponding high-resolution digital elevation models and hill shades were developed and used within 2D (ArcMap 10.3). The aim of these was the mapping of geomorphic features and landforms in the sections of interest with a much greater accuracy than is possible through available free DEM's

(ALOSPALSAR Global Radar Imagery 12.5 m), in addition to a considerable better visualization of the 3D surface.

2.4 Geological slip-rate measure in geomorphological markers

In this study, geomorphological markers are used to determinate the MFS offsets in Argentine and Chilean portions of TdF. The fault locations were previously determined in satellite imagery (Worldview) and ALOSPALSAR 12.5 m data set (slope-shades elevation model visualizations, contour maps, and topographic index maps) according to the location of fault scarps, vegetation alignment and peat bogs deposits. This provides the framework in which to interpreted displacement values in offset markers (Zielke et al., 2015). After the fault was located and traced as an idealized planar fault trace, displaced geomorphic markers was located along those traces (Burbank & Anderson et al., 2012; Zielke et al., 2015). These offset clusters are interpreted as the cumulative slip associated to the earthquakes since the ice retreat during the Late Pleistoscene, as the study area is mostly cover by glacial, fluvio-glacial and glaciolacustrine degraded deposits leaved by the glaciers in their westward retreat before the Last Glacial Maximum (LGM). These markers were inspected in detail to avoid doubtful landforms that possibly were modified by other reasons, for example, channel deflection or meanders. A first type of uncertainties related to the offsets measurements are due to the quality of the offset value, for which was assigned a degree of validity (A to C for a very good to a low degree of confidence, respectively), depending on factors as the orientation of the offset landform respect to the fault (lower angles correspond to a lower quality, while sub-perpendicular piercing lines give high-quality measurements), and fault zone width delineation (a wider and imprecise fault trace delineation correspond to a lower quality, while a unambiguous and well-defined fault zone allows high confidence measurements), other factor that

influence the degree of validity are the estimates of the preservation of the markers and the pre-deformation shape reliability, considering also related background of the area. The recognition of the moraines and surfaces covered by till and glaciofluvial deposits is based on fieldwork descriptions and correlation with previous geomorphological and glaciology studies in the area (Coronato et al., 2009; Waldmann et al., 2010; Rabassa et al., 2011). For hillslopes of glacial origin, the most representative offset contours were chosen as markers, while for recent alluvial deposits were used the contours that delimited each side of the creek and thalweg of the channel.

Due to the remote study area, scarce resources and available days in the field and poor accessibility to the full fault trace, including the dense vegetation a peat deposit cover, only sites with category A and B were considered to sites for the acquisition of drone images for SfM, where certainly was a causal relationship between the displaced landform and the fault slip and whether the amount of separation was an accurate measure of the offset associated to cumulative earthquakes (Zielke et al., 2015; Cowgill et al., 2007). In the SfM data set obtained after the photos processing, which includes contour lines, slope maps and hillslopes, the marker section north and south the fault and them respectively interpolation was traced along the Lake Fagnano valley and Lake Azopardo valley area in Chile, and in Lainez river area in Argentina. Subsequently, the pre-earthquake morphology was inferred considering possible modifications related to erosion and deposition process. For the prospect markers with category C, only a first order estimation was made with a lower resolution (12.5 m/pix), with a wider confidence interval in the offsets (See Annexed III, See Discussion chapter).

For determinate the horizontal offset in each marker, an appropriate projection of the piercing lines marker both sides the fault onto the linear fault trace was made, in addition to elevation profiles both sides the

fault processed on the software ArcMap 10.3, where the offset were defined as clear variation within the imagery or the horizontal distance needed for back-slip the marker north both sides the trace. For the interpolation of the markers and profiles an estimation of the original morphology for the feature or landform was done. A range of plausible offsets amounts was given as a minimum and maximum for each marker related to the range of values that credibly restored the original morphology in a specific site (Zielke et al., 2015, Salisbury et al., 2015). The acceptable offset range is dependent on the scale of geomorphic features versus magnitudes of offset, the clarity of landform features and the precision of measurement tools (Salisbury et al., 2015). Linear features that could be followed right up to the fault on both sides have small uncertainties that those features that needed to be projected (McGill & Sieh, 1991). Was intended to measure the largest number of representative markers in each site with the aim of more consistently estimates of offset. The offsets for each feature are reported to the nearest 0.1 m.

Geological slip-rates were estimated by combining the minimum and maximum offsets from each marker together with the available age data. These ages were obtained after a review of the regional quaternary dating. Dalibrated ages are used instead of carbon years. A mean value with its standar deviation were calculated to determinate the minimum and maximum slip-rate for the site as a whole. A closure criterion was used to estimate the overall relative slip along the fault system in case that two fault traces are assumed as parallel, the sum of the slip rates are considered approximately match the overall slip rate (Tong et al., 2014).

1.11 Climate and vegetation

The maritime climates triggered by the South Pacific high-pressure systems and the Polar depression controlled the glacial environment in southernmost South America (Coronato et al., 2009). Currently, the climate of this region is alpine, with a strong winter subpolar Antarctic influence and under the south-westerly wind effect during austral summers, which brings moisture, precipitation and humidity to the region (Waldmann et al., 2008).The climate is temperate in the south and temperate-oceanic in the north, with and overall mean annual temperature of ca. 5°C (Rabassa et al., 2000). Rainfall distribution is affected by the mountain ranges and present and strong gradient from the southwest (600 mm/yr), to the northeast (300 mm/yr), with the moisture derive primarily from the south and southwest. Also exist east-west precipitation gradient in the south with an increase of precipitation from the eastern mouth of the Beagle Channel toward the eastern end of Isla Grande in Isla de los Estados (1000 mm/yr), where oceanic masses are not obstructed by mountain ranges. Moreover, according to the classification of Köppen (1936), the Lake Fagnano area climate correspond to a humid temperature (Cfc) in his eastern region and a polar tundra (ET) in his western region, both with an oceanic influence.

The area is included in the Subantarctic phytogeographic province, represented by the Deciduous Magellanic Forest (Pisano, 1977). The main vegetation type is Nothofagus forest (a.k.a Lenga trees), with N. pumilio and N. Antarctica species. Several types of peatland deposit are abundant in central and southern part of the island, with maximum development in the higher part of the Fuegian Andes, near the Argentina-Chile border. (Rabassa et al., 2000), but also can be found in the lowland areas, with poor drainage together with grasslands (Coronato et al., 2009). These accumulations contain important paleoenvironmental and paleoclimate information (Rabassa et al., 2000). Abandoned river channels, shallow ponds, or poorly drained areas were colonized by peat since Late glacial to early Holocene. An average peat accumulation of about 0.1-0.025 cm/yr south and east of Lake Fagnano (Rabassa et al., 2000). Peatlands are still actively forming today (Coronato et al., 2006).

CHAPTER 3: THE NARROWEST AND SIMPLEST STRIKE-SLIP PLATE BOUNDARY ON EARTH?

Chapter overview:

This chapter presents the main result of this investigation and is a standalone case study that is submitted for peer review. The object of this manuscript is to encompass a concise version of the background, methodology, main results, brief discussion and main conclusions of this thesis. The main contribution of this document es to present the first long-term geological slip-rates based on direct geomorphologic evidence of recent activity of the main and secondary segments of the most active fault system in the southern Patagonia region, the MFS, along its onshore portion in TdF. The figures on this section are also include in Chapter 4.

Abstract

Plate boundaries are zones where deformation is concentrated due to motion along plates and understanding their behaviour is critical to unraveling geologic history and contemporary seismic hazard. The up to 3000 km long Magallanes-Fagnano Fault System (MFS) is the southernmost on-shore strike slip plate boundary (between the South American and Scotia Plates), however slip-rates, a key factor for understanding neotectonics and seismic hazard are only available from geodetic models. In this study, we present the first direct geologic evidence of slip rates. Long-term Late-Cenozoic slip rates along the main MFS fault is 5.4 ± 3.3 mm/yr (2.1 to 8.7 mm/yr), based on geological separations found in regional mapping. Late-Quaternary deformation from offsets geomorphological markers was documented along the MFS in Chile and Argentina based on a combination of satellite mapping, fieldwork, and Structure from Motion (SfM) models developed from drone photography. By combining displacements observed in

remote sensing models with regional Late-Quaternary dating, we obtain sinistral slip-rates for the MFS of 10.5 ± 1.5 mm/yr (9.1 to 12.0 mm/yr, Chile) and 7.8 ± 1.3 (6.5 to 9.1 mm/yr, Argentina). By comparing our results with regional geodetic models, motion here is concentrated along a very narrow zone, approximately <30 km wide from Tierra Del Fuego and east, but widening and becoming more defuse from Cabo Froward north and west to >100 km wide. Because the MFS here is straight, generally narrow and concentrated, we postulate that this plate boundary may be the narrowest and simplest on Earth which provides insight into Plate Boundary evolution, neotectonics, and associated seismic hazard.

Key words: Magallanes-Fagnano fault system, strike-slip faults, Patagonia, Plate Boundary, seismic hazard

Plate boundary faults are first order neotectonic structures which accommodate large proportions of crustal scale deformation along narrow zones and are important sources of seismic hazard. At the southern end of South American, the Patagonian Andes (between Chile and Argentina) are characterized by the curvature of the Fuegian belt, which progressively shifts from an N-S trending structural grain to an E-W strike along the Island of Tierra Del Fuego (TdF; Fig. 3.1; Menichetti et al., 2008; Poblete et al., 2014). There, a continental-scale system of transform faults (Tuzo Wilson, 1965) called the Magallanes-Fagnano System (MFS; Winslow, 1982; Pelayo & Wiens, 1989; Klepeis, 1994; Lodolo et al., 2003), accommodates sinistral (left-lateral) motion along the plate boundary between the Scotia and South American Plates (Barker & Dalziel, 1983; Klepeis et al., 1994; Lodolo et al., 2007) and is the southernmost onshore-strike-slip plate boundary on Earth. High magnitude historical seismicity at depths <15 km (Fig. 3.1), along the MFS in 1879 (Mw 7.0-M7.5), 1949 (Ms 7.8 and Ms 7.5), 1950 (Mw 7.8) and 1970 (Mw 6.2) (Fig. 3.1; Lomnitz, 1970; Jaschek, 1982) demonstrates the seismic hazard. Scant

paleoseismic records estimate recurrence intervals for high magnitude earthquakes from 750 to 2,000 years (Costa et al., 2006; Waldman et al., 2010; Bonorino et al., 2012). To date, faults within the MFS are poorly mapped, with unknown geological slip-rates. Short-term modeled slip-rate estimations from geodetic data based on a limited number and distribution of GPS stations and limited timeframes (Fig. 1; 6.6 ±1.3 mm/yr, Smalley et al., 2003; 7.0 ± 3.5 mm/yr, Thomas et al., 2003; 9.6 ± 1.4 mm/yr, De Mets et al., 2010). This demonstrates the need for geological data to better understand long-term neotectonics along this plate boundary and evaluate the geophysical models. This paper presents new field and remote sensing mapping and offset data that provide geological slip rates along this plate boundary for the first time.

The MFS is a up to 3000 km long transform boundary (e.g. Pelayo &Wiens, 1989; Barker et al., 1991; Klepeis, 1994) with limited neotectonic data likely because few portions of the fault are onshore or not below lakes, only ~65 km of the MFS are onshore in Chile and 60 km in Argentina respectively (Fig. 1). Broad east-west trending fault segments were identified because of their geomorphological expression along the valleys of the Fagnano Lake, Turbio and Irigoyen rivers (Klepeis, 1994; Lodolo et al., 2003; Menichetti et al., 2008). West of TdF, the main fault trace passes through towards the Almirantazgo fiord until it intersects the Chile Trench (52ºS, 76ºW), 500 km from TdF, defining the triple junction between the South American, Antarctic and Nazca plates (Fig. 3.1; Winslow 1982). East of TdF the MFS extends along the North Scotia Ridge up to 1800 km, for a combined length of ~ 3000 km for this plate boundary (Fig. 1).

In order to understand the long-term behavior and rates along the MFS, a review of the origins of the fault are necessary. The northern tip of the Antarctic Peninsula and the southernmost Patagonia probably

formed a continuous rectilinear margin at the end of the Early Cretaceous (Poblete et al., 2015). The relative motion history between Southernmost South America and the Antarctic Peninsula commenced in the Upper Cretaceous (Cunningham et al., 2005) and according to Cunningham et al., (1993), this separation and associated wrenching tectonic would trigger the development of the Patagonian bend since the Upper Cretaceous. Other authors suggest that the current plate boundary development is related to the onset of seafloor spreading in the western Scotia Sea and the opening of Drake Passage (Winslow, 1982; Klepeis & Austin, 1997; Ghiglione & Ramos, 2005). According to this model, the strike-slip deformation in TdF started after 30 Ma, superimposing the contractional deformation dominant during Cretaceous times (Winslow, 1982; Klepeis & Austin, 1997). Between 46 to 20 Ma, the spreading rates in the Western Scotia ridge increase and change to an WNW-ESE direction, resulting in a transpressional tectonics along the NSR during this period (Eagles et al., 2005). At 20 Ma, a change in the motion to an E-W direction lead to the initiation of spreading at the East Scotia Ridge and an important drop in the spreading rates on the West Scotia Ridge (Eagles et al., 2005). Thus, the MFS-NSR transform system development may have occurred much later, 6.6 to 5.9 Ma (Lodolo et al., 2003; Eagles et al., 2005; Betka et al., 2016), coeval with cessation of western Scotia seafloor spreading and a significant increase in the Sandwich Ridge activity (Eagles et al., 2005), which led to the current plate geometry with the inactive West Scotia Ridge and ongoing sinistral motion (Eagles et al., 2005; Lagabrielle et al. 2009). An uplift and exhumation in the eastern domain of Patagonian fold and thrust belt was also be related to the Upper Miocene (~6Ma; Fosdick et al., 2013).

To evaluate the long-term motions, we reviewed previous geological mapping (e.g. Klepeis, 1994; Olivero & Martinioni, 2001; Sernageomin, 2003) to better understand long-term Late-Cenozoic geological separations along the MFS. This was followed by mapping of faults within the MFS by using Google

Earth and a 12.5 m/pix resolution digital elevation model (DEM) of the region derived from corrected ALOSPALSAR Global Radar Imagery (2006-2011), acquisition date: 2010-12-30, 2011-01-11. to identify potential fault traces and displaced Quaternary features. Sites identified during remote sensing were visited in the field. Field airphotos were collected with a DJI Phantom 4 drone at sites identified during desktop mapping (supplemental data). In Chile we screened from the Beavouir Range to the edge of Lake Fagnano to best identify the trace of the fault (Fig. 3.2). These aerial photographs were modeled using Agisoft Standard Photoscan Pro 1.3.2 in order to develop Structure from Motion (SfM) site models (Westoby et al., 2012) including 3D DEMs, and full colour orthophotos (<1m/pix; see supplemental materials). These models were imported into ArcMap for analysis. During fieldwork, field reconnaissance permitted characterisation of deposits, and tectonic geomorphology. We note this process was iterative, because drone flights allowed for identification of additional field sites to characterise the MSF.

Using the SfM models, the faults within the MFS were located and traced as an idealized planar trace, and displaced geomorphic markers were viewed along those traces (e.g. McGill and Sieh, 1991)). Displaced geomorphic features (e.g. river channels, terrace risers) were identified and measured and uncertainties related to the offset measurements are due to the quality of the offset value, for which was assigned a degree of validity (A to C from high to low degree of confidence, respectively. See supplemental data (e.g. McGill & Sieh, 1991, Zielke et al., 2015). An appropriate projection of the piercing points was made to the faults, and the horizontal distances measured. Possible post-rupture modifications by erosion and deposition were considered to estimate of the original morphology of the feature. A range of plausible offsets amounts was given as a minimum and maximum for each marker associated to the range of values that credibly restored the original morphology in a specific site (Zielke et al., 2015, Salisbury et al., 2015). Although the resolution of the DEMs were generally a 1 m for these sites, we ascribe uncertainties (based

on creek modifications and vegetation) of ~5 to 10 m per site measurements. The Late-Quaternary slip-rates were obtained by combining the measured offsets derived from the SfM models (with uncertainties) combined with published ages (with uncertainties) from surfaces and deposits.

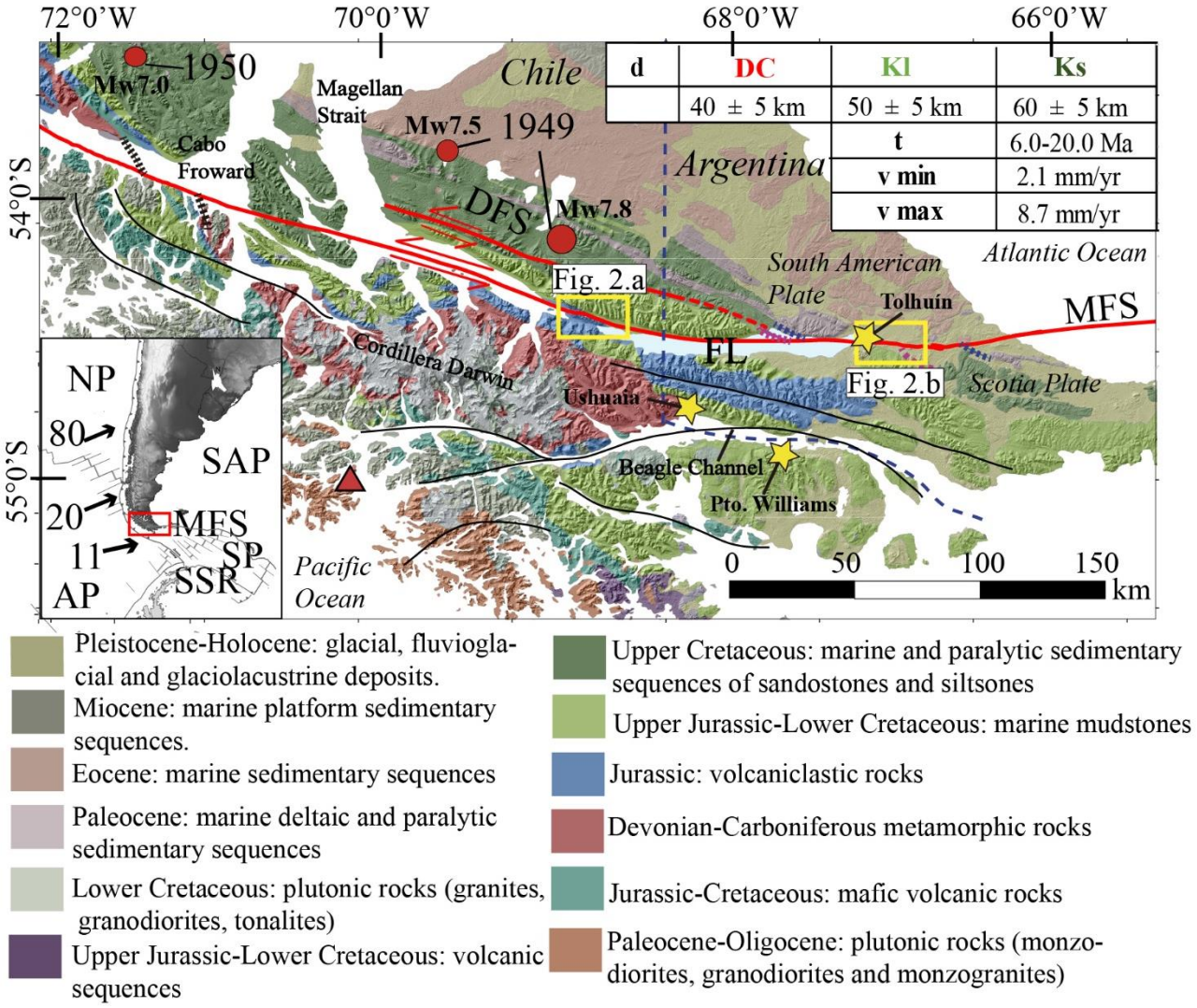

Figure 3.1: Geological map of the Southern Patagonia region (modified from Sernageomin, 2003; Olivero & Martinioni, 2001; Klepeis, 1994). Table indicates Late-Cenozoic MFS slip-rates based on a mean of the plausible sinistral separation of the Devonian-Carboniferous metamorphic unit (DC, red), Upper Jurassic-Lower Cretaceous marine sequences unit (Kl, light green) and Upper

Cretaceous marine sedimentary sequences (Ks, dark green) and proposed ages for the beginning of activity (20.0 to 6.0 Ma; Eagles et al., 2005). Dotted lines are the projection of the contacts to the MFS. Yellow boxes are field study areas. Red circles indicate historical epicenters (Jaschek et al., 1982). MFS: Magallanes-Fagnano Fault System, DFS: Deseado Fault System, FL: Fagnano Lake, NP: Nazca Plate, SAP: South American Plate, AP: Antarctic Plate, SP: Scotia Plate.Red triangle indicates Cook Quaternary Volcano. Blue dotted line indicates international border. Black solid lines indicate lineaments possible related to tectonic activity (Lodolo et al., 2003; Sue & Ghiglione, 2006). Plate velocities are from Pelayo & Weins (1989) and DeMets (1990).

Geological separations (Fig. 3.1), we identified along the MFS main trace suggest that total slip ranges from 40 ± 5 km to 60 ± 5 km yielding long-term (Late Cenozoic) geological strike-slip slip rates from 5.4 ± 3.3 mm/yr based on the ages of this rocks. Previous offsets were reported by Torres-Carbonell et al., (2008); 48 ± 20 km conntact between Ks and Pl), Klepeis, (1994; 25 km, cumulative separation of the contact between Js and Kl) and Winslow (1982; 80 km of apparent offset in the Patagonian Batholith), however none of these data were previously used to determine long term MFS slip rates. The large range here is based on uncertainties in timing from 20 Ma to 6.0 Ma (Fig. 3.1; Eagles).

We believe the master MFS fault (i.e. the Magellan fault, MF) in Mount Hope area in Chile (Fig. 3.2.a) is north of Fagnano Lake. Here, the trace of the fault is a well-defined-single rectilinear ~N70°E strand with clear evidence of Late Quaternary surface rupture and is expressed by a south-facing scarp of about 5-10 m high delineated mainly by aligned vegetation and peat along the southern dropped side (Fig. 3.3.a). This trace continues to east along the lake main axis the lake until the eastern portion of Lake Fagnano where it was identified in a seismic profile reported by Waldmann et al. (2011). A creek channel left of the road is sinistrally displaced by the main fault trace in 80 ± 5 m to 95 ± 5 m (Fig. 3.3.c). Offsets were measured in each side of the river and in the thalweg of the channel, additionally, parallel elevation

profiles were made to the north and south the fault trace and the channel was back-slipped (Figure 3.3). The elongated strips of undifferentiated till along the northwestern shore of Lake Fagnano cut by the fault suggested they are the last depositional stage of the Fagnano paleo-glacier before its definitive recession (i.e. third Recessional phase) once it reached the Azopardo valley (Coronato et al., 2009; Waldmann et al., 2010a). A maximum age of 12.5 ka is considered for these deposits and is correlated with the Younger Dyras event in TdF (Waldmann et al., 2010). Furthermore, an age of 10.2 ka is proposed as a definitive deglaciation for the Southern Patagonia and therefore forms a minimum age for these landforms (Rabassa et al., 2000; McCulloch et al., 2005). Thus, the deglaciation ages when combined with the slip (Fig.3.3; after e.g. Ludwig, 2013) allow us to estimate a long-term (Late Quaternary) geological slip-rate of 7.8 ± 1.1 mm/yr along the MF here.

Another fault, the Hope Fault (HF; Menichetti et al., 2008), only ~5 km and sub-parallel with the MF was evaluated in the Azopardo Valley south of Mount Hope (Fig. 2; Supplemental data). Onshore it is ~11 km long but likely continues offshore within the Almirantazgo Fiord according to seismic reflection data (Winslow, 1982), and possibly to the east running parallel or merging with the MF in Lake Fagnano. SfM data allowed identification of a clear fault trace along the center of the valley (parallel with the river) including of two displaced till deposits with offsets from 16 ± 3 m to 23 ± 2 m in the central-eastern portion of the valley (supplemental data). When combined with the deglaciation records outlined above, these data suggest Late-Pleistocene Hope Fault slip-rates of 1.3 to 2.1 mm/yr. A combined MF and HF slip-sites in the Chilean portion of TdF and including the Deseado fault which we believe to be at least 1 mm/yr based on geomorphology (supplemental data), provides a total Late-Quaternary geologic strike-slip rate across the parallel MFS of at least 9.1 to 12.0 mm/yr.

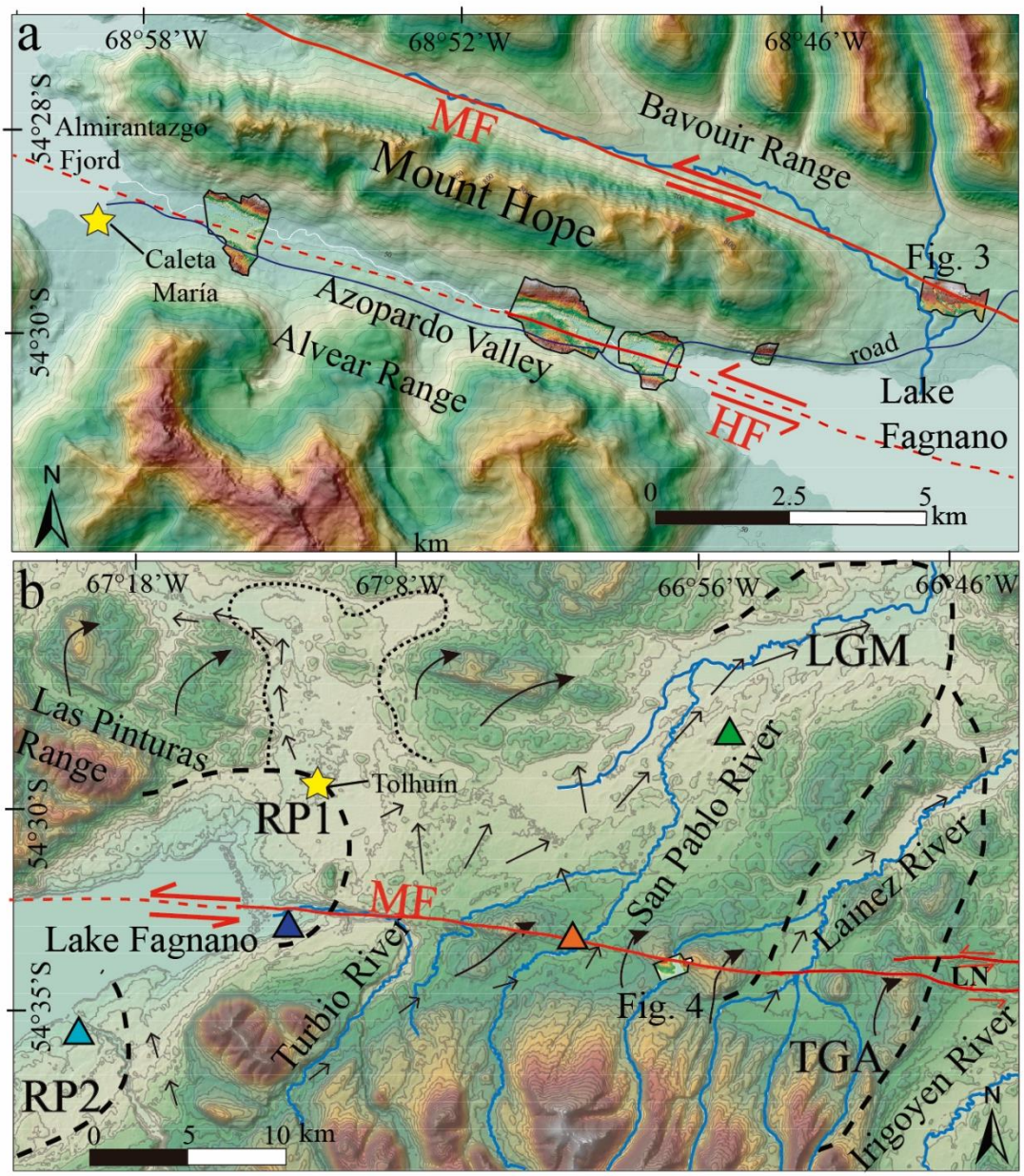

Figure 3.2: a) Chilean study area in TdF. SfM DEM shows over the 12.5 m resolution DEM (See Supplemental data). MF: Magallanes fault, HF: Hope fault. Solid red lines are observed faults and dashed red lines are inferred faults. b) Argentina study area. Thick dashed black lines show glacial boundaries identified by Coronato et al., (2009). Thin dotted lines show ice disintegration landscape area triggered by the ice retreat (Coronato et al., 2009). MF: Magallanes Fault, LGM: Last Glacial Maximum (Proposed ages for deglaciation TGA: Tributary glaciers area, RP1: Recessional Phase 1, RP2: Recessional Phase 2. LN: Laguna Negra bog. Thin black arrows indicate flow direction of outwash paleo-streams triggered by the melting of Fagnano Paleo-lobe post RP1 (Coronato et al.,

(2009). Thick black arrows indicate glacial overridden hills (Coronato et al., 2009). Colored triangles are radiocarbon dating of peat bogs (Coronato et al., 2005; 2009; green, 13.8-14.4 kyr; orange, 13.4-13.9 kyr; light green, 13.8-14.2 kyr; blue, 8.9-9.3 kyr). . 50 meters contours shown.

In Argentine side of TdF east the Fagnano Lake, the MF extends east (e.g. Costa et al., 2006; Waldmann et al., 2010) to the Claro River and Lainez River areas (Fig. 3.2.b). The eastern tip of the trace reaches the Laguna Negra bog area (Fig. 3.2.b), where forms part of the southern boundary of a pull-apart basin of ~13 km long in an overlapping left-stepping extensional geometry (Figure 3.2.b). Despite of the thick vegetation, the main MF scarp is visible in satellite images as a clear, straight, linear geomorphic trace. In the SfM derived DEMs obtained where the western tributary branch of the Lainez River cut the fault (Figure 3.2.b), the MF strikes 80º with clear left-lateral offset the River channel and adjacent hillslopes (Figure 3.4.c). Geomorphological offsets in geomorphological markers are from 110 ± 5 m to 130 ± 10 m (Fig. 4), considering possible post-events modification by sedimentary process. Fieldwork reveals classic strike slip tectonic geomorphology with sag ponds, and shutter ridges, in addition to clear sinistral offsets (supplemental data). The MF here cuts LGM glacial and post-glacial deposits related to Recessional phase 1 (Coronato et al., 2009) superimposed in some segments by recent alluvial deposits (Figure 3.2.b). A maximum age for these deposits is LGM deglaciation, which began shortly after 18 ka (Rabassa et al., 2000; McCulloch et al., 2005) and a minimum age of 13.4 ka is used, according for the basal peat bogs radiocarbon dating (Fig. 3.2; Coronato et al., 2009), whose deposition occurred after the area was free of ice. The offsets measured here combined with the available age data in the area provide Late-Quaternary slip-rates from 7.8 ± 1.3 mm/yr

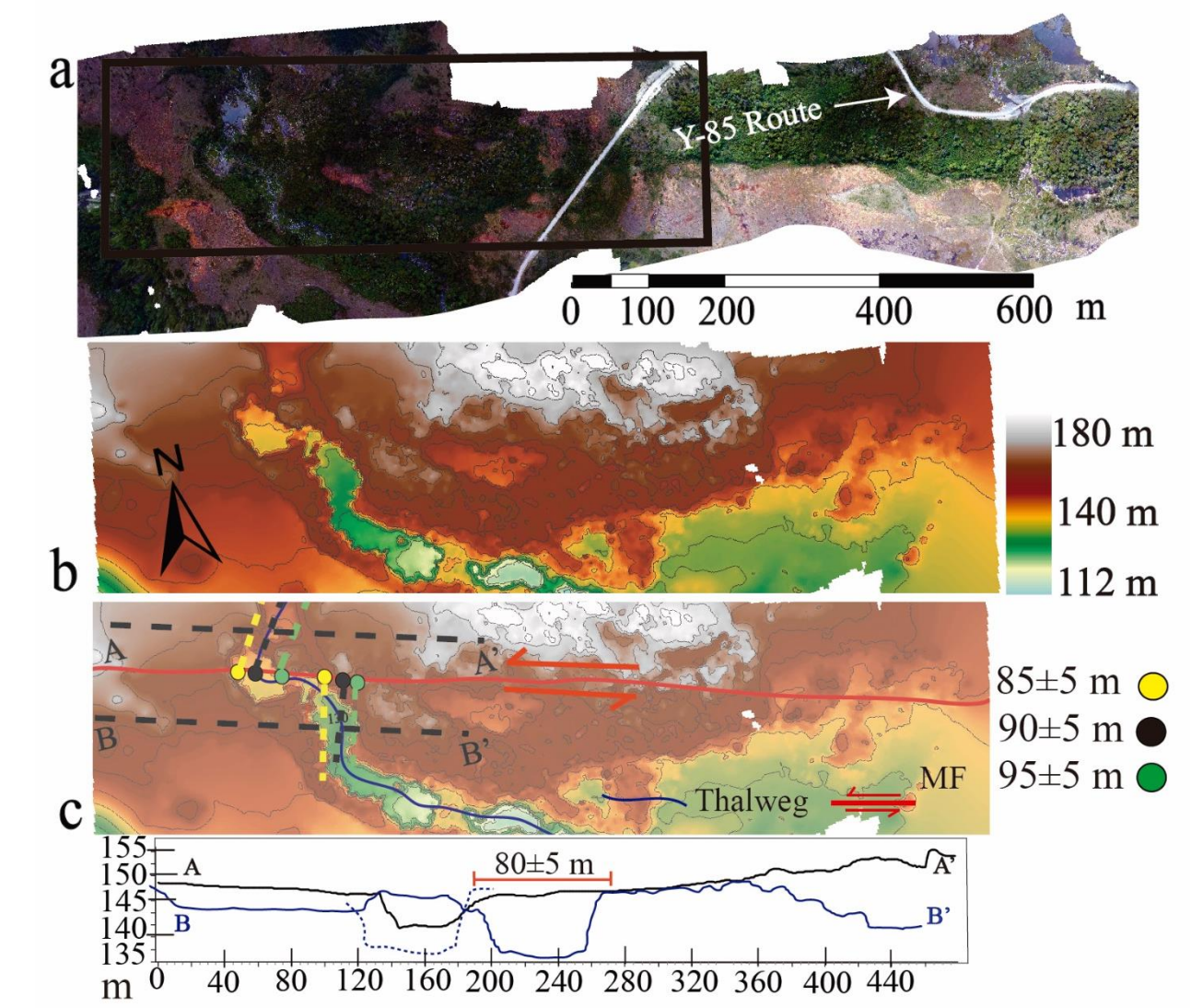

Figure 3.3: a) SfM Ortophoto near Mont Hope in Chile (Fig. 2.a). A 1-2 meters high fault scarp with its southern side dropped is observed east the road with peat bog deposits. Vegetation is aligned along the fault trace. b) High resolution SfM DEM for MF section without interpretation and c) with interpretations. The topographic profile shows the horizontal distance needed for back-slip the channel and glacial deposits north and south the fault trace. The displacement corresponds to the offsets measured in the western (yellow), eastern (green) and thalweg (black). White dotted lines represent the elevation profiles traceS A-A' and B-B'. 5 m contour interval.

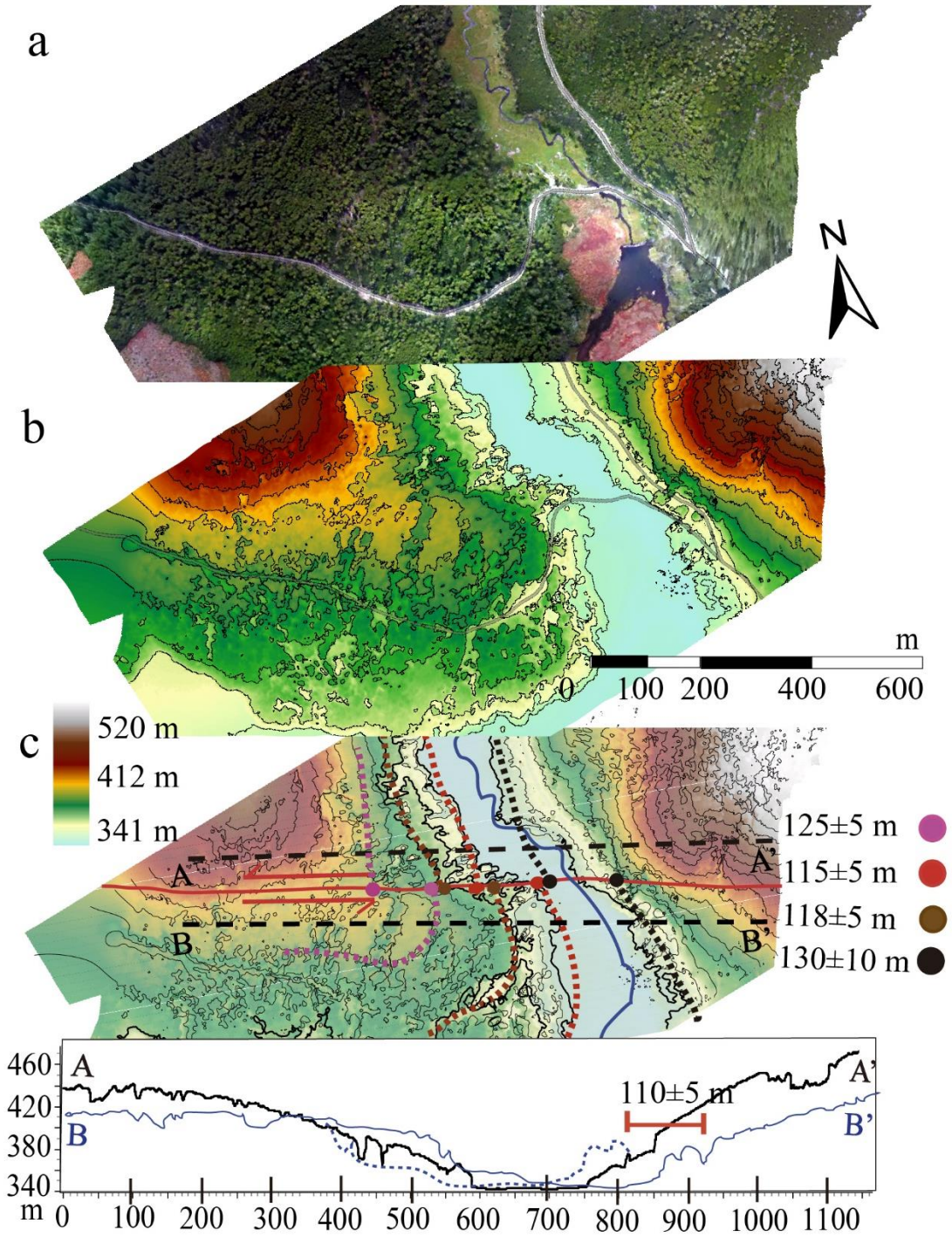

Figure 3.4: a) Ortophoto in MF section in the western arm of Lainez river in Argentina (for location see Figure 2.b), b) Key Slip rate Argentina, in a western arm of Lainez river cutting glacial and recent alluvial deposits c) High resolution DEM showing the left-lateral displaced channel, the offset can be observed both in recent alluvial and fluvio-glacial deposits. The profile shows the horizontal distance needed for back-slip the channel north and south the fault trace. The

displacement corresponds to the offsets measured in the 350 m (red and black), 380 m (brown) and 400 (pink) contours. White dotted lines represent the elevation profiles tracesa A-A' and B-B'. Green start indicates fault zone with parallel ridges and sag ponds (supplemental info). Yellow star is MFS trace cutting glaciofluvial deposits overlying till deposits. 5 meters contour intervals.

The plate boundary MFS, from Cabo Froward east is a classic, strike-slip crustal plate boundary, with localized deformation on sub-parallel crustal faults and an important source of seismic hazard (Fig. 3.1). Based on our first geologic quantification of slip-rates along the MFS, this plate boundary fault system has Late-Cenozoic slip-rates from5.8 ± 3.7 mm/yr. As slip-rates can change over long-time scales (Meade and Hager, 2005), future fieldwork and dating will better constrain timing of MFS initiation and thus the long-term slip rate. Late-Quaternary (Late-Pleistocene) strike-slip rates of 7.8 ± 1.1 mm/yr (Chile) and 7.8 ± 1.3 (Argentina) for the MFS main strand (MF). Fault planes and striations along the Deseado Fault (DF) ~15 km north Lake Fagnano (Klepeis, 1994), and there in the field, we found clear geomorphic evidence of recent tectonic activity including offset creeks, shutter ridges, and sag ponds (supplemental data) consistent with a slip rate of at least 1 mm/yr. Thus combining the slip rates of the three main known strands of the MFS, the MF, HF, DF at this location in Chile gives a combined strike-slip rate of at least 9.1 to 12.0 mm/yr. According to Smalley et al. (2003) based on GPS velocities and modeling, the faults mapped south the MF are not currently active. Geophysical models provide MFS slip rates that are within the same range however slower than the geologic rates we present here (6.6 ±1.3 mm/yr, Smalley et al., 2003; 7.0 ± 3.5 mm/yr, Thomas et al., 2003; 9.6 ± 1.4 mm/yr, De Mets et al., 2010). Our geologic rates are also support the NUVEL-1 model after De Mets et al., (1990), which suggested the MFS should accommodate a minimum of 40% of the rate of separation between South American and the Antarctic Peninsula (22 mm/yr). Nevertheless, the higher geologic rates versus the geodetic rates along the MFS could possibly be explained by the style of modelling and based on the thickness of the geodetic model

and recency of recent earthquakes (Tong et al., 2014). Although the location information for historical earthquakes has high uncertainties due to a sparse seismic network, recent historical events (Fig. 3.1; two Mw 7.5 events in 1949, Mw 7.0 in 1950, and Mw 7.2 in 1970) may have enough influence on the geodetic models to underestimate the motions here.

Since the MFS is fast slipping, and long-lived (since at least 6 Ma and up to 20 Ma), and apparently narrow, is it the narrowest of all strike slip plate boundaries? Low to moderate seismic events from adjacent to the MFS up to 30 km north the MF superimpose the contractional structures of the Magellan Fold and Thrust belt (Figure 3.1; Jaschek et al., 1982, Sabbione et al., 2007; Fosdick et al.,2005). According to Smalley et al., (2003) major faults mapped south the MFS at Lake Fagnano (e.g. Beagle Channel fault (Cunningham, 1993); Lasifashaj fault) are not currently active, however, based in our experience in New Zealand (e.g. De Pascale et al., 2016), generally along major plate boundaries deformation is partitioned along both sides of the master faults, and slower slipping faults should be expected. The area south of Lake Fangano is wilderness and poorly mapped and future work there may yield additional insight. Therefore, along TdF a total width of deformation along the MFS of 30-50 km would make it a candidate for one end member of plate tectonics, the narrowest strike slip plate boundary on Earth.

Compared with the width of surface deformation along other continental strike slip plate boundaries (e.g. North America/Pacific Plate along the San Andreas up to 200 km; the Marlborough Fault System in New Zealand up to 150 km), the main deformation in TdF is narrow, localized and straight, the MFS is a mature Plate boundary with minimal stepovers and thus consistent through-going large-magnitude earthquakes (Wesnousky, 1988). According to Stirling et al. (1996), the MFS well-developed geometry,

simplicity and remarkable lengths, could suggest a low ratio of small to large earthquakes due to smoothing along these faults and thus magnitude-frequency distributions derived from seismology may not reflect the actual seismic hazard along these faults. West of TdF, however, according to Betka et al. (2016) from work near Cabo Froward (Fig. 3.1), the MFS widens, forming a more diffusely distributed fault system partitioned onto splays increasingly further apart. These structures may correspond to reactivated faults within the pre-existing fold and thrust belt and would be localized along mechanical anisotropies defined by the structural trend of the orogen (Betka et al., 2016). However, from TdF and east, it appears that the MFS could be one of the narrowest and simplest transform (strike slip after Tuzo Wilson, 1965) plate boundaries on Earth.

CHAPTER 4: STUDY CASES

Chapter overview:

The next chapter presents the results obtained in this thesis work in an extended format, including detailed field observations and interpretation of the high resolution DEM's from Structure for Motion technique and derivatives. Portions of this chapter are included in the supplemental data for the submitted manuscript. The results are divided across the two study areas, the first is located in the Chilean portion of TdF Island, Southern Patagonia, from the western portion of Fagnano Lake until the Almirantazgo fjord. The second area is in the Argentinean portion of the Island, where a rectilinear path was followed between the easternmost shore of Fagnano Lake south the city of Tolhuín until approximately 30 km at east.

Before making observations on a local, site-specific scale, first order left-lateral geological separations were observed using regional mapping along the MFS onshore trace in TdF Island and the along the sub-aquatic trace in the Fuegian Fjords (Sernageomin, 2003). The Devonic-Carboniferous metamorphic unit in the highest peaks of the Fueguian Andes is separated along the MFS trace in 40 ± 5 km along Cabo Froward (Figure 3.1). Additionally, in the Argentine part of Isla Grande, the contact between the Upper Jurassic-Lower Cretaceous Beauvoir Formation (Olivero & Martinioni, 2001) and the Upper Cretaceous Cerro Martero-Policarpo Formation (Olivero & Malumián, 1999) have a geologic separation of 50 ± 5 km north and south the fault in the northeastern portion of Fagnano Lake. Finally, the upper limit of the last one is also displaced in 60 ± 5 km (Figure 3.1). An uncertainty of 5 km was given to each estimation in the horizontal plane, considering the error in the regional scale of the mapping given by the geographic

reference and the errors due to digital mapping. These observations allow us to made first order estimation of long-term slip-rates from 2.1 to 8.7 mm/yr of the Magallanes-Fagnano fault system, considering as a range the ages proposed for the beginning of the MFS activity. At 20 Ma, a change in the motion to an E-W direction lead to the initiation of spreading at the East Scotia ridge and an important drop in the spreading rates om the western Scotia ridge (Lagabrielle et al., 2009). Moreover, the MFS-NSR transform system development may have occurred much later, in the Late Miocene (6.6 to 5.9 Ma; Lodolo et al., 2003; Eagles et al., 2005; Lagabrielle et al., 2009; Betka et al., 2016), coeval to the cessation of western Scotia seafloor spreading and a significant increase in the Sandwich ridge activity (Lodolo et al., 2003; Eagles et al., 2005; Livermore et al., 2005). This period is also coeval with uplift and exhumation in the eastern domain of Patagonian fold and thrust belt (Fosdick et al., 2013).

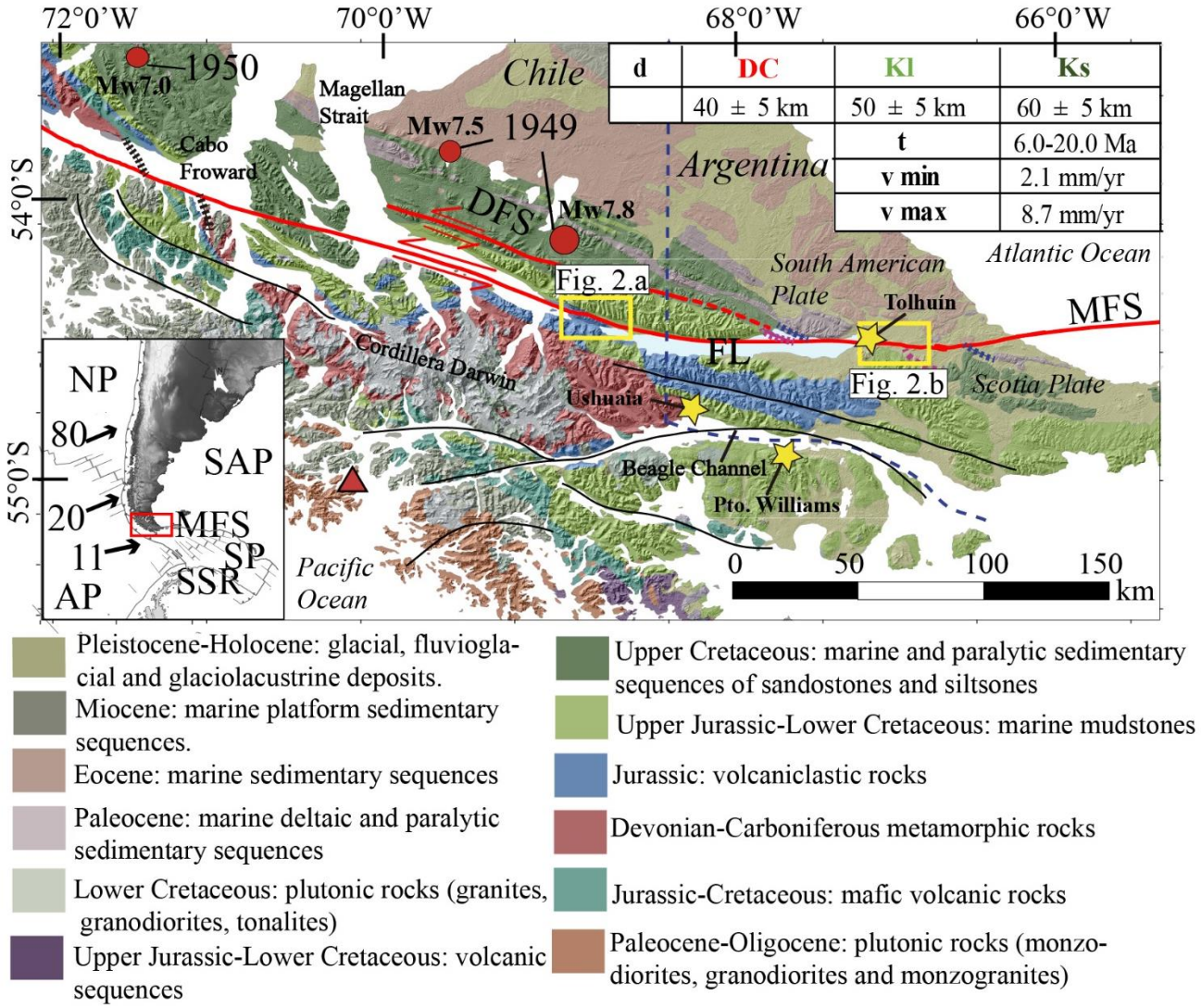

Figure 4.1 Geological map of the Southern Patagonia region (modified from Sernageomin, 2003; Olivero & Martinioni, 2001; Klepeis, 1994). Table indicates Late-Cenozoic MFS slip-rates based on a mean of the plausible sinistral separation of the Devonian-Carboniferous metamorphic unit (DC, red), Upper Jurassic-Lower Cretaceous marine sequences unit (Kl, light green) and Upper Cretaceous marine sedimentary sequences (Ks, dark green) and proposed ages for the beginning of activity (20.0 to 6.0 Ma; Eagles et al., 2005). Dotted lines are the projection of the contacts to the MFS. Yellow boxes are field study areas. Red circles indicate historical epicenters (Jaschek et al., 1982). MFS: Magallanes-Fagnano Fault System, DFS: Deseado Fault System, FL: Fagnano Lake, NP: Nazca Plate, SAP: South American Plate, AP: Antarctic Plate, SP: Scotia Plate.Red triangle indicates Cook Quaternary Volcano. Blue dotted line indicates international border. Black solid lines indicate

lineaments possible related to tectonic activity (Lodolo et al., 2003; Sue & Ghiglione, 2006). Plate velocities are from Pelayo & Weins (1989) and DeMets (1990).

To obtain the long-term (Late Pleistoscene) slip-rates based directly on the geological record, SfM- high resolution DEM's (2 to <1 m/pixel resolution) and derivatives were obtained in a Chilean and Argentine portion of the MFS main onshore trace in the previously chosen sites. These displacements are interpreted as the cumulative offsets of successive earthquakes since the Upper Paleocene (Rabassa et al., 2000; Coronato et al., 2009), which together with the correlation with available age data of previous authors allowed the geological slip-rate estimations for both sections. The sites were chosen between other more marker prospects in sites along the fault after stablish a causal relationship between the displaced geomorphic features and the fault slip by a confidence estimation for the offset (McGuill & Sieh., 1991; Cowgill et al 2007; Zielke et al., 2015), which depends on the quality and reliability of the individual slip measurements, taking into account the angle of the landform with the fault trace and the width and definition of the fault zone, besides the grade of preservation estimated for a specific marker (A,B and C for high, medium and low reliability, respectively; McGuill & Sieh, 1991). Only the landforms with category A and B were chosen for the photo acquisition and post-processing. Later, a minimum and maximum values for the offset measured in each marker was established to quantify the range of values that probably restored the original morphology in that specific site, this value is related to the DEM resolution (1-2 m/pix) used for mapping and the reliability in the reconstruction of the geometry of the markers before to modifications by erosional and depositional process (Cowgill et al., 2007).

4.1 Chilean Slip sites: Mount Hope area and Azopardo valley

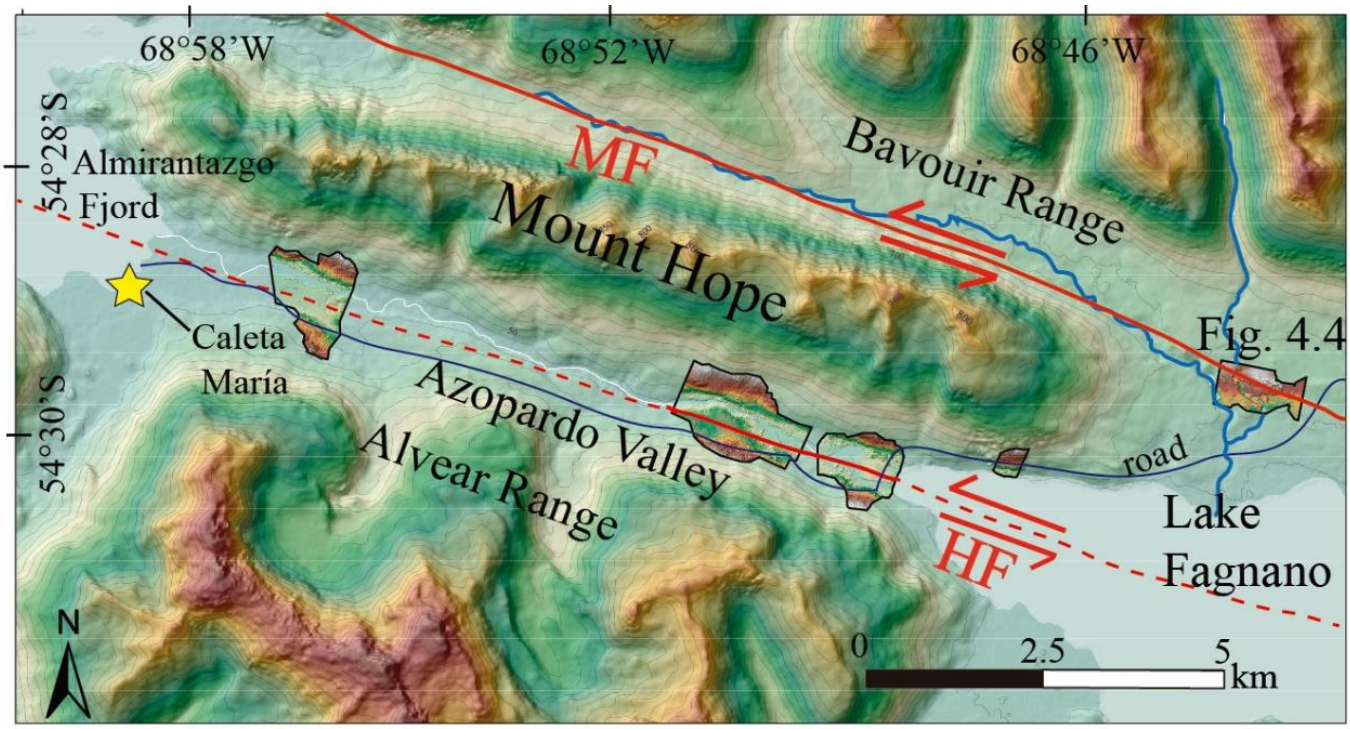

Figure 4.2: Study area in Chilean portion of TdF Island. Black boxes indicate the locations of the five high resolution DEM obtained in the MFS area, which has been associated to the 3rd recessional phase after the LGM. MFS: Magallanes-Fagnano principal fault. AF: Azopardo fault. Red solid lines indicate observed fault location either in satellite imagery or in the field. Dotted red lines indicate location of inferred faults. 50 m contour interval.

The study area in Chilean side of TdF Island comprises from the eastern portion of Fagnano Lake valley until the shore of the Almirantazgo Fjord (Figure 4.2). Valleys morphologies in this area are largely as result of glacial processes with later modifications of alluvial and landslide process (Coronato et al., 2009; Rabassa et al., 2011). The deposits observed in the sides of the road presents between 70-80% of matrix of clay to coarse sand and ~20-30% of polymictic clasts between 2 and 20 cm, interpreted as result of glacial process, combined with abundant peat deposits that cover a large part of the areas in the

northwestern shore of the lake and in the valleys north and south Mount Hope (Figure 4.2), an NW/SE trending Jurassic ridge of volcanoclastic rocks (Tobífera formation, Caminos et., 1981; Winslow., 1982) bounded by the Azopardo river valley on the south (Figure 4.2.a) and by a narrow valley covered by sag ponds infill with peat and alluvial deposits on the north. Intercalations and lenses of 10 to 30 cm of dark brown and dark grey clay and peat are present, probably related to glaciolacustrine environments. Moreover, alluvial deposits are restricted to the valleys and ravines, while landslides and gravitational deposits cover a big part of the slope ranges (Figure 4.2.a; Mount hope to center and Beauvoir and Alvear range at north and south respectively).

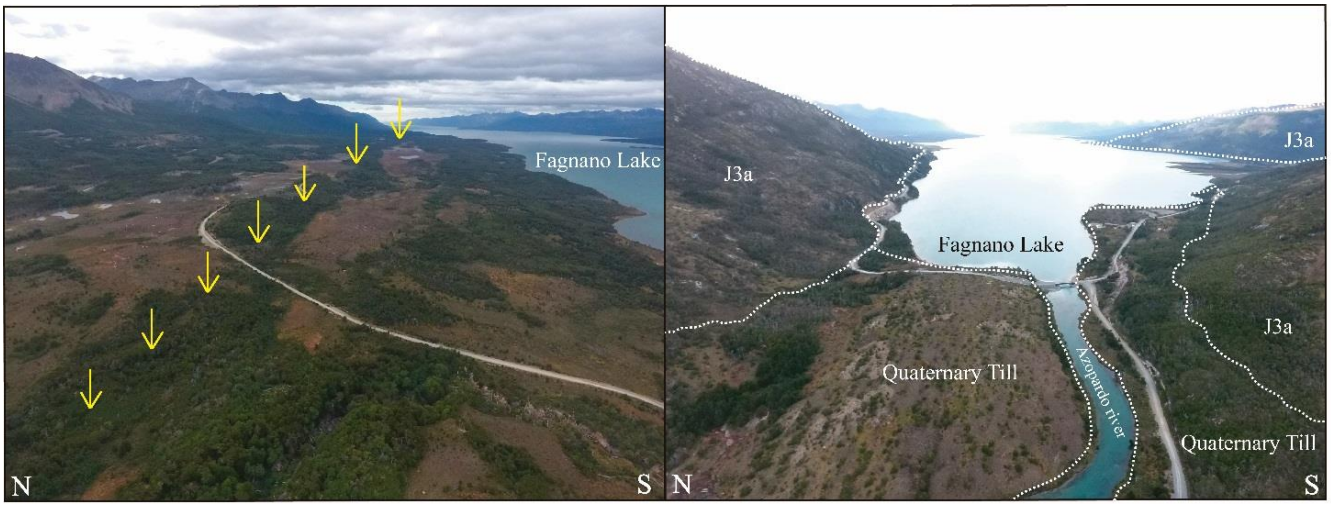

Figure 4.3: a) Aerial drone photography of the northeastern shore of the lake crossed by the Y-85 Route, yellow arrows indicate the main MFS fault trace in this area in glacial, postglacial and peat bog deposits. b) View to the east in Azopardo valley, bounded on the north and south by Jurassic volcaniclastic rocks of the Beauvoir fm. (Caminos et al., 1981), a lobular till deposit entrenched to the south by the Azopardo river is cut and left-lateral offset by the Azopardo fault.

The MFS main and current active fault (MF) in this portion goes onshore from the western boundary of Isla del Fuego along the northern slope of Mount Hope through east along the northwestern shore of Lake Fagnano (Figure 4.3). In this shore, the trace of the fault is a well-defined-single rectilinear ~N70°E strand with clear evidence of Late Quaternary surface rupture and cut peat deposits covering moraine deposits with elongated morphologies parallel to the lake shore (Coronato et al., 2009; Waldman et al., 2010a). The fault here is expressed by a south-facing scarp of about 5 m high delineated mainly by vegetation and peat in the southern dropped side (Figure 4.3.a, Figure 4.4). In the northwestern and southeastern shore of the lake, elongated strips of undifferentiated till in remnants moraines were correlated by Coronato et al., (2009) with the third Recessional phase or Latest Late glacial, suggested as the last depositional stage of the Fagnano paleo-glacier before its definitive recession, once its edge reached the Azopardo valley. Although no absolutes ages exist for this deposit, an age of 12.5 to 11.7 ka age was proposed in the central-western portion of Lake Fagnano by Coronato et al., (200), by comparing this phase with "Stage E" in the Bahía Inútil model (McCulloch et al., 2005). Furthermore, Waldmann et al., (2010a) based on seismic data and lithological and chronological analyses from a core in the western sub-basin identified a series of terminal moraines formed during a series of repeated glacier advances and westward net retreat. An age for a submerged moraine structure in the westernmost part of the western sub-basin was suggested by correlating the moraine depth with a guide level in the core at east and estimating a sedimentation rate for the sedimentary package constrained between an upper tephra level with known age and this guide level. The more reasonable sedimentation rate was estimated of 1 mm/yr by comparing other rates calculated for other similar lacustrine settings and proglacial environments elsewhere, suggesting a most probable age of ~11,170 cal yrs BP, coinciding with the Younger Dryas chronozone (YR, 12.800-11.5). Subsequently, a maximum age of 12.5 ka is considered for the undifferentiated till along the northwestern shore, due to its location with respect to the boundary from the last re-advance and stillstand of the

Fagnano paleoglacier before its definitive recession through the Azopardo valley. Furthermore, a 10.2 kyr are proposed by several authors as a definitive deglaciation for the Southern Patagonia region (Rabassa et al., 2000; McCulloch et al., 2005). This stage is characterized in the Lake Fagnano area by a complete retreat of the ice from the basin, followed by a drainage switch of the lake and a concurrent lake lever lowering (Waldmann et al., 2010a). Indeed, the age obtained in a sediment core in Seno Almirantazgo indicated that the deglaciation here occurred prior to 14.300 cal yr BP and became a predominantly saline fjord environment with near-modern oceanographic conditions by 9800 cal yr BP, as indicated by an increase in the alkenone and organic carbon of margin origin content, which is well correlated with the Holocene sea level rise (Bertrand et al., 2017).

A channel on a creek 450 meters to the left of the road is left-lateral displaced by the main fault trace (Figure 4.4.a, Site 1 in Table 4.1). As observed in the field and in satellite images, the channel follows a general NW/SE trend and its boundaries are mostly covered by vegetation, nevertheless in the DEM a stepped trend in the channel by the fault strike slip is noted (Figure 4.4.b). Offsets were measured in each side of the creek and in the thalweg of the channel by projecting them into the fault trace, additionally, parallel elevation profiles were made to the north and south the fault trace, and the northern and southern river channel profile were back-slipped with respect to one another to determinate the optimal offset estimate (Figure 4.4.b; Table 4.1). Due to the left-lateral displacement of the fault the western wall of the southward flowing channel is more prone to fluvial erosion because the south segment was faulted into the active channel (McGill & Sieh., 1991, Cowgill et al., 2007). Thus, the actual eastern limit is considered to better represent the total offset of the river and the projection of the three markers and the retro-deformation of the channel were estimated by considering this erosion process (Figure 4.4.b). Offset were measured several times in each of the three markers, obtaining a range of plausible values considering its

definition and geometric properties (Figure 4.4.b). With the bounding values, the arithmetic mean and standar deviation was calculated (Table 4.1). These observations together with the previous estimated ages allow us to estimate geological slip rates of 6.7 to 8.9 mm/yr in this segment of the MFS (Table 4.1, Ludwig, 2013).

Table 4.1: Offset measurement synthesis for site 1, located in the northwestern shore of Lake Fagnano, Chile (Figure 3.4).

Chile- Site 1	**Projection 1**	**Projection 2**	**Projection 3**	**Profile**
Confidence degree	A	A	B	A
Offset (m)	95 ± 5	85 ±5	90 ± 5	80± 5
Geomorphological marker description	Right limit of the channel (Figure 3.4.b)	Left limit of the river (Figure 3.4.b)	Thalweg of the channel (Figure 3.4.b)	River channel back-slip
Age max 12.5 ka				
Age max 10.2 ka				
Arithmetic mean (μ)±Standard deviation (σ) **7.8±1.1 mm/yr**				
Slip-rate 6.7 to 8.9 mm/yr				

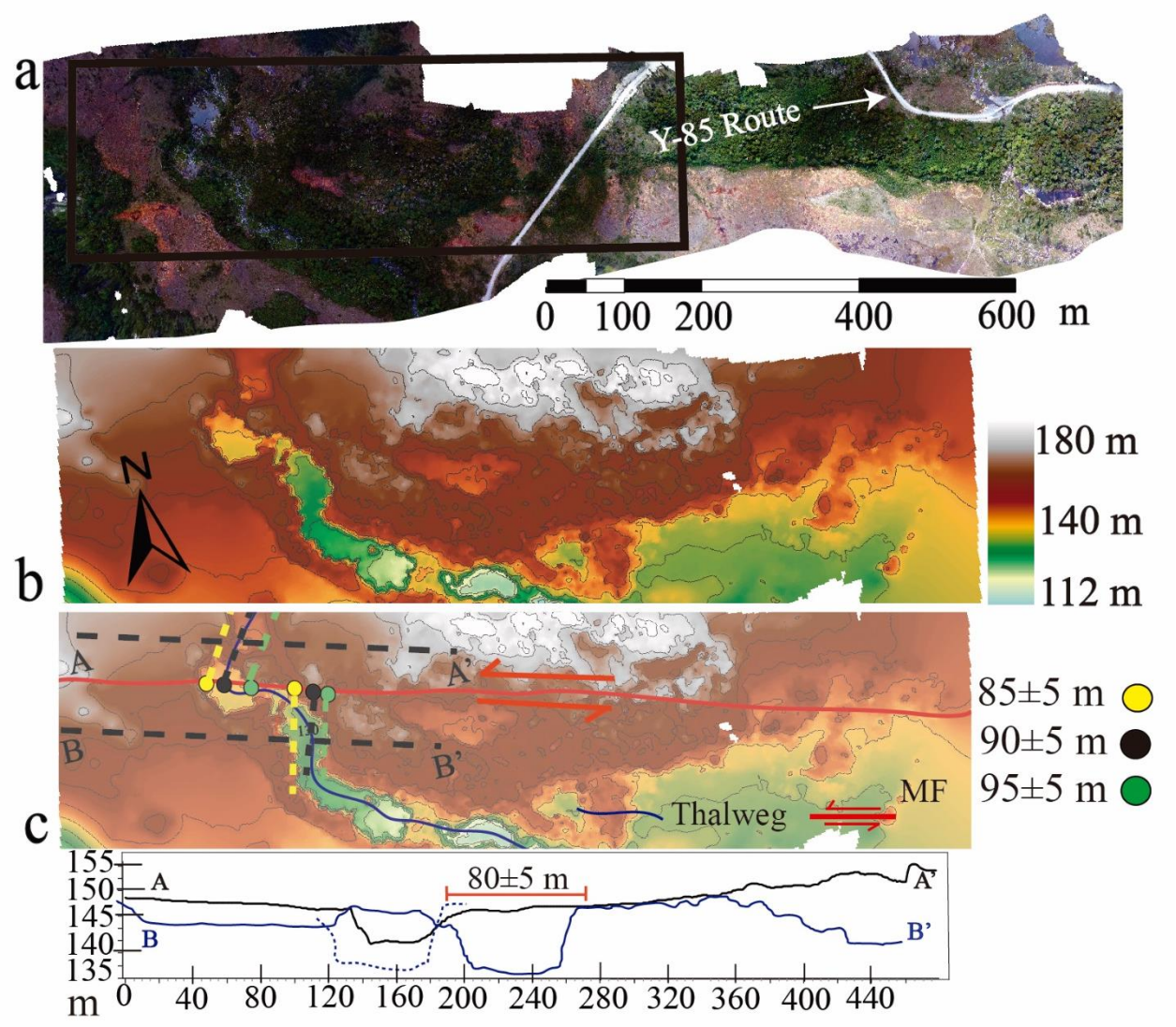

Figure 4.4: a) Slip rate estimation site in Chile, a left-lateral displaced channel can be observed (see Figure 2.a for location). A 5-7 meters high fault scarp with its southern side dropped is observed east the road with peat bog deposits. Vegetation is aligned in the fault trace b) High resolution DEM with the measured displacements along the river boundaries and thalweg of the channel. The profile shows the horizontal distance need for back-slip the channel north and south the fault trace. 5 meters contour interval.

South of the MFS main fault, the southeastern portion of Mount Hope presents a high grade of fragile deformation with different scales N-S, NNE-SW, NE-SW oblique extensional faulting noticeable next

the road along the northwestern shore of Lake Fagnano, conforming a faulted area of ~5 km of extension along the southern slope of Mount Hope (See Annexed I). I observed a fault in an N-S trending and ~ 5 m width fracture in the slope cutting the volcanoclastic rocks. A ~100 m width damaged area around this fracture is marked by a high grade of fracturing and a pervasive light-colored hydrothermal alteration. The block east is topographically higher than the block at west, and apparently the fault splays in two faults which continue to the north (See Annexed I). Inside of the cave the original volcanoclastic rock has turned totally brecciated and is crossed by abundant quartz veins, at least 3 fault planes ~N-S and ~70°-80°SW dipping is observed according to the presence of slickensides and cemented and uncemented fault rocks. Sub-vertical parallel striations were observed in the fault planes indicating an extensional component for most of these structures.

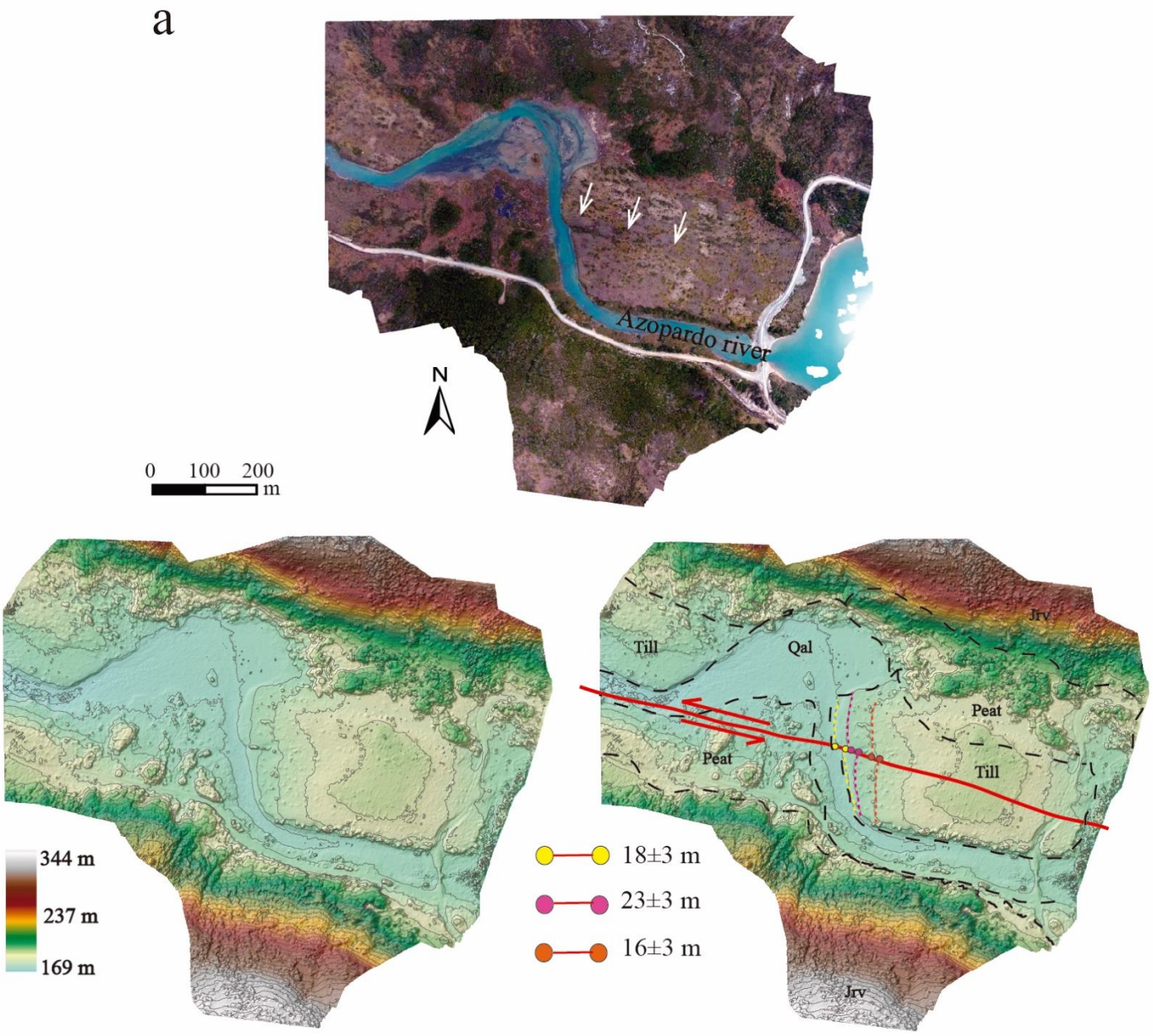
a
Azopardo river
N
0 100 200
m
344 m
237 m
169 m
Till
Qal
Jrv
Peat
Peat
Till
Jrv
18±3 m
23±3 m
16±3 m

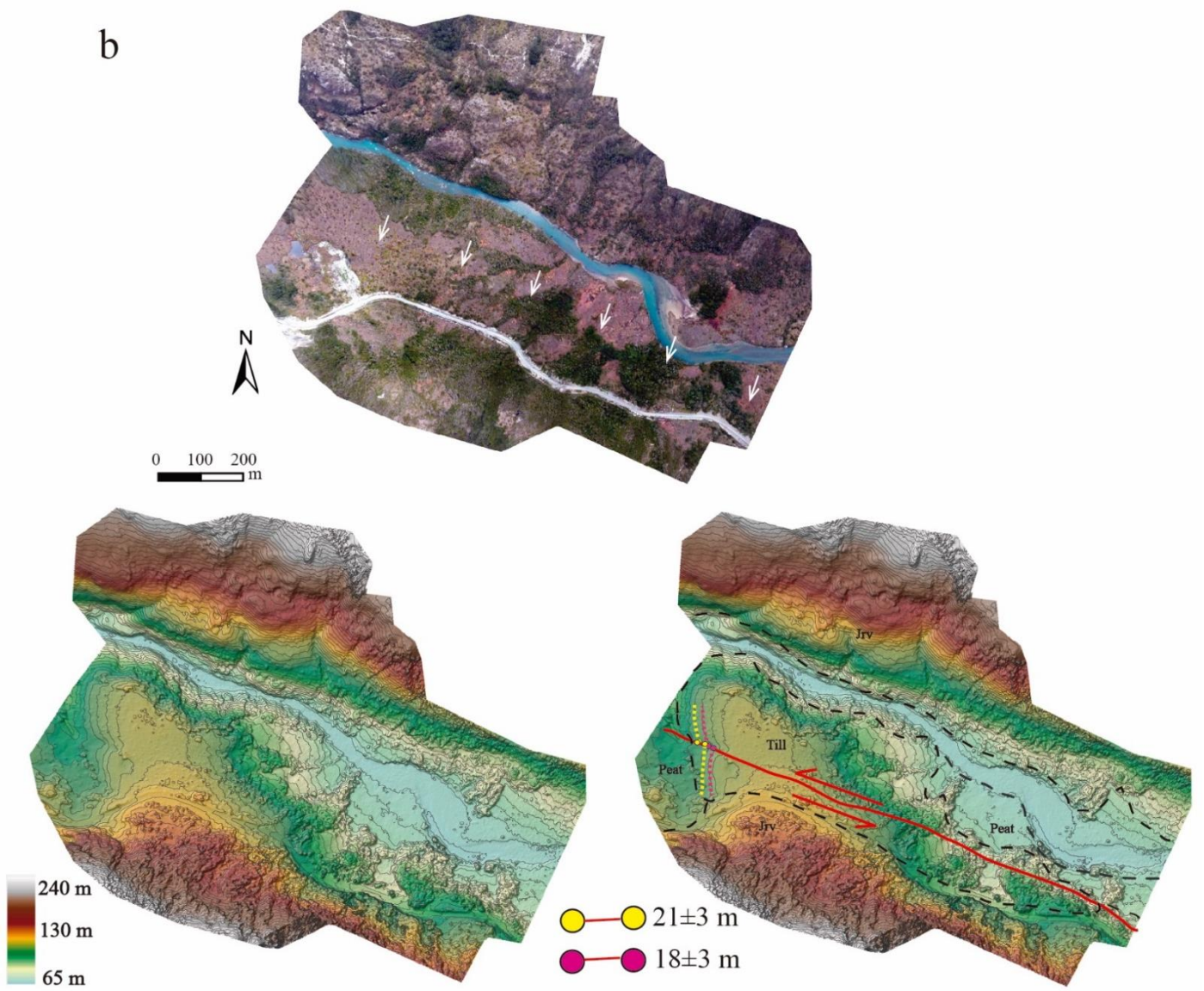
b
N
0 100 200
m
240 m
130 m
65 m
Jrv
Till
Peat
Jrv
Peat
21±3 m
18±3 m

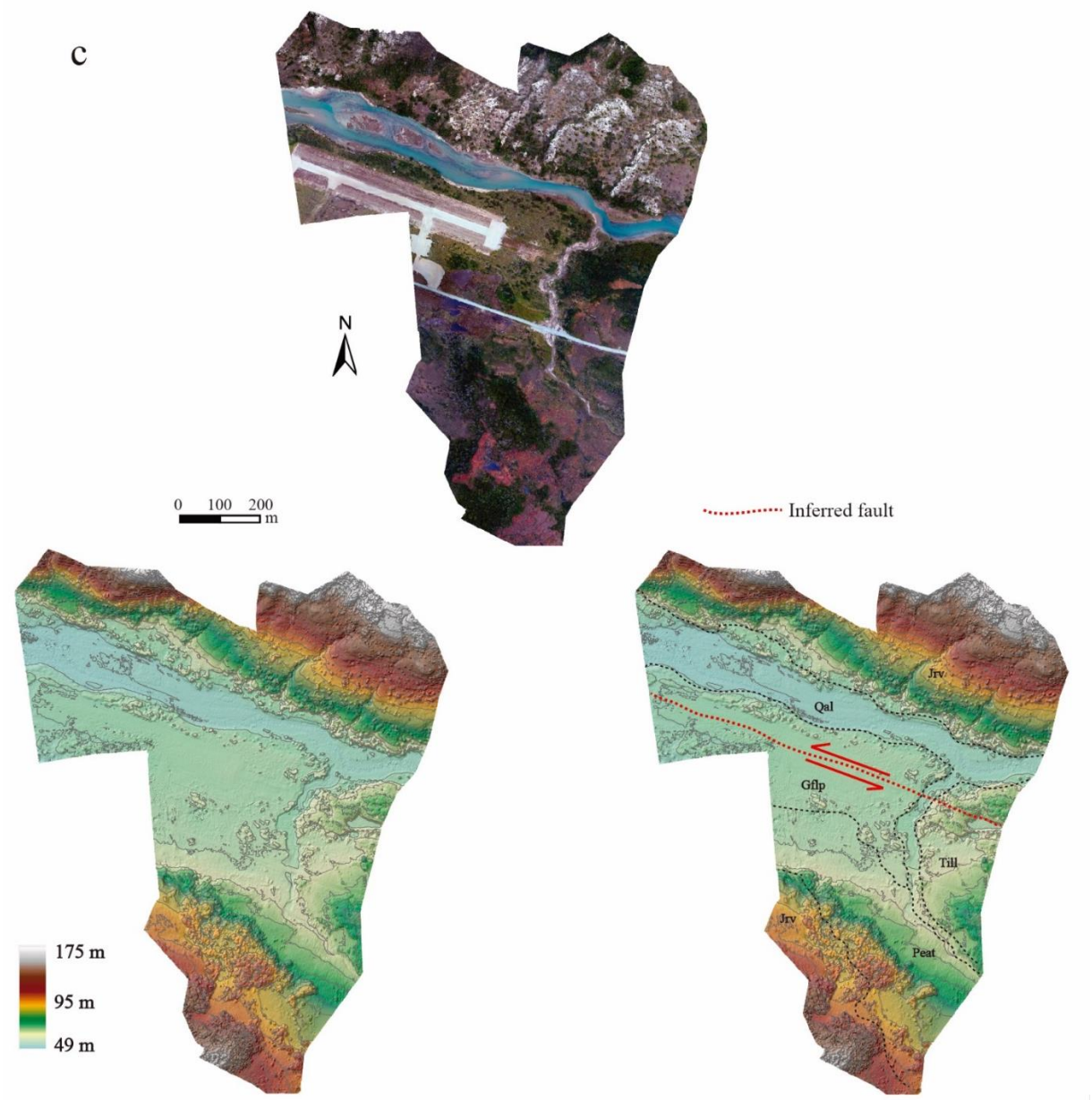

Figure 4.5: a) Azopardo fault in the eastern portion of Azopardo valley, Chile. The fault trace cut a till deposit west Fagnano Lake. b) Azopardo fault rupture continuation at west, in the ortophoto the fault trace is delineated by vegetation and left-lateral offset a glacial deposit. c) Western models in Azopardo valley, the fault rupture is not observed, probably because it is covered by peat, and recent deposits with plain morphology. The fault trace would continue parallel to the airstrip in Caleta María area. For figures locations see Figure 4.2. Qal: recent alluvial deposits, Till: undifferentiated till, Jrv: Jurassic volcaniclastic rocks from Lemaire fm. (Caminos, 1981), Qflp:

Quaternary glaciofluvial plain. Solid red lines indicate the fault trace observed along the valley. Dotted red line indicates the inferred fault continuation at west. 5 meters contours interval.

Immediately west Lago Fagnano, another fault trace is observed along the Azopardo River valley (Figure 4.2). This structure was previously defined as the Hope fault by previous works (HF, Menichetti et al., 2008; Damian Esteban et al., 2014; Zanolla et al., 2017), although no slip-rate or fault length have been proposed. The fault has an onshore length of 11 km from the easternmost portion of the lake until de Caleta María Bay. Three high resolution DEM were obtained by SfM with a total length of about 4 km in the eastern, central-eastern, and western section of the valley (Figure 4.2). A portion of about 200 m of the fault trace was identified in the ortophotos and contour maps in the two eastern models (Table 4.1), with two left-lateral offset till deposits south the river that were used for estimating the fault slip-rate since the deposition of these sediments (Figure 4.6.a, b, Table 4.2). In the western model, the rupture trace is observed in the lobed shaped deposit next to the lake coast, but is mostly overlaid by peat deposit and vegetation (Figure 4.6.a), nonetheless, an small south-facing scarp of <1 m with a left-lateral offsets of 16 ± 3 m to 23 ± 3 was identified on the DEM-derived maps (Figure 4.5.a). In the model at west, the fault trace is delineated by vegetation where is not covered by peat, and others left-lateral offset of 18 ± 3 and 21 ± 3 were measured in an elongated till deposit (Figure 4.5.b). At west, the trace is unclear or totally covered by vegetation and peat, and in the area next to bay in the western model, is overcast by a plain which covers the base of the valley (Figure 4.6), This plain, which reaches the 10-12 meters high, is observed in the bays north and south of Mount Hope, suggesting that could be related to the sea level rises during the Holocene due to glacio-isostatic rebound proposed by some authors in the Lago Fagnano basin and in the Azopardo valley area. (Lodolo et al., 2007; Bertrand et al., 2017; Waldmann et al., 2010a), or could be related with flooding plains of the river channel flowing west triggered by the planar topography in the western portion of this valleys. Anyway, these flat deposits are probably younger and overlaps the

glacial deposits leaved by the paleo-lobe recession at east. In the slope of the southern ridge next to the shore bay, striations and a possible recent fault scarp with a rockslide deposits triggered by the MFS activity could take place, specifically associated to the 7.8 Ms 1949 event (Klepeis, 1994). Nonetheless, there is limited evidence of surface rupture, scarps or lineaments east or west the supposed fault scarp neither in the field, drone photos nor satellite imagery.

These data together with available age estimations for the glacial deposits in the Azopardo valley, which are considered to be the same range as east, suggests a slip-rate of 1.3 to 2.1 mm/a for the HF (Ludwig,2013), considerably lower than its parallel trend at north. Compared with the fault trace observed east Mount Hope, where the fault slip measured is higher and the scarp expression is clearer, the Hope fault would not exert a predominant structural control during the Holocene after the deposition of the plain.

A closure criterion for the slip sites 1 (MF) and 2 (HF) was used assuming that the fault traces north and south of Mount Hope in Chile are parallel and that the sum of the slip-rates on this parallel strand should approximately match the overall slip-rate. According to this, the overall displacement in this area associated with the current observed MFS active structures in this western portion of TdF Island is around 8.1 and 11.0 mm/yr.

Table 4.2: Offset measurement synthesis for site 2 in Chile.

Chile- Site 2	**Projection 1**	**Projection 2**	**Projection 3**	**Projection 4**
Confidence degree	A	A	A	A
Offset (m)	18 ± 2	23 ± 2	16 ± 3	21 ± 3
Geomorphological marker description	180 Contour, in glacial deposit next the lake (Figure 3.5.a	185 Contour, in glacial deposit next the lake (Figure 3.5.a	112 Contour, in glacial deposit in the central eastern portion of the valley (Figure (Figure 3.5.b)	112 Contour, in glacial deposit in the central eastern portion of the valley (Figure 3.5.b)
Age min **10 ka**				
Age max **12,5 ka**				
Arithmetic mean (μ)±Standard deviation (σ) **1.7±0.4 mm/yr**				
Slip-rate for site 2 **1.3 to 2.1 mm/yr**				

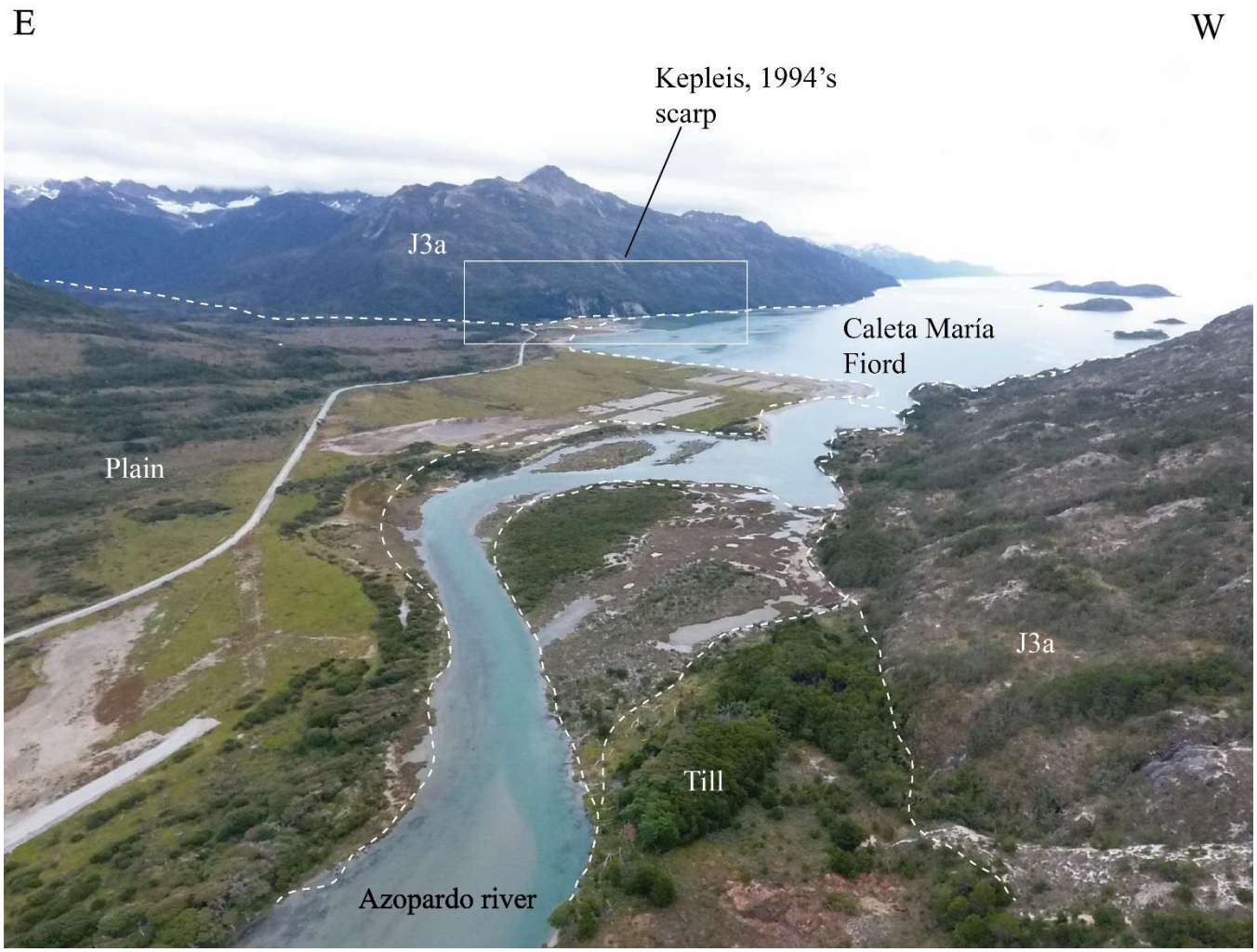

Figure 4.6: Drone photograph looking. Southwest view of Azopardo valley at Caleta María, Chile. Glaciofluvial cover the western portion of Azopardo valley showing a planar morphology.

4.2 Chilean slip sites: Deseado lake zone

Klepleis (1994) defined a fault zone of about 3.5 km wide located along the Deseado valley, about 14 km north of the Fagnano Lake in the external portion of the Magallanes Fold and Thrust belt (MFTB). The fault system crosses parallel to the MFTB and extends for ~150 kilometers divided in at least three fault segments with an NWW/SEE strike crossing the center portion of TdF (Figure 4.1). A central trace of about 35 kilometers long is located along the Lago Deseado valley, a glacial ~E-W trending valley whose bottom is mostly cover by peat and recent alluvial deposit in its western portion and by the Lake Deseado in its eastern portion. Till deposits cover the piedmont of the mountain chains north and south the valley, with alluvial fan deposits in the gorges and rockslide deposits in areas of steeper slope (Figure 7.1). The southern ridge reaches more than 1000 meters and corresponds to Lower Cretaceous marine mudstones of the Yaghan Formation (Caminos, 1981), while the northern ridge is about 200 meters lower and it's formed by Upper Cretaceous marine sandstones and siltstones (Klepeis. 1994).

The main fault trace leaves the lake to the west by its northern boundary and it is located approximately in the course with the road in the northern ridge (Figure 7.1). The outcrops both north and south the valley present high grade of fragile deformation associated with the MFTB in the Late Cretaceous times and with a most recent fracturing and sliding. A damaged area of about 20 meters wide can be observed next to the road in the northern ridge of the valley with a clear change in the grade and dip of the fracturing respect to the surrounding less damaged outcrops. A fractured zone with a stratification of ~228/50 is cut by a pervasive and more vertical fracturing of ~285/85 (Figure 7.2).

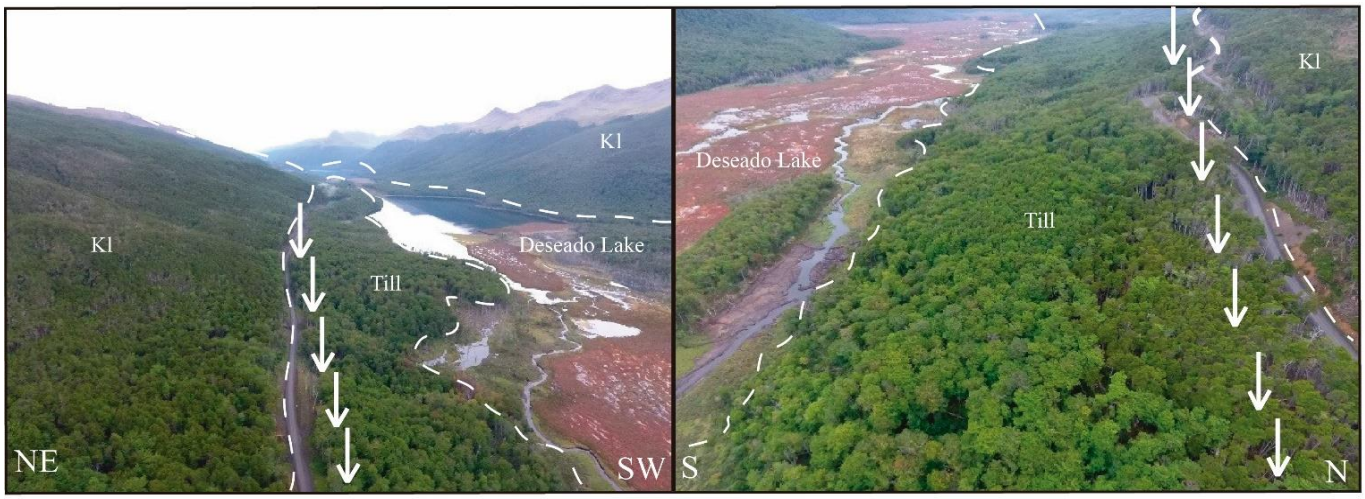

Figure 4.7: Deseado principal fault along the northern slope of Lago deseado valley, cutting Upper Cretaceous mudstones of Beavouir Formation.

Moreover, a series of geomorphological evidence of recent activity are present in the Quaternary deposits along this area. In the western part of the valley, a series of sag pond of about one kilometer long covered by water, peat and alluvial deposits are present in the valley floor (Figure 7.1). Vegetation truncated by the fault activity can be observed parallel to the valley's limits. Also, next to the road, an uphill fault scarp in alluvial deposits of about 3 to 5 meters high was observed with an approximately east-west orientation (Figure 7.3).

Figure 4.8: Deseado main fault cutting marine mudstones of the Upper Cretaceous Beavouir Formation.

Klepeis., (1994) realize a structural analysis along a 10 km wide zone affected by secondary strike- slip faulting located north of the Deseado valley. The author defined two series of strike-slip fault populations cutting the previous thrust faults, folds and steeply dipping strata of the MFTB. The structural data collected by Klepeis., (1994), reflects a Riedel shear-type geometry for the entire fault zone. These results suggest that the Deseado fault zone corresponds to a left-lateral system with a normal motion component. Nevertheless, the length and orientation of the overall slip vector for the fault system is unknown, since the generation of a single plane solutions using a moment tensor sum for all the known faults in the fault system is not possible because of the lack of enough structural data related to the main fault trace and other parallel faults within the valley (Klepeis., 1994).

Figure 4.9: Uphill fault scap in the Deseado fault zone.

4.3. Argentine Slip site: The Rio Turbio and the Rio Lainez area

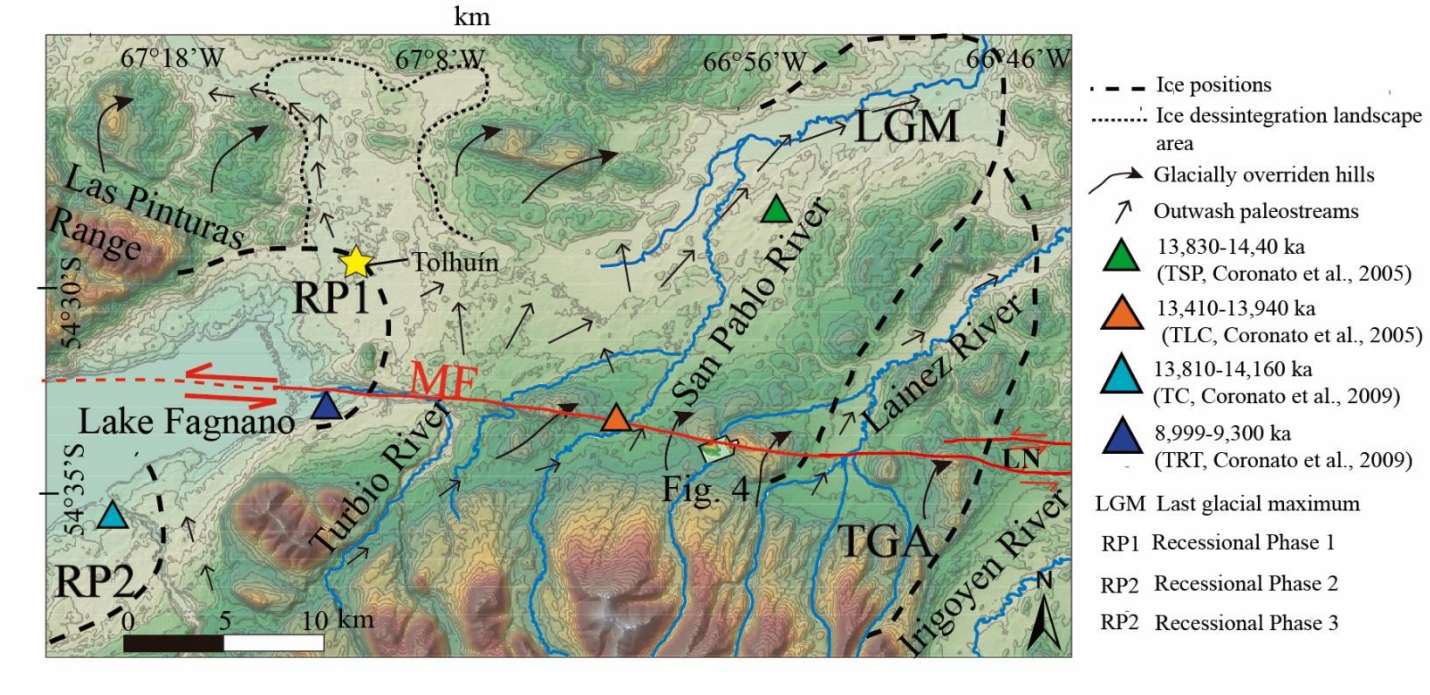

Figure 4.10: Study area in Argentina, TdF. Red line indicated locations of the Las Pinturas- Río Lainez fault segment, corresponding to the MFS main active fault during Holocene times in the central-eastern portion of TdF, Argentina, LN: Laguna Negra bog. Recessional Phases limits, landscape area positions and ice flow direction are from Coronato et al., (2009). Colored triangles indicate the locations for radiocarbon dating of basal peat bog in the area. Dotted square indicates additional offset measurements site with a 12.5 m resolution DEM (Annexed III). 50 meters contour interval.

In Argentine side of TdF Island, from the eastern shore of Fagnano Lake until the Atlantic coast, the geomorphological evidence of the MFS main trace it is much better delineated in the field and aerial images than west, which has allowed the identification of a relatively smooth and continuous well-defined fault trace with small and local scale step-over and bends geometries (Figure 4.10). These structures cut glacial and post-glacial deposits associated to the Last Glacial Maximum and the subsequent Earliest Late

Glacial or Recessional phase 1 (a.k.a Tolhuin Recessional Phase RPT), superimposed in some segments by recent alluvial deposits of the four main rivers in this area (from east to west the Irigoyen River, Lainez River, San Pablo river and Turbio river).

In the western Lake Fagnano, the MFS correspond to ~65 km length continue segment goes from the lake from the Claro river valley area to the Lainez river area in the argentine portion of TdF. As the fault zone reported by Waldmann et al., (2011) in the center of a seismic profile at the lake central sub-basin it is not evident on the seismic profiles on the eastern sub-basin in Argentina, the master fault is probably goes through the northern shore of the lake and the southern slope of Las Pinturas range (Figure 3.2.b), as a continuations o maybe forming a small scale (< 2 km) step over with the MF in Chile. Along the onshore segment southern facing scarps from 3 to 15 m were observed in glacial and glaciofluvial deposits intercalated with loess and glaciolacustrine deposits. Both downhill and uphill facing scarps were identified depending on the slope orientation. Two high resolution DEMS and ortophotos were obtained in the western and eastern portion of Río Turbio area by Structure for Motion method (Figure 4.10). South Tolhuín, the trace rupture from the 1949 earthquake is observed the 0.5 to 1 m high quite degraded scarp, which was previously reported by Costa et al., (2006) in unconsolidated gravels paleo-shorelines of the Lake. (Figure 4.11). Moreover, where Turbio river changes its trend from ~E-W to ~N-S, a 30 meters high shutter ridge was observed in the field going parallel to a downhill fault scarp of 5 to 8 meters (Figure 4.12.b). Nevertheless, no reliable markers or clear fault traces were observed in neither of the two models due to the large amount of Lenga trees cover both in bent and upright positions, the fault location is constrained only by field observations, thus other methods in which a correction can be made are necessary for an optimum geomorphic marker identification.

The eastern tip of the MF reaches the Laguna Negra bog area, where forms part of the southern boundary of a pull-apart basin of ~13 km long in an overlapping left-stepping extensional geometry (Figure 4.10). Based on satellite imagery the northern boundary of the basin forms part of series of a ~35 km segments that goes from the Lainez river until the Atlantic coast forming small-scales bends and step-over geometries, no larger than 1 km.

In the area where the western tributary branch of the Lainez River cut the fault, the MF present a N80°E strike and left-lateral offset the river channel and the unconsolidated deposit on both sides (Table 4.3, Figure 4.13). The deposits in this area are mostly massive, with grain size from clay to 40 cm blocks with 70% of the clast lower than 10 cm, polymictic and with middle to high rounding, intercalations and lenses of grey clay and fine sand are presents as well as peat layers. Based on this description, aerial imagery interpretation, previous geomorphological mapping and glacial chronology in the area, the 250-400 meter highs lobed hills both side the river are correlated with the Last Glacial Maximum extension, where the Fagnano paleoglacier would reach an elevation of 800 to 200 m a.s.l from the accumulation area to the ice snout, respective. Moreover, the hilly massive deposits are superimposed by glaciofluvial deposits related to the 1rst Recessional Phase or Earlier Late Glacial (Figure 4.10; Coronato et al., 2009), where a re-advance or possibly stillstand of the Fagnano lobe in the eastern shore of Lake Fagnano occurred and whose melting gave rise to the currents flowing from the fusion point of the ice tto the Atlantic ocean through outwash plains (San Pablo, Lainez and Irigoyen valleys). This glacio-fluvial deposition continued until the final retreat of the paleoglacier in the western side of TdF through the Azopardo valley, which changed the drainage patter on the lake causing the ceasing of the deposition of several fluvial outwashes along the valleys in Argentina (Coronato et al., 2009; Waldmann et al., 2010a; Rabassa et al., 2011). Thus, a maximum age for the till offset deposits is considered to be the estimated age for the LGM termination,

which began shortly after 1cal. Ka BP (Rabassa et al., 2000 Kaplan et al., 2004; McCulloch et al., 2005). Moreover, a minimum age these deposits of 13.4 cal. Ka BP is used, according for the basal peat bogs radiocarbon dating in La Correntina and San Pablo area (Coronato et al., 2009), whose deposition occurred after the area was free of ice.

Different geomorphic evidence of strike-slip tectonic activity was observed in this site, as 2-4 meters high ridges and elongated sag ponds in a damaged area along the fault trace (Figure 4.11). Despite of the thick cover of vegetation in the hilly deposits both sides the river, the scarp is still preserved and visible in satellite images by the alignment of vegetation (Figure 4.9.a), and according to the local topography changes from downhill to uphill in the central and eastern are of the hill, respectively, indicating a left-lateral displacement (Figure 4.10). The original glacial hillslopes both sides the river was modified by postglacial erosion and deposition. Indeed, the north flowing channel probably changed the configuration of the slope thus the contour lines in the eastern boundary of the river, considering that the downstream segment was faulted into the active channel (McGill et al., 1991). In the western hill, the scarp is about 8-10 meters high, while a 500 meters long shutter ridge was developed in the southern side due to the left-lateral displacement. Four offset geomorphological markers were measured from 110±10 to 130±10 meters based on the contour offsets in the high-resolution DEM (Figure 4.3). For this, the markers were interpolated when these were not continuous to the fault trace, and a back-slip estimation for the channel north and south the fault was made in two profiles considering aforementioned post-events modification by the river erosion (Figure 4.10.b). The channel thalweg offset were not used considering the high sinuosity relative to presumed offset amount, so the projection to the fault plane would not be well constrained. The offsets measured together with the available age data in the area suggest velocities from 6.5 to 9.1 mm/yr since the Late Pleistocene along this MFS segment (Table 4.3; Ludwig, 2013).

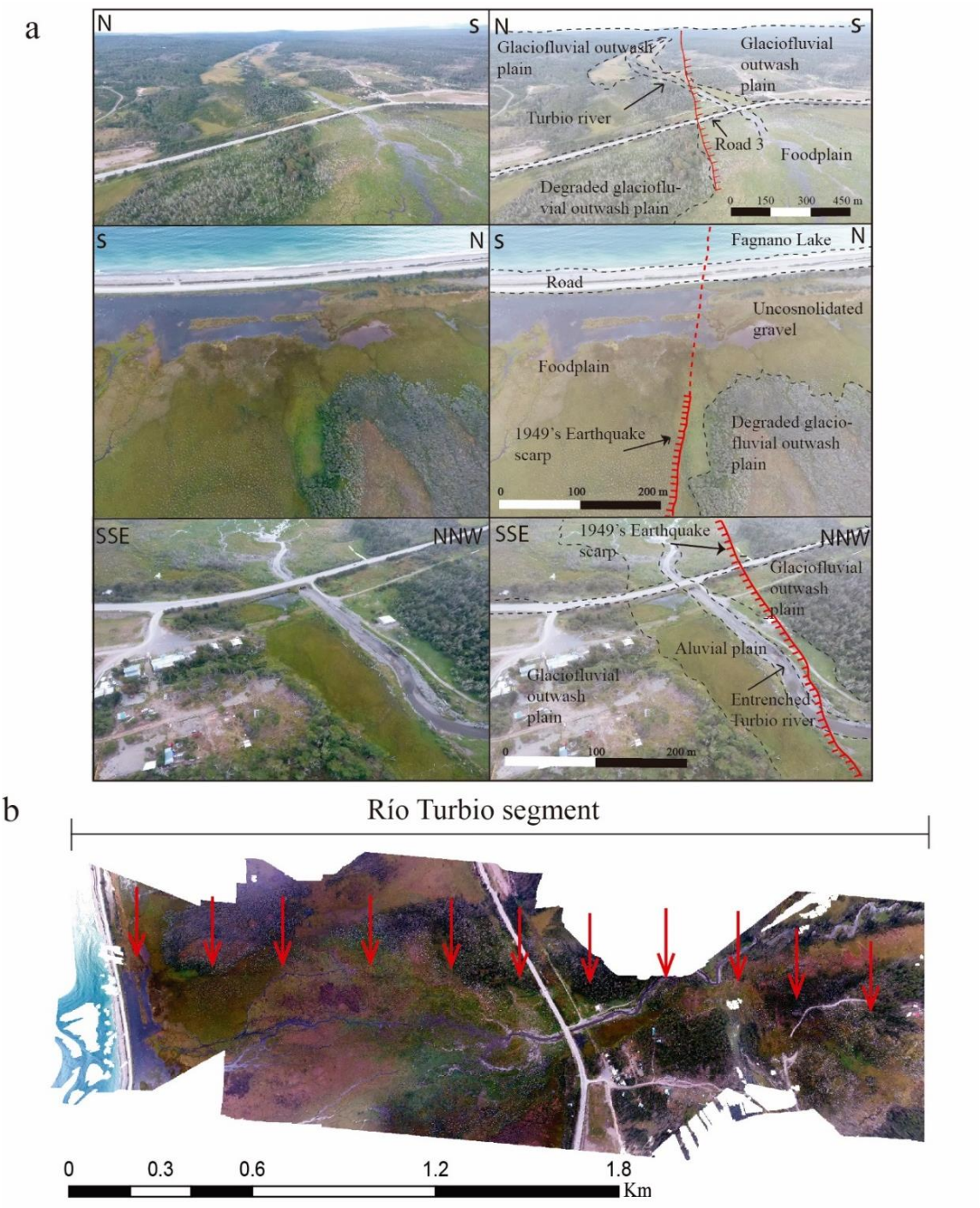

Figure 4.11: a) Drone images for the MFS portion in the eastern shore of Fagnano Lake, south to Tolhuín, Argentina. b) Photogrammetry-derived orthophoto of the the Las Pinturas-Río Lainez fault segment along Río Turbio segment valley in TdF, Argentina. Red arrows indicate location of the surface rupture described by Costa et a., (2006).

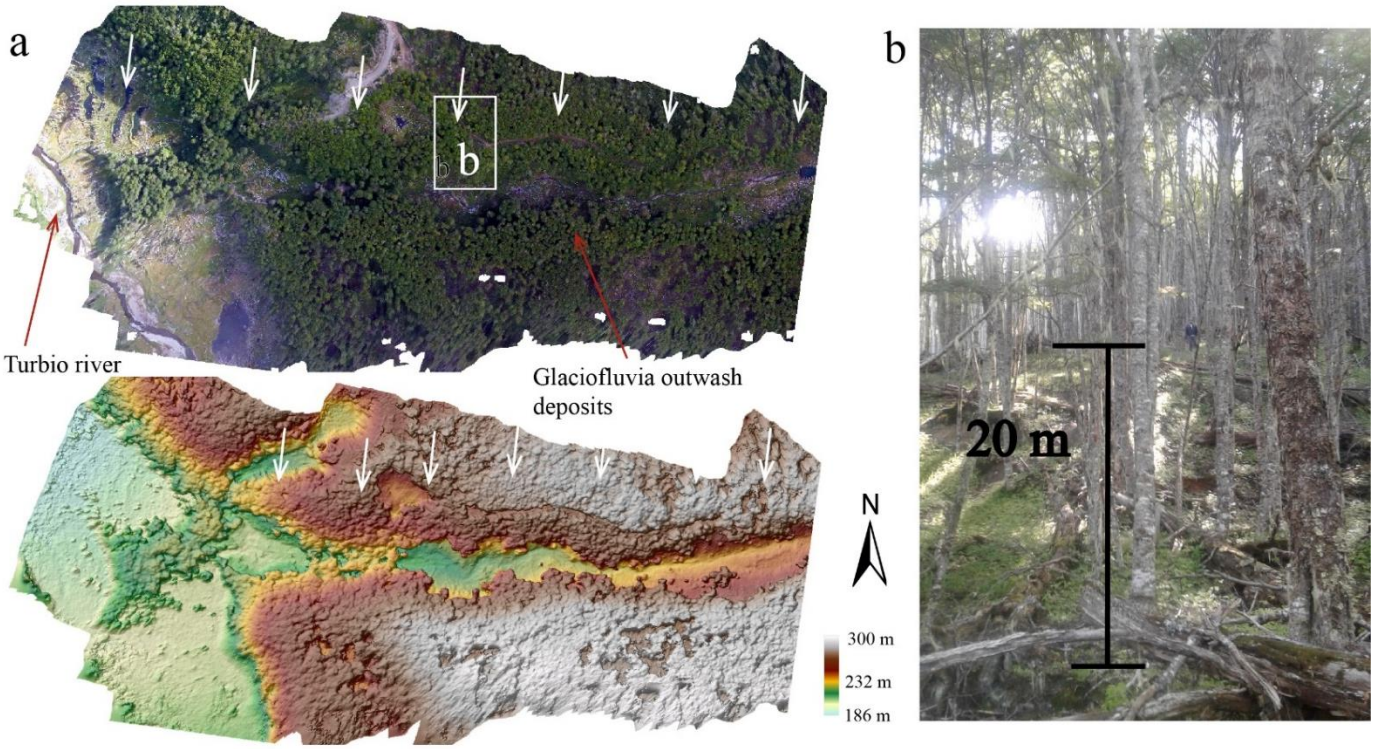

Figure 4.12: a) Ortophoto and DEM of the eastern portion of Río Turbio valley, Argentina (For location see Figure 4.8), white arrows indicate fault trace location. b) 20 meters-high shutter ridge north the fault segment (note person for scale).

Table 4.3: Offset measurement synthesis for site 3 in Argentina.

Argentina-Site 3	**Projection 1**	**Projection 2**	**Projection 3**	**Projection 4**	**Profile**
Confidence degree	A	A	A	A	B
Offset (m)	115±5	118±5	125±5	130±10	110±10
Geomorphological marker description	380 Contour, glaciofluvial outwash deposit (Figure 3.7.b)	400 Contour, glaciofluvial outwash deposit (Figure 3.7.b)	350 Contour, left limit of Lainez river deposits (Figure 3.7.b)	350 Contour, right limit of Lainez river deposits (Figure 3.7.b)	River channel backs-lip
Age min **134 kyr**					
Age max **17.8 kyr**					
Arithmetic mean (μ)±Standard deviation (σ) **7.8±1.3 mm/yr**					
Slip-rate for site 3 **6.5 to 9.2 mm/yr**					

East of the Lainez river branch bridge the fault trace is exposed next the road (Figure 4.12, for location see Figure 4.7.b) in a 4-meter-high deposit next the road. An abrupt change in the cohesion of the matrix is observed in the area surrounding the fault. Away of the trace, the deposit is composed mostly little or non-cohesive and matrix supported gravel with a grain size from clay to 20 cm blocks, which would be associated to the retreat if the Fagnano paleoglacier into its westward retreat after its maximum extent (LGM), superimposed by glaciofluvial and alluvial deposits. Near the trace, the matrix of the deposit is brown fine clay with high cohesion (Figure 4.12). The fault trace in this section has an 80/70°E azimuth/dip, and the clasts are imbricated along the fault zone. A normal displacement is observed in the

layered deposits near the top of the sequence, which would indicate an extension component in the failure with a displacement of less than 1 meter (Figure 4.12).

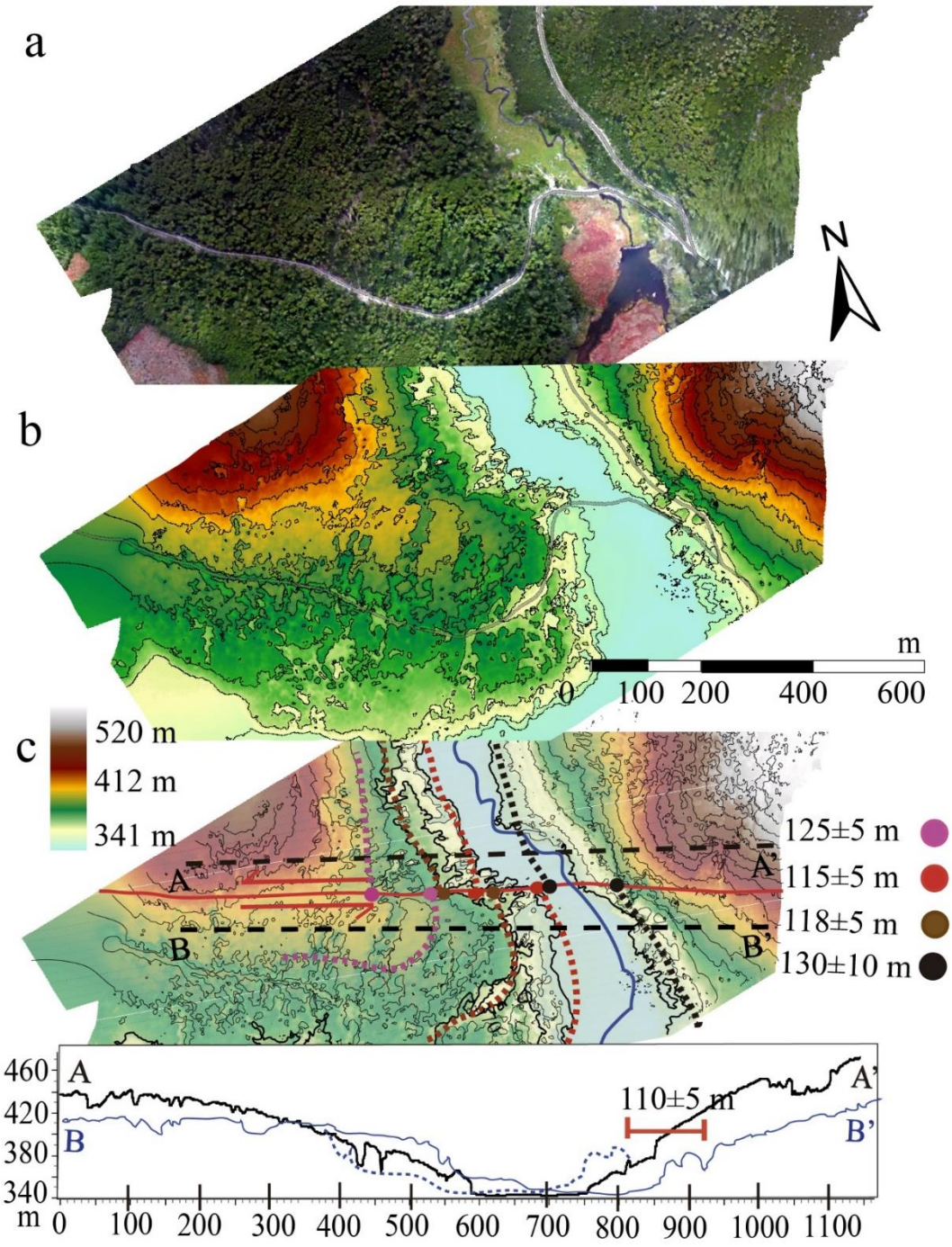

Figure 4.13: a) Slip-rate estimation site in Argentina, in a western arm of Lainez river cutting glacial and recent alluvial deposits b) High resolution DEM showing the left-lateral displaced channel, the offset can be observed both in recent alluvial and fluvio-glacial deposits. The profile shows the horizontal distance need for back-slip the channel north and south the fault trace. See Figure 4.2.a for location. The displacement corresponds to the offsets measured in the 350 m (dark orange and pink), 370 m (purple), 380 m (yellow) and 390 (light blue) contours. White dotted lines represent the elevation profiles traces. Stars indicate the locations for Figure 3.11 (green star) and Figure 4.12 (yellow start). 5 meters contour interval.

Figure 4.14: a) 2 meters shutter ridge parallel to the MFS with abundant fallen trees. b) Sag ponds south the ridge in a 50 meters width damaged area in the MFS area. For locations see green start in Figure 4.10.a).

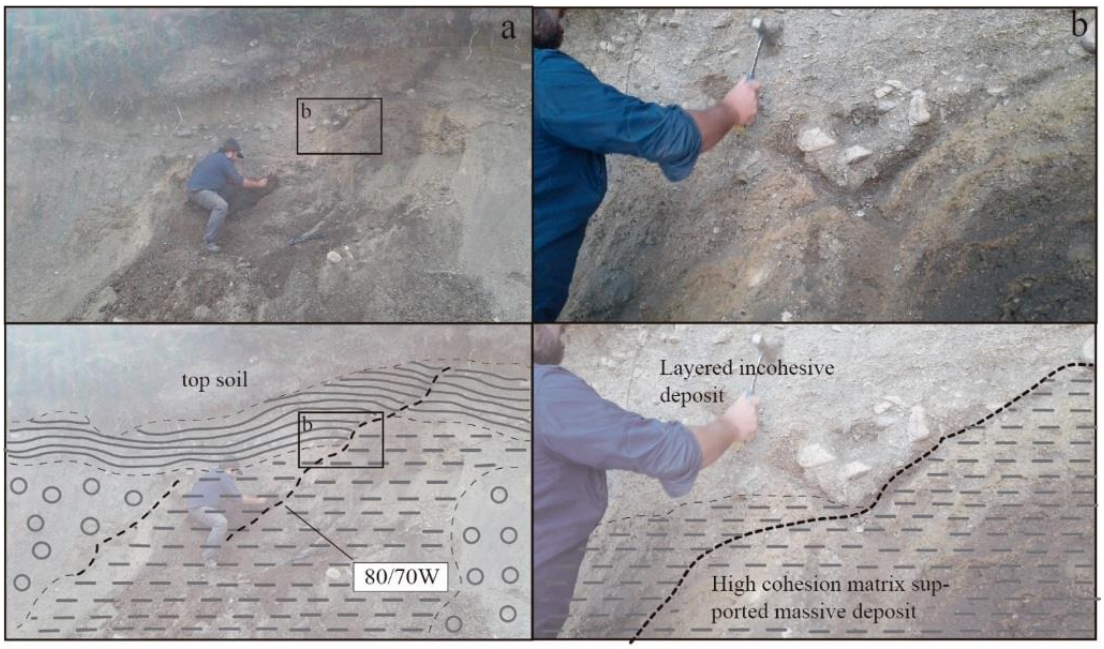

Figure 4.15: MFS fault trace the Lainez river area in glaciofluvial deposits covering glacially overridden low hills. (For location see Figure 4.7). The circular plot indicated the massive, matrix-supported and non-cohesive gravel. Striped plot marks the high cohesion matrix-supported gravel both sides the fault trace. Finally, the layered plot indicated the parallel stratification deposit on the top of the sequences.

CHAPTER 5: DISCUSSIONS

5.1 Faults locations and geomorphologic evidence of active tectonic

Long-term (millennial scale) geological slip-rates estimations were obtained in this work based on left-lateral displaced geomorphological markers along the MF fault trace in Chile (6.7 to 8.6 mm/yr) and Argentina (6.5 to 9.1 mm/yr) (Figure 5.1). The MFS main strand (MF) plus the Hope fault (HP) at this location in Chile gives a combined strike-slip rates of 8.1 to 11.0 mm/yr here. The higher values obtained at west than east along the MFS trace are consistent with the gradually decrease from west to east along the NSR according to the MORVEL plates rates (De Mets, 2010). These displacements represent the cumulative offsets of successive earthquakes since the Upper Pleistocene, since the sedimentary cover was shifted since the last glacial advance and retreat in the region during de LGM (McCulloch et al., 2005; Coronato et al., 2009) and there are no reports of aseismic creep in the area (Mendoza et al., 2015). Nevertheless, if some of the surficial offset measured correspond to post-seismic slip in the next month following large events, this amount added to the co-seismic surface slip would be a good estimation of the net seismic slip at depth than is the co-seismic surficial slip by itself (McGuill & Sieh 1991).

Fault mapping of the MFS was reported by previous authors based on kinematic data, bathymetric mapping, seismic profiling interpretation and geological offsets. As seeing in Figure 5.1, the faults location in Chile and Lake Fagnano area is imprecise, and the kinematic data-based mapping (Esteban et al., 2014) could may also correspond to shear motion along secondary fracture planes with no reports of significant amount of slip. Moreover, neither reports of rock faults (gouch- cataclasite) nor geological slip-rate or location of the active fault traces of the MFS in the western portion of TdF was reported according to its surface geologic and geomorphic expression, so it is uncertain to know if previously mapped faults

accommodated remarkable amount of slip or are currently active. The most reliable and clear expression of a recent faulting in Lake Fagnano stratigraphy in which a fault trace ruptured the surface was reported by Waldman et al., (2011), located at the center of a seismic profile (Figure 5.2) in the central sub-basin from NE to SW (Blue star in green dotted line (Figure 5.1), where a vertical slip component is also shown. In Argentina, the main MFS active fault segment (a.k.a. Río Turbio fault by previous authors) was characterized in based to the rupture scarp and slip during the last high magnitude 1949 events (Costa et al., 2006). Nevertheless, neither was reported a geological slip-rate for this structure in Argentina.

A prevailing left-lateral kinematics were observed along the three fault traces visited in the field based on a clear geomorphological expression (Figure 5.1.b). The main MFS fault (MF) in the western portion of TdF goes along the northwestern lake shore and the valley north Mount Hope. This fault is the fast-slipping structure (6.7 to 8.9 mm/yr) with the strongest geomorphologic expression in this portion of TdF, and therefore would exercise a first order control and concentrate the largest partitioning in the deformation along the MFS during Holocene time. This statement is contrary to that indicated by Klepeis et al., (1994), which suggested that the MFS current main structure is the fault south Mount Hope (a.k.a. Hope fault, HF; Figure 5.1). This is evidenced by the 5-10 me scarp and a left-lateral offset creek, together with several sag ponds orientated parallel to the fault, geomorphological lineaments and hydrothermal alteration along the slopes in the northern valley.

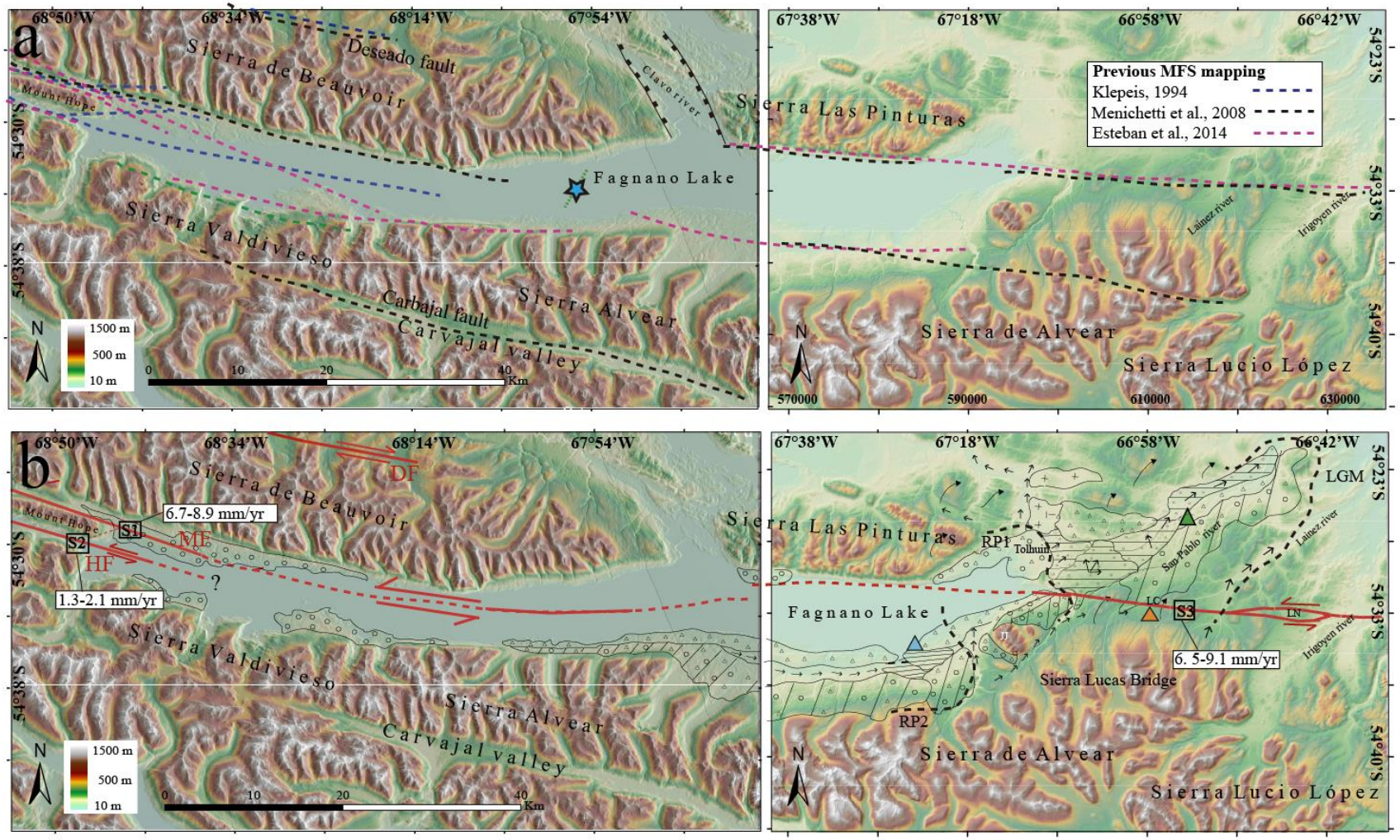

Figure 5.1 a) MFS mapping compilation in Lago Fagnano area by Klepeis, (1994) (blue dotted lines); Menichetti et al., (2008) (black dotted lines) and Esteban et al., (2014) (Pink dotted lines). Green dotted line indicate location for seismic profile in the Lake Fagnano by Waldmann et al., (2010). Light blue star indicate location for a well define fault zone observed in the profile.

a) MPF mapping in this work based on field and remote sensing data observations. Red solid lines indicate locations for fault reported in this study. Dotted red lines indicate locations for inferred fault continuations along Fagnano Lake. S1, S2 and S3 indicate site for geological offset measurements and boxes indicate long-term (Late Pleistocene) slip-rates for these structures based on measured geomorphological markers offsets and regional dating available in previous works (Coronato et al., 2009; McCulloch et al., 2005).

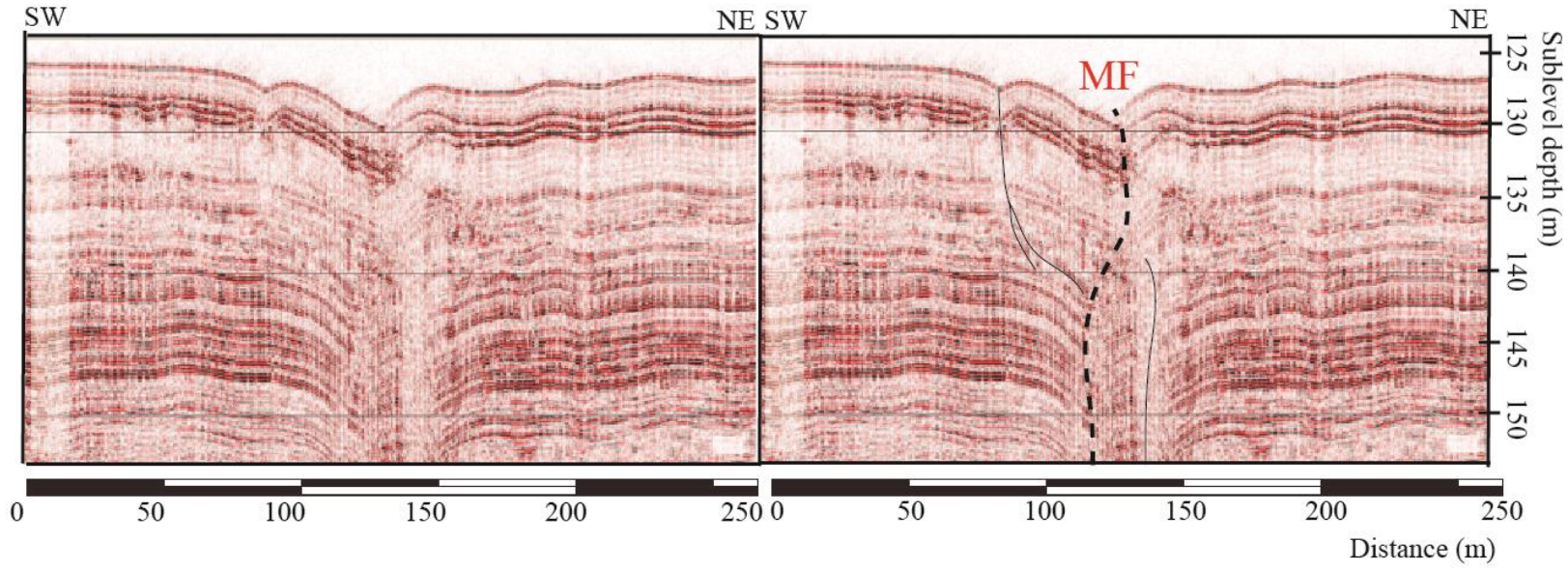

Figure 5.2 a) NE-SW seismic profile crossing the central sub-basin of Lake Fagnano (after Waldmann et al., 2011). .b) Interpreted NE-SW seismic profile crossing the central sub-basin of Lake Fagnano. The black dashed line indicates MF location. For location on floor see light blue star in Figure 5.1. Modified from Waldmann et al., (2011).

Based on the bathymetric studies in the Lake Fagnano basin the MF fault reported in the northwestern shore could correspond to the limit between the minor western sub-basin and the central main sub-basin separated by a structural high of less than 100 m depth extending 6 km in a WNW-ESE trend identified by Esteban et al., (2014) as the Martínez fault. Nevertheless, according to the noticeable and well-defined 50 m wide faulted zone in the seismic profile along the central sub-basin reported by Waldman et al., (2011), the fault trace would continue to east along its axis until at least the central section of the lake (Figure 5.1.b). To west, would connect or possibly form a small-scale (< 2 km) step over with the MF main segment in Argentina (a.k.a Río Turbio fault by previous works) towards the northern lake boundary along the southern slope of Las Pinturas range, as in seismic profiles located in the eastern sub-basin this fault zone is not that obvious along the main axis as it is in the western profile. Similarities in the slip-rates obtained in this study for the MFS main segment in Chile (6.7-8.9 mm/yr) and Argentina (6.5-9.1 mm/yr) supports the idea both faults correspond to the same continuous fault segment.

South the MF, the continuation of the HF at east is uncertain (Figure 5.1.b). But the most likely option is that this structure goes parallel to the MF or both merge at some point in the western portion of the lake. Nevertheless, the 8.1 to 11.0 mm/yr estimate by sum the slip-rates for the two active structures observed in this area, MF and HF along the valleys north and south Mount Hope, respectively, would be a minimum estimation if other active faults were north or south Mount Hope area. Previous structural mapping based on seismic profiling reported subparallel strands along the southern slope of Beavouir Range (Figure 5.1.a; Menichetti et al., 2008, Esteban et al., 2014), nevertheless, no evidence of neotectonic activity was observed in fieldwork and satellite imagery, and more data is necessary to determinate if these structures are currently active and accommodate some deformation partitioning. Moreover, geomorphic evidence of recent tectonic activity was reported in this work along the Deseado valley, north Beavouir Range, were

the Deseado fault area was previously reported by Klepeis, (1994) (See Section 4.2). This suggests an overall Late-Quaternary combined sinistral slip-rate near the Chile and Argentina border at Lake Fagnano of 9.1 to 12.0 mm/yr.

According to some authors the relative motion since the beginning of the separation between the Antarctic Peninsula and the southern tip of South America could been temporally and spatially partitioned in the different fault systems that cross southern Patagonia region (Lodolo et al., 2003; Cunningham et al., 2004; Menichetti et al., 2008). Moreover, several E-W and NW-SE lineaments are observed in the valleys and fiords of the Fueguian archipelago (Figure 5.3; Winslow., 1982; Klepeis, 1994; Lodolo et al., 2003; Torres-Carbonell et al., 2008). Between this several major sub-parallel faults stand out the Magallanes-Fagnano fault system and the Deseado fault system because them clear morphological expression, but other several lineaments including along the Lasifashaj Valley, the Beagle Channel (Cunningham., 1993), the Carbajal valley (Caminos., 1981) and the Isla Clarence lineaments and Isla Iloste lineaments could also currently or previously accommodate part of the plate motion (Figure 5.3). This partitioning in the amount of displacement since the late Cretaceous explain the difference between the even 1500 km of offset estimated in the NSR by some authors (Cunningham.,1993). Furthermore, strike-slip fault systems were reported south the MFS which could have distributed a portion of the offset along the plate boundary Caminos, (1981) reported a fault zone along the Carbajal valley southeast Mount Hope dissecting and brecciating Upper Jurassic to Lower Cretaceous rocks of the Magallanes Fold and Thrust Belt, while Menichetti et al., (2004) identified in the center of the valley a left-lateral strike-slip fault with a sub-vertical axial plane pervasive cleavage deforming E-W mesoscopic folds. Cunningham et al., (2005) reported E-W trending faults pertaining to the sinistral strike-slip Canal Beagle fault system offsetting thrust along the northern shore, and a small cluster of low-magnitude earthquakes was also found here (Febrer et al., 2000). However, there is no geomorphic neither geologic evidence that these structures are

currently accommodating some amount of deformation. Moreover, according to the GPS velocities the major faults mapped south the MFS are not currently active (Smalley et al., 2003).

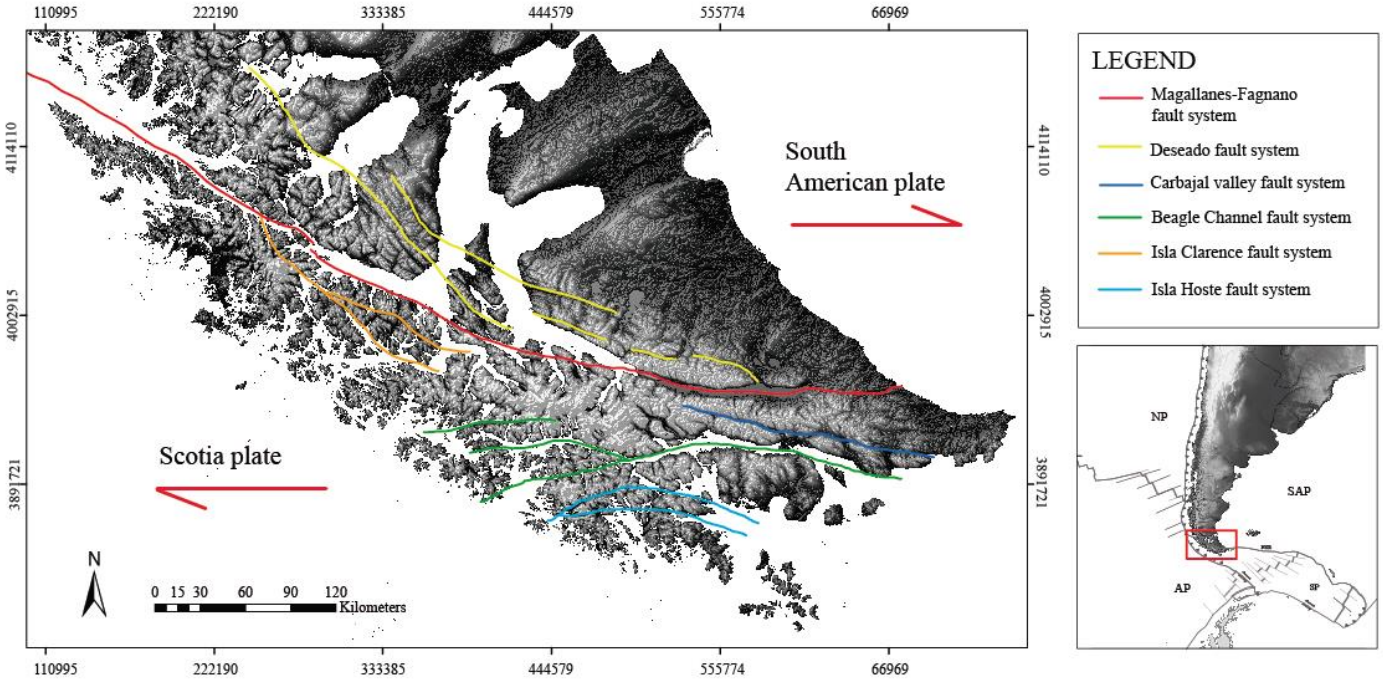

Figure 5.3: Overall fault systems previously mapping in Patagonia region, according to geomorphological lineaments. Modified from Lodolo et al., (2003) and Sue & Ghiglione (2006).

Adittionally, the role of the MFS in the tectonic evolution and dynamics of the Scotia plate was previously disputed in previous works. The northern tip of the Antarctic Peninsula and the southernmost Patagonia probably formed a continuous rectilinear margin at the end of the Early Cretaceous and were very close in the middle to late Cretaceous (Poblete et al., 2015). The relative motion history between Southernmost South America and the Antarctic Peninsula could commenced around 84 Ma, when South American continent had a significantly more rapid westward motion and a non-parallel trajectory with the Antarctic

Peninsula relative with fixed African continent. According to Cunningham et al., (1993); this separation and associated wrenching tectonic would trigger the development of the Patagonian bend. Since this time, approximately 1320 km of east-west, left-lateral strike-slip motion has developed and approximately 900 km of the motion occurred after the 50 Ma (Cunningham., 1995).

Other authors suggest that the current plate boundary development is related to an increase in the continental separation rates at 55-40 Ma related during a global Eocene plate reorganization event, which led to the onset of seafloor spreading in the western Scotia Sea and the opening of Drake Passage. According to this model, the strike-slip deformation in TdF occurred after the 60 Ma and dominantly since 30 Ma, superimposing the contractional deformation dominant during Cretaceous times (Winslow, 1982; Klepeis & Austin, 1997; Ghiglione & Ramos, 2005). Between 46 to 20 Ma, the spreading rates in the Western Scotia ridge increase and change to an WNW-ESE direction, possibly related to the onset of the subduction of oceanic seafloor of southern South American beneath the eastern side of the Antarctic Peninsula (Livermore et al., 2005; Lagabrielle et al., 2009). This configuration resulted in a transpressional tectonic along the NSR during this period (Eagles et al., 2005; Lagabrielle et al., 2009) At 20 Ma, a change in the motion to an E-W direction lead to the initiation of spreading at the East Scotia ridge and an important drop in the spreading rates on the western Scotia ridge (Eagles et al., 2005). According to this, the MFS-NSR transform system development may have occurred much later, in the Late Miocene (6.6 to 5.9 Ma; Lodolo et al., 2003; Eagles et al., 2005; Lagabrielle et al., 2009; Betka et al., 2016), coeval to the cessation of western Scotia seafloor spreading and a significant increase in the Sandwich ridge activity (Eagles et al., 2005), which led to the current plate geometry with the extinct West Scotia Ridge and sinistral motion along the plate boundary (Eagles et al., 2005; Lagabrielle et al. 2009). This period is also

coeval with uplift and exhumation in the eastern domain of Patagonian fold and thrust belt (Fosdick et al., 2013).

According to the said above regarding to the estimates ages for the beginning of the MFS activity, first order estimations for long-term slip-rates were made according to offsets in bedrock units both sides the MFS trace at regional scale. A Lower (20.0 Ma) to Upper Miocene (6.0 Ma) age for the onset of the MFS as a first order control as the current plate boundary activity suggest an average long-term slip-rate of 2.1 to 8.7 mm/yr. Moreover, an Upper Miocene age agreed with the short-term estimations obtained in this and previous works, and moreover, this period is related to important changes in the Scotia Plate dynamics due to the imposition of a dominant wrenching tectonics and corresponding left-lateral strike-slip faulting along the northern boundary of the Scotia plate, compatible with the extinction of the spreading direction along the West Scotia ridge (Eagles et al., 2005) and the exhumation of the eastern thrust domain of the Patagonian Fold and Thrust belt (Fosdick et al., 2013). Nevertheless, considering that the slip-rate is not constant along the history of a strike-slip fault system more data is lack for determinate a deformation history for this structure (Meade & Hager, 2005).

Moreover, the role of the fault system proposed south the MFS area in the tectonic rotation observed in the southern tip of south America has also been disputed (Diraison et al., 2000; Cunningham et al., 2003; Glasser & Ghiglione 2009; Poblete et al., 2016).Some authors proposed that the structural control in the deformation has been migrated further north since the Upper Cretaceous-Oligocene starting in the inherited basement detachment of the Late Cretaceous Andean compressional phase into strike-slip faults along the Beagle Channel fault zone and other fjords (Figure 5.2; Winslow., 1981; Cunningham., 1993;

Menichetti et al., 2008). Nonetheless, paleomagnetic studies made by Poblete et al., (2016) discard a considerable magnitude of strike-slip deformation south the Darwin Cordillera in Cenozoic times according to tectonic rotations and the variability on the orientation of the magnetic fabric recorded by the plutons of the Fueguian batholith. In his model, the Paleogene rotations observed south the Darwin Cordillera are mostly related to large-scale regional block rotations driven by the shortening in the Magallanes Fold and Thrust Belt and no correspond to in-situ small block rotations related to Cenozoic strike-slip structures.

5.2 Offsets measurement and uncertainties estimations

Potentially, every large earthquake on a strike-slip fault could be recorded by these offset markers, if new features form during the inter-seismic period and if these features are preserved at the time of observations (McGuill & Sieh, 1991; Ludwig et al., 2010). Nevertheless, based on to the available data, no reliable lower offset clusters are identified in younger geomorphological markers along the MFS, precluding to stablish a consistent cumulative offset probability distribution (COPD, Zielke et al, 2015). However, it was only possible to certainly determinate the cumulative offset in some deposits resulted from past events since Late glacial times (<18 ka). Most of the major river that cross the fault (Río Turbio, San Pablo, Irigoyen) doesn't exhibit reliable offset in satellite imagery (Wordview, ±5 m of horizontal uncertainty) and cross the fault trace flowing north to the Atlantic Ocean without major disturbance despite the northern side is topographically higher. This suggest high incision rate for these channels compared with earthquakes occurrence. On the other hand, offsets deposits consist in minor channels or secondary strands of the major rivers flowing north, and several glacial deposits with plains and hilly morphologies. This are the oldest landforms in the area resulted from the replacement of the sedimentary cover in the area after the LGM ice recession Furthermore, for greater number of events and therefore time registered

in an offset cluster, this will be wider and with smaller amplitudes, thus is more difficult to distinguish the slip per-event and to reconstruct the single-event slip accumulation pattern, due to geomorphic markers will be altered by further degradational or buried process (McGuill & Sieh, 1991; Zielke et al., 2015). Furthermore, a high variability in environmental conditions was stablished during Holocene times by the sedimentary record in Lago Fagnano, suggesting the onset of humid conditions in the region during Neoglacial times related to an increase in the sediment supply to the basin and rain-storm frequency (Waldman et al., 2010b). Then, the recurrence rate for storm events exceeds in two or three orders of magnitude to the recurrence rate of surface rupturing earthquakes. Another influence factor to considerate is the profuse cover of vegetation, peat and disturbances in the terrain leaved by beavers (castores). Nevertheless, more data is necessary for determinate if it is possible to determinate a reliable COPD, either a greater coverage area for SfM-derived high resolution DEM's or Light Detection and Ranging (lidar) data with vegetation filtered.

Beyond the uncertainties proper to the offset measurements described in the results chapter, it was necessary to delimit an age to these landforms. The most common method is radiocarbon dating published by previous authors, where age of the basal peat is taken to indicate the approximate initiation of the peatland development, which would be started at the latest when the glaciers leaved the area (Coronato et al., 2009). The date itself has associated an analytic error, and possible additional errors in the calibration for ages older than Holocene times (Norris & Cooper et al., 2000). Moreover, scarce local age data was proposed in previous local studies, and regional correlation was done by Coronato et al., (2009) for the LGM and recessional phases by comparing the glacial boundaries identified in the Lake Fagnano area with the glacial chronology in the Bahía Inútil and Magellan Strait after McCulloch et al., (2005). As the paleo-glaciers covering these areas belong to the same outlet glacier, the glaciological behavior is assumed to be under the same conditions. Provided the dating are correct, the uncertainty on doing this correlation

do not add large uncertainties to the slip-rates estimations, in the order of 10% due to the length of time involved (Norris & Cooper et al., 2000). Additionally, subsequent re-advanced are discarded for the Lake Fagnano area during the Neoglacial period in TdF, whose onset is marked by the mid-Holocene times (~6 ka; McCulloch et al., 2005; Waldmann et al., 2010a). In this period, the Fagnano lobe advanced again but the ice was probably confined to the high mountain region of Cordillera de Darwin to the west, so the ages used for the correlation of the deposits documented in the field range between the LGM and Latest Late glacial for these landforms.

5.3 Seismic potential and seismic hazard implications

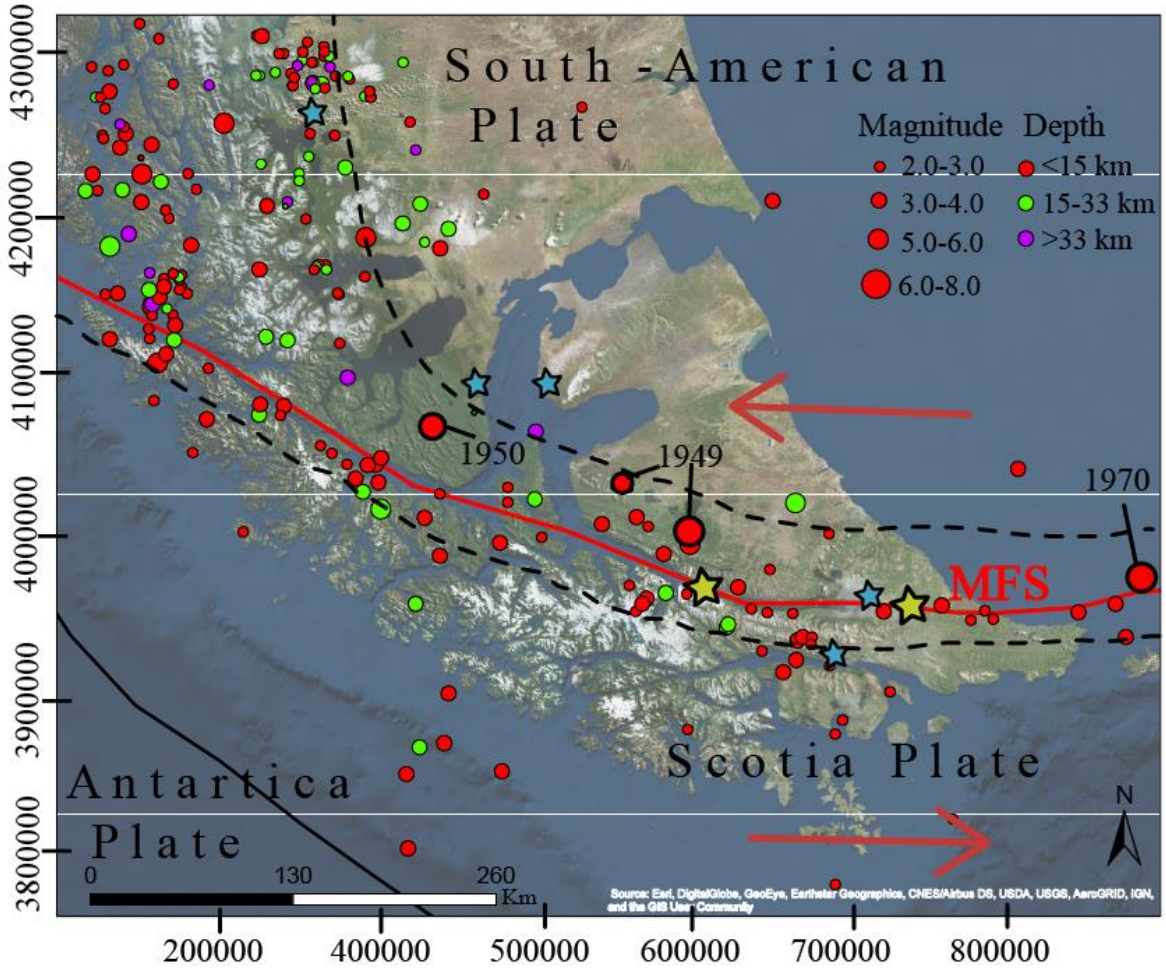

Figure 5.4 Seimicity in Southern Patagonia region (ISS – ISC: Catalogue of the International Seismological Centre, Berkshire, Great Britain. (http://www.isc.ac.uk), UNLP (Universidad Nacional de La Plata, Jaschek et al., 1982). The circles with thick edge indicate locations of epicenter for historical high magnitude earthquakes, from east to west: Mw7.8 1949 (10 km), Mw7.5 1949 (10 km), Mw7.0 1950 (15 km) Yellow start indicate locations for the geological slip-rate measurement sites in Chile (west) and Argentina (east). Light blue stars indicate locations for urban centers (Puerto Natales, Punta Arenas and Porvenir at west and Tolhuín and Ushuaia at east). Coordinates on UTM, 19S.

Seismic zoning of INPRES for TdF reflect a tectonic model where the main seismogenic source is located along the margin of South American continent that borders the Pacific Ocean. South the Chilean ridge (52°S), the Antarctic plate converges at a lower speed of 2 cm/yr triggering a low seismicity with no risk for the western sector of TdF (Adaros, 2003). Nevertheless, this zoning needs to be modified to considering the MFS as the main seismogenic source (Abascal & Bonorino, 2014), and better constrained parameters for this first order structure are needed for improve seismic hazard assessment.

Left-lateral coesismic slip reported by previous authors for the 1949 events in Argentina indicate displacements from 0.4 to 6 meters according to horizontal offset of fences (Smalley et al., 2003; Costa et al., 2006). No information is provided for the co-seismic displacement in the second events or in paleo-earthquakes, and the estimation have quite low realibiliy. Considering the 120 m of cumulative post-glacial offset obtained in Argentina during this work together with these only left-lateral coesismic slip estimations for the 1949 first event, these segments would have recurrence intervals for large earthquakes of 60 to 900 yrs between events, assuming that the majority of the seismic moment is released during the repeated occurrence of large magnitude earthquakes (Schwartz & Coppersmith, 1984; Stirling et al., 1996)**.** The lower value agreed with the time span between the two most recent high magnitude earthquakes related to the MFS in Argentina in 1879 and 1949 (Pedrera et al., 2014). Moreover, since there are no reports of creep in the area, the average long-term slip-rate of 8mm/yr obtained in this study suggest that perhaps ~0.6 m of slip is accumulated since the 1949 event.

Although the location information for historical earthquake have limited spatial resolution here due to a sparse seismic network, epicenter distribution for historical (Fig. 5.4; Mw7.5 and Mw7.5 in 1949, Mw 7.0

in 1950, Mw7.2 in 1970) and low to moderate seismic events from adjacent to fault up to even 30 km north the MFS fault trace superimpose the contractional structures of the Magellan Fold and Thrust belt (Figure 5.4; Jaschek et al., 1982, Sabbione et al., 2007), together with geomorphologic evidence of neotectonics activity along the Deseado fault (Figure 1: Klepeis et al., 1994; this work, Supplemental data) suggest that there is other active seismogenic strike-slip structures along the plate boundary, likely accommodating some partitioning of the deformation along the Antarctic and Scotia Plate boundary.

Moreover, in the study area in TdF to the east across te the main deformation belt perhaps is not more than a total width of 30-50 km as there is no geomorphic neither geologic evidence that structures suggested south the MFS, as the Beagle Channel fault zone (Cunningham, 1993), are currently accommodating some amount of deformation, and according to Smalley et al., (2003) based on GPS velocities the major faults mapped south the MFS are not currently active. Compared with the width of surface deformation along other continental strike slip plate boundaries, e.g. Along the San Andreas (50 to 100 km, Mount & Suppe, 1987; Meade & Heager, 2005); and the Marlborough Fault System in New Zealand (150 km; T.A Little & A. Jones, 1998; Wilson et al., 2004), the main deformation here is relatively narrowand well developed, and therefore the Scotia-South American plate boundary in its central and eastern portion would be composed by a well-defined deformation belt with a main relatively smooth and long trace bounded by secondary active but slower parallel faults, as the Hope fault and Deseado fault, with a total belt width of no more than 50 km (Figrue 5.4). Its relatively simple geometry and remarkable length would suggest a small ratio between small and large earthquakes due to smoothing of the fault zone, as the size of the largest earthquakes on a fault increases and the number of small event decreases as individual fault strands and fault coalesce for form a long, smooth fault trace (Stirling et al., 1996). The relatively simplicity of the onshore trace in TdF with well-defined fault traces and small-scale steps and

bends along Tdf would support this assumption. If this is true, a Gutenberg-Richter log-linear frequency-magnitude relationship (logN= a-bM; Gutenberg & Richter, 1944; Figure 5.5) based on modern and ongoing seismicity monitoring provide an estimate of the long-term rate of small to moderate earthquakes but will underestimate the hazard related to a greater frequency of occurrence of large earthquakes (Stirling et al., 1996). The shape of the magnitude-frequency distribution for high-magnitude earthquakes on the MFS would then be described by a non-linear relationship estimated independently with geological and long-term fault slip-rate data in a characteristic earthquake model (e.g. Mw 7.8in 1949, and Mw 7.0 in 1950) , which is based on that the slip distribution of the characteristic event along a fault zone or fault segment is repeated in successive events (Schwartz & Coppersmith, 1984, Figure 5.5). Although making this statement is complex because historical records of seismicity in Southern Patagonia and TdF is much shorter than a complete seismic cycle, the occurrence of several largest earthquakes in historical and Holocene times is consentient with this assumption.

According to the equation $D=2.8 \times 10^{-5} \times L$ (The working group on California WGCEP, 1988), which relates coseismic slip (D, 50% uncertainty) and length of rupture, a coseismic slip of 0.4 to 6 meters for the first 1949 event in Argentina implies a rupture of approximately 14.2 km to 214 km, respectively. The higher value corresponds to the entire length of the MFS onshore in Tierra del Fuego, from the Atlantic coast to the Magellan Strain. More seismological data are needed to better constrain a reliable recurrence interval for the faults on this system and the length of the surface ryt

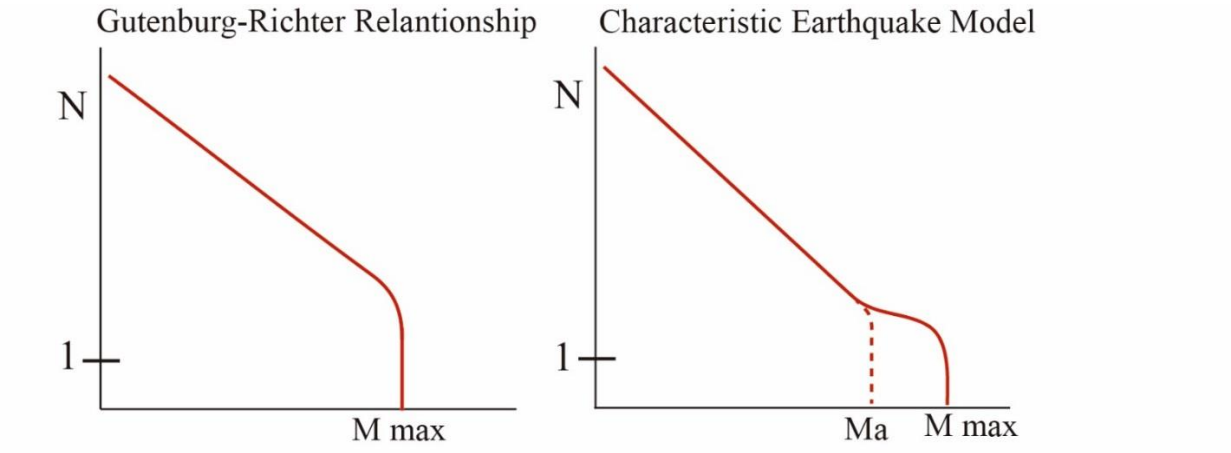

Figure 5.5: Gutenberg-Richter log-linear relationship versus a Characteristic earthquake model. Modified from Stirling et al., (1996).

Northwest the study area, according to fault slip data along the Magallanes retroact fold and thrust belt near Peninsula Brunswick and Seno Otway, strike slip and oblique-slip normal faults sets reflects a regional bulk transtension and the MFS form a plate-bounding strike slip fault zone diffusely distributed and partitioned (Betka et al., 2016) onto splays reverse reactivated faults within a pre-existing fold and thrust belt (Figure 5.4; Klepeis & Austin, 1997; Lodolo et al., 2003; Betka et al 2016). Betka et al., (2016) mapped left-lateral faults belonging to the MFS north the main segment (MF) west TdF. One of them, the Bahía del Indio fault, strikes NW for 100 km across Peninsula Brunswick between Estrecho de Magallanes and Seno Otway forming a left-lateral, left-stepping releasing zone with the main MFS trace.in the northwestern trending segment of the Magellan Strait. More studies are needed to better determinate the amount of partitioning between the different segments in the Southern Chilean Patagonia and how much the deformation belt width changes approaching to the trench, especially where potentially active structures go through populated areas or crossing terrestrial and submarine infrastructure. Moreover, this

partitioning along the western portion of the plate boundary could have an influence on the geometry and definition of the triple point between the Scotia, Antarctica and South American plates.

5.4 Geological versus Geodetic data-based slip-rates

Table 5.1 resume the previous short-term geodetic data-based slip-rate estimations along the MFS and offshore in the NSR. Particularly, the MORVEL model (De Mets, 2010) and the rates estimated by Smalley et al. 2003 differ in more than 4 mm/yr (Table 5.1). The difference between these two estimates are caused mainly by the different closure constraints that must be satisfied by the two estimates, as the different constraints that are imposed for the Antarctic-South America plate motion. De Mets, (2010) suggest that better constrained estimates for plate motion in this region await more data, while Smalley et al., (2003) indicated that the scarce number and poor distributions of stations decrease the confidence the results.

Although geodetic data-based rates reported by De Mets et al., (2010) fit within the ranges for geological slip-rate estimations both in Argentina and Chile sites obtained in this study, with no evidence of Quaternary secular variation, these results are 3-5 mm/yr higher than Smalley et al., (2003) and Mendoza et al., (2015)'s results, possible more if the Deseado fault system would have an slip-rate higher than 1 mm/yr, which is likely considering the remarkable geomorphic evidence of strike-slip tectonic reported in this work (See Section 4.2).

Both similarities and systematic differences between geologic and geodetic slip-rates are observed in several major strike-slip fault systems (North Anatolian fault, Dolan et al., 2017; San Andreas fault, Dixon

et al., 2003,Tong et al., 2014; Altyn Tagh fault, Cowgill et al., 2009), suggesting a complex relationship between long and short-term fault system behaviors. Misfits between these two estimations can be due to several reasons. First, the results obtained in this study can be slightly overestimated due to uncertainties in the projections of the piercing lines and in the estimation of the preservation of the markers and pre-deformation shape. Nevertheless, the unambiguous and well-defined trace in the slip sites, together with a ponderation of the plausible offsets on at least three marker's elements in each site and considerations about the erosion susceptibility on each of them and estimated qualitatively incision rates allowed us to obtain high reliability measurements with well-defined uncertainties. An overestimation by an incorrect age correlation for the quaternary deposits also is unlikely, as subsequent re-advanced are discarded for the Lake Fagnano area during the Neoglacial period in TdF during mid-Holocene times (~6 ka; McCulloch et al., 2005; Waldmann et al., 2010a), so all of the glacial deposits in the area are from the LGM and its recession period during the uppermost Late Pleistoscene.

A second explanations is systematic errors in the modeling and geologic constraints in geodetic studies which has led to a systematic underestimation of the short-term slip-rates. Smalley et al., (2003) modeled the deformation of the MFS as a single ~E-W plane in the central and western portion of TdF using a simple two-dimensional homogeneous elastic half-space model and assumes a 15 km of locking depth. The fault model not considerate deviations of the geometry from a straight plane as bending or in echelon segments, resulting in transtension or transpresion regimes and neither could define locking depth or fault inclinations because of the limitations of the GPS network. Mendoza et al., (2015), on the other hand, used a denser GPS networks and covered a longer time span (20 years) and also used a homogenous elastic-space to model the fault, but defines more geometric parameters although the spatial resolution were not enough to resolve the slip partinioning between the different fault segments.

Previous works suggested that this misfit could be related to the rheological model considered in the geodetic-based estimation. If the earth surface is modeled as a continuous elastic half-space (Dixon et al., 2003, Tong et al., 2014), this modeling ignores the viscoelastic behavior of the rocks under the brittle-ductile transitions temperature (lower crust and upper mantle). Otherwise, the earthquake cycle effect produces time-dependent deformation in the asthenosphere by viscoelastic relaxation, reflected on the preset-day surface velocity. Therefore, a three-dimensional model with an elastic plate layer overly a viscoelastic half-space is more realistic to predict the surface inter-seismic velocity than the elastic-half-space model (Dixon et al., 2003). If the lower cosesimic slip estimate by Costa et al., (2006) is correct (0.4 m), the recurrence rates estimations obtained in this study according to the cumulative offset since glacial times suggest that this fault is currently on a later period of the earthquake cycle. In this case the observation time is much later than the Maxwell relaxation time, defines as twice the effective viscosity divided by the shear modulus (Savage & Prescott, 1978; Tong et al., 2014). This would lead to an underestimation of the geodetic slip-rates, which would be lower than the cycle average (Tong et al., 2014). If the slip-per event is higher (up to 6 meters), the resulting recurrence rates would indicate that he observation time is earlier in the earthquake cycle (earlier the Maxwell relaxation time), and the geodetic rates would be higher than the cycle average (overestimated), which is unlikely taking into considerations the geological estimations presented in this study.

Furthermore, recent studies discard the diagnostic character of the ratio between geodetic to geologic rates before an earthquake to determinate the time of the next event, so there is a no single relationship between these two rates data that can be applied all faults. According to this, single existing earthquake cycle-model can descript all the diversities of earthquake- cycle behaviors (Dolan et al., 2017). Furthermore, Savage & Prescott (1978) suggest that in the case of a small ratio between the locking depth and

lithosphere thickness the effect of the asthenosphere relaxation is disposable. As the Moho depth calculated by Buffoni ,(2009) rounds the 30 km and considering a locking depth of 10-12 km determined by Mendoza et al.,(2005) and a 15 km estimated by Smalley (2003), this ratio should be relatively smaller and the earthquake cycle effect should not be significant.

Beyond the rheological model used for the velocity inversion and the period in which the fault is found respect to the earthquake cycle, the geological constraints have the advantage of not depending on temporal and spatial limitations, and present a long-term estimations becaused includes in its time span several earthquake cycles, unlike the geodetic and instrumental seismicity data.

Table 5.1 Short-term slip-rates obtained by previous authors (Smalley et al., 2003; De Mets, 2010; Mendoza et al., 2015), compared with long-term slip-rates obtained in this study.

Study	Time spans	Slip-rate	Data set
This study	Upper Pleistoscene (~18 kyr)	9.1-12.0 mm/yr in Chilean segment and 6.5-9.1 mm/yr in Argentina segment	Geomorphological marker offset in the central-eastern portion of the MFS in Argentina
Smalley et al., 2003	Campaigns measurements over a total observation spans of 2 to 6 years.	6.6±1.3 mm/yr	17 GPS stations in the South American (9) and Scotia plates (8)
De Mets et al., 2010	1999-2008	9.6±1.4 to 8.9±1.2 mm/yr at the western and eastern end of the NSR, respectively	Velocities of three Scotia plate stations from Smalley et al., (2003), (2007) study
Mendoza et al., 2015	1993-2013	5.9±0.2 mm/yr	Interseismic velocities from 48 sites in South American (31) and Scotia /17) plates together with Global Navigation Satellite System observations.

-* The western NSR is considered in De Mets et al., (2010) to be in the eastern limit of TdF.

CHAPTER 6: CONCLUSIONS

6.1 Main conclusion of this work

Available restricted data suggest a complex geotectonic environment and rupture dynamics along the MFS area related to the current active dragging between the Southern tip of South America and the Antarctic Peninsula. Several question about the seismic hazard related to this first-order tectonic structure exist due to the lack of a geologically consistent Late Quaternary slip-rate for the main and minor active structures along the Scotia and South American plate boundary. In this work, remote sensing mapping were combined to determine locations of fault traces and offset geomorphological markers along them, together with fieldwork and SfM-derived high-resolution topographic data and geological observations. This allowed the combination of short (<150 m) left-lateral offsets on these markers and available regional dating to constraint the first long-term (Late-Pleistocene) slip-rate for structures within the MFS.

Based on a review of the regional geology, cumulative long-term geological separation of 40 to 60 kilometers exists along the MFS based on the left lateral separation in three bedrock geological units (Figure 4.1). Considering a Lower Miocene to Upper Miocene age for onset of the current boundary between he South American and Scotia plates, the MFS (Lodolo et al., 2003; Eagles, 2005; Lagabrielle et al., 2009), this structure accommodates a large amount of deformation along the South American and Scotia plates boundary, based on the average long-term slip-rate of 5.4 ± 3.3 mm/yr for this fault system derived from these long-term Late-Cenozoic separations.

Remote sensing and field mapping reveal classic strike-slip geomorphology along the main strand of the Magallanes fault (MF), Hope fault (HP) and Deseado fault (DF). Specifically, linear valleys and shutter ridges, elongated sag ponds, fau lt scarps and sinistrally offsets landforms were documented along these faults. Although no dating was done as part of this work, by combining these geomorphic offsets at specific sites with age estimations for these deposits based on field dating reported in the literature suggest Late-Quaternary (Late-Pleistocene) strike-slip-rates of 7.8 ± 1.1 mm/yr (6.7 to 8.9 mm/yr) in Chile and 7.8 ± 1.3 mm/yr (6.5 to 9.1 mm/yr) in Argentina, for the MF. By combining the slip rates for the MF plus the HP at this location in Chile gives a combined strike-slip rate of 9.5 ± 1.5 mm/yr (8.1 to 11.0 mm/yr). Nevertheless, this rate would be a minimum estimation considering other active fault in the area, as the slip rate for the Deseado fault (Klepeis, 1994; this work), remains uncharacterized. Although the DF has clear tectonic geomorphology that suggests slip rates at least of 1 mm/yr, this suggests an overall Late-Quaternary combined sinistral slip-rate near the Chile and Argentina border at Lake Fagnano at least of 10.5 ± 1.5 mm/yr (9.1 to 12.0 mm/yr). Moreover, according to rates separation between South American and the Antarctic Peninsula (22 mm/yr, De Mets, 1990), the MFS would accommodate at minimum a 40% of this deformation.

Geologic and seismological data suggest that the Scotia-South American plate boundary in its onshore portion in TdF and possibly in most of its length from approximately the 54°S to the east, , the MFS consist in a narrow-localized (30-50 km) and well-defined deformation belt composed of the main MF by a straight and relatively smooth and long fault traces bounded by parallel secondary active but slower-slipping faults, such as the HF and DF. The relatively simple geometry (straight) and length (up to at least 1500 km and perhaps up to 3000 km) suggest a small ratio between small and high magnitude events (Stirling et al., 1995) and perhaps a recurrence rate for high magnitudes earthquakes given by a

characteristic earthquake model (Schwartz & Coppersmith, 1984; Ludwig, 2013). to smoothing along these faults and thus magnitude-frequency distributions derived from seismology may not reflect the actual seismic hazard along these faults. West of TdF, however, according to Betka et al. (2016) from work near Cabo Froward (Figure 4.1), the MFS widens, forming a more diffusely distributed fault system partitioned onto splays increasingly further apart (Figure 5.4). These structures may correspond to reactivated faults within the pre-existing fold and thrust belt (Klepeis & Austin, 1997; Betka et al., 2016). and would be localized along mechanical anisotropies defined by the structural trend of the orogen (Betka et al., 2016). However, from TdF and east, it appears that the MFS could be one of the narrowest and simplest transform (strike slip after Tuzo Wilson, 1965) plate boundaries on Earth.

This model possibly predicts higher occurrence rates than a Gutenberg-Richter relationship based on the extrapolation of curves fit to the log-linear distribution of lesser-sized earthquakes (Gutenberg & Richter, 1944). Additionally, the cumulative post-glacial offset of 120 meters measured in Argentina together with 0.4 to 6.0 m of left-lateral displacement (Smalley et al., 2003; Costa et al., 2006) for the first Ms 7.8 1949 event suggest recurrence intervals for large earthquakes between 60 to 900 yrs, assuming that most of the strain along the MFS is released during the repeated occurrence of large magnitude in a characteristic earthquake model (Schwartz & Coppersmith, 1984), although there are large uncertainties (0.4 to 6.0 m) in the slip-per event data reported by Costa et al. (2006) and Smalley et al., (2003).

These new results are in the same range of previous short-term GPS data-based slip-rate estimates made by the MORVEL model (De Mets et al., 2010), but are 3-5 mm/yr lower than the most recent geodetic-based estimations made by Smallet et al., (2003) and Mendoza et al., (2015), although it is not clear if this misfit could be related to the rheological model considered in the geodetic-based estimation or to other

factors . This work provide better constrained geological parameters to consider for seismic hazard assessment in Patagonia region, which is currently underestimated as the MFS is a fast-slipping, even slightly faster than already knew, able to trigger high magnitude events and closer to urban areas both in Chile (Punta Arenas, Puerto Natales, Porvenir) and Argentina (Tolhuín, Ushuaia). Moreover, as TdF is a major zone for hydrocarbon exploration and extraction both in Chile and Argentina, understanding the locations and nature of the faults here are critical to perhaps reduce risk of seismic triggering due to hydraulic fracturing operations (Holland et al., 2011; Ellsworth, 2013).

6.2 Suggestions for future work

There is still much to know about the MFS and Southern Patagonia region, future work in this area need to be focused on better constrained the parameters for this first order structure to improve seismic hazard assessment. Paleoseismological dating of earthquakes by trenching and dendrochronology would improve the knowledge about rupture process along the MFS and conduct statistically substantial recurrence models for this structure. Better constrained radiometric ages for the Quaternary deposits and more knowledge about glacial chronology history in Tierra del Fuego and Southern Patagonia would lead to obtain better bounded geological slip-rates with shorter uncertainty ranges. Moreover, a denser network with higher spatial and temporal resolution is needed for better constrained geodetic data, with the aim to address the questions of plate movement and the partitioning among the different fault segments that compose the MFS. A greater coverage of high-resolution topographic data with filter for vegetation as Light Detection and Ranging (lidar), will allow to overcome the limitations by the thick cover of trees along the trace and possibly, to stablish a highly reliable density probability function for cumulative offsets along the MFS trace. Finally, as more than a half of the MFS trace would be underwater conditions, both onshore to east and to west by the Patagonian Fjord until the triple junction. Thus, marine bathymetry is needed for a better mapping of the fault geometry and location of the main and secondary strands, and marine cores west Tierra del Fuego in Almirantazgo fjord and Cabo Froward, constrained by quality age models, should improve the knowledge about the intensity, magnitude and epicenter locations of past earthquake.

BIBLIOGRAPHY

Abascal, L. D. V., & González Bonorino, G. (2014). Evaluación del riesgo sísmico para Tolhuin, Tierra del Fuego, Argentina, aplicando el programa Selena.

Adaros Cárcamo R.E. (2003). Sismicidad y Tectónica del extremo sur de Chile. Tesis Magíster, Universidad de Chile, 82 pp.

Barker P.F., Burrell J (1977). The opening of Drake Passage. Mar Geol 25:15–34.

Barker, P. F., Dalziel, I. Y., & Storey, B. C. (1991). Tectonic development of the Scotia Arc region.

Bertrand, S., Lange, C. B., Pantoja, S., Hughen, K., Van Tornhout, E., & Wellner, J. S. (2017). Postglacial fluctuations of Cordillera Darwin glaciers (southernmost Patagonia) reconstructed from Almirantazgo fjord sediments. Quaternary Science Reviews, 177, 265-275.

Betka, P., Klepeis, K., & Mosher, S. (2016). Fault kinematics of the Magallanes-Fagnano fault system, southern Chile; an example of diffuse strain and sinistral transtension along a continental transform margin. Journal of Structural Geology, 85, 130-153.

Bonorino G.G., Rinaldi V., del Valle Abascal L., Alvarado P., Bujalesky G.G., Güell A. (2012). Paleoseismicity and seismic hazard in southern Patagonia (Argentina-Chile; 50°–55°S) and the role of the Magallanes-Fagnano transform fault. Nat Hazards 61(2):337–349.

Boyd, B. L., Anderson, J.B. Wellner, J. S., & Fernandez, R.A. (2009). The sedimentary record of glacial retreat, Marinelli Fjord, Patagonia: Regional correlations and climate ties. Marine Geology, 2009, vol 22.5, no 3-4, p. 165-178.

Buffoni C., Sabbione N.C., Connon G., Ormaechea J.L. (2009). Localización de hipocentros y determinación de su magnitud en Tierra del Fuego y zonas aledañas. Geoacta 34:75–86.

Burbank, D. W., & Anderson, R. S. (2012). Tectonic Geomorphology, 454 pp.

Bujalesky, G. G., Heusser, C. J., Coronato, A. M., Roig, C. E., & Rabassa, J. O. (1997). Pleistocene glaciolacustrine sedimentation at Lago Fagnano, Andes of Tierra del Fuego, Southernmost South America. Quaternary Science Reviews, 16(7), 767-778.

Caminos R., Haller M., Lapido .J., Lizuain O., Page A., Ramos V.A. (1981). Reconocimiento geológico de los Andes Fueguinos, Territorio Nacional de Tierra del Fuego. VIII Congreso Geológico Argentino (San Luis) Actas 1:759–786.

Caldenius, C. C. Z. (1932). Las Glaciaciones Cuaternarias en la Patagonia y Tierra del Fuego: Una investigación regional, estratigráfica y geocronológica. Una comparación con la escala geocronológica sueca. Geografiska Annaler, 14(1-2), 1-164.
Costa C.H., Smalley R., Schwartz D., Stenner H., Ellis M., Ahumada E., Velasco M.S. (2006) Paleoseismic observations of an onshore transform boundary: the Magallanes-Fagnano fault, Tierra del Fuego, Argentina. Rev Asoc Geol Argentina 61:647–657.

Coronato, A., Roig, C., & Mir, X. (2002). Geoformas glaciarias de la región oriental del Lago Fagnano, Tierra del Fuego, Argentina. In Actas XV Congreso Geológico Argentino. El Calafate, Argentina (23-26 de abril, 2002). CD-Rom. Artículo (Vol. 24, No. 5).

Coronato, A., Meglioli, A., & Rabassa, J. (2004). Glaciations in the Magellan Straits and Tierra del Fuego, Southernmost South America. In Developments in Quaternary Sciences (Vol. 2, pp. 45-48). Elsevier.

Coronato, A., Roig, C., Collado, L., & Roig, F. (2006). Geomorphologic emplacement and vegetation characteristics of Fuegian peatlands, southernmost Argentina, South America. Developments in Earth Surface Processes, 9, 111-128.

Coronato, A., Seppälä, M., Ponce, J. F., & Rabassa, J. (2009). Glacial geomorphology of the Pleistocene lake Fagnano ice lobe, Tierra del Fuego, southern South America. Geomorphology, 112(1-2), 67-81.

Cowgill, E. (2007). Impact of riser reconstructions on estimation of secular variation in rates of strike–slip faulting: Revisiting the Cherchen River site along the Altyn Tagh Fault, NW China. Earth and Planetary Science Letters, 254(3-4), 239-255.

Cowgill, E., Gold, R. D., Xuanhua, C., Xiao-Feng, W., Arrowsmith, J. R., & Southon, J. (2009). Low Quaternary slip-rate reconciles geodetic and geologic rates along the Altyn Tagh fault, northwestern Tibet. Geology, 37(7), 647-650.

Cunningham W.D. (1993). Strike-slip faults in the Southernmost Andes and the development of thePatagonian Orocline. Tectonics 169–186.

Cunningham W.D., Dalziel I.W., Lee T.Y., Lawver L.A. (1995). Southernmost South America-Antarctic Peninsula relative plate motions since 84 Ma: implications for the tectonic evolution of the Scotia Arc region. J Geophys Res-Sol EA 100(B5):8257–8266.

Cunningham, W. D., & Mann, P. (2007). Tectonics of strike-slip restraining and releasing bends. Geological Society, London, Special Publications, 290(1), 1-12.

Dalziel, I. W. D. (1981). Back-arc extension in the southern Andes: a review and critical reappraisal. Philosophical Transactions of the Royal Society of London. Series A, Mathematical and Physical Sciences, 300(1454), 319-335.

Dalziel, I.W.D., (1989). Tectonics of the Scotia Arc, Antarctica, Field Trip Guidebook T180, 206pp.

Del Cogliano D, Perdomo R, Hormaechea J (2000) Desplazamiento entre placas tectónicas en Tierra del Fuego. XX Reunión Científica de la AAGG, Mendoza.

DeMets C., Gordon R.G., Argus D.F. (2010). Geologically current plate motions. Geophys J Int 181:1–80.

De Pascale, G. P., & Langridge, R. M. (2012). New on-fault evidence for a great earthquake in AD 1717, central Alpine fault, New Zealand. Geology, 40(9), 791-794.

De Pascale, G. P., N. Chandler-Yates, F. Dela Pena, P. Wilson, W. May, A. Twiss, and C. Cheng (2016). Active tectonics west of New Zealand's Alpine Fault: South Westland Fault Zone activity shows Australian Plate instability, Geophys. Res. Lett., 43, doi: 10.1002/2016GL068233.

Dolan, J. F., & Meade, B. J. (2017). A comparison of geodetic and geologic rates prior to large strike-slip earthquakes: A diversity of earthquake-cycle behaviors? Geochemistry, Geophysics, Geosystems, 18(12), 4426-4436.

Diraison M., Cobbold P.R., Gapais D., Rossello E.A., Le Corre C. (2000). Cenozoic crustal thickening, wrenching and rifting in the foothills of the Southernmost Andes. Tectonophysics 316:91–119.

Dixon, T. H., Norabuena, E., & Hotaling, L. (2003). Paleoseismology and Global Positioning System: Earthquake-cycle effects and geodetic versus geologic fault slip rates in the Eastern California shear zone. Geology, 31(1), 55-58.

Duelis, C., (2015). Análise estructural de descontinuidades baseada em técnicas de Structure From Motion: Aplicaçao em mina a céu aberto. Tesis Mag. São Paulo, Universidad de São Paulo, Instituto de Geociências, 158 p.

Eagles, G., Livermore, R.A., Fairhead, J.D., Morris, P., 2005. Tectonic evolution of the west Scotia Sea. J. Geophys. Res. 11, B02401. doi:10.1029/2004JB003154.

Ellsworth, W. L. (2013). Injection-induced earthquakes. Science, 341(6142), 1225942.

Esteban, F., Tassone, A., Menichetti, M., Rapalini, A. E., Remesal, M. B., Cerredo, M. E., ... & Vilas, J. F. (2011). Magnetic fabric and microstructures across the Andes of Tierra del Fuego, Argentina. Andean Geology, 38(1).

Esteban, F. D., Tassone, A., Lodolo, E., Menichetti, M., Lippai, H., Waldmann, N., ... & Vilas, J. F. (2014). Basement geometry and sediment thickness of Lago Fagnano (Tierra del Fuego). Andean geology, 41(2), 293-313.

Febrer J.M., Plasencia M.P., Sabbione N.C. (2000). Local and regional seismicity from Ushuaia broadband station observations (Tierra del Fuego). Terra Antartica 8:35–40.

Fosdick, J. C., Grove, M., Hourigan, J. K., & Calderon, M. (2013). Retroarc deformation and exhumation near the end of the Andes, southern Patagonia. Earth and Planetary Science Letters, 361, 504-517.

Ghiglione M.C. (2002). Diques clásticos asociados a deformación transcurrente en depósitos sinorogénicos del Mioceno inferior de la Cuenca Austral. Rev Asoc Geol Argentina 57:103–118.

Ghiglione, M.C., (2003). Estructura y evolución tectónica del cretácico terciario de la Costa Atlántica de Tierra del Fuego. Tesis Doctoral, Universidad de Buenos Aires.

Ghiglione, M. C., & Ramos, V. A. (2005). Progression of deformation and sedimentation in the southernmost Andes. Tectonophysics, 405(1-4), 25-46.

Graells, G., Corcoran, D., & Aravena, J. C. (2015). Invasion of North American beaver (Castor canadensis) in the province of Magallanes, Southern Chile: comparison between dating sites through interviews with the local community and dendrochronology. Revista chilena de historia natural, 88(1), 3.

Gutenberg, B., & Richter, C. F. (1944). Frequency of earthquakes in California. Bulletin of the Seismological Society of America, 34(4), 185-188.

Hervé, F., Nelson, E., Kawashita, K., & Suárez, M. (1981). New isotopic ages and the timing of orogenic events in the Cordillera Darwin, southernmost Chilean Andes. Earth and Planetary Science Letters, 55(2), 257-265.

Heusser, C. J. (2003). Ice age southern Andes: a chronicle of palaeoecological events (Vol. 3). Elsevier.

Holland, A. (2011). Examination of possibly induced seismicity from hydraulic fracturing in the Eola Field, Garvin County, Oklahoma. Oklahoma Geological Survey.

Jaschek E., Sabbione N., Sierra P. (1982). Reubicación de sismos localizados en territorio argentino (1920–1963). Observatorio Astronómico de la Universidad Nacional de La Plata Serie Geofísica, Tomo XI, No 1.

Klepeis K.Y.R. (1994). The Magallanes and Deseado fault zones: Major segments of the South American-Scotia transform plate boundary in southernmost South America. Tierra del Fuego. J Geophys Res 99(B11):22001–22014.

Klepeis K.Y.R., Austin J.A. (1997). Contrasting styles of superposed deformation in the Southernmost Andes. Tectonics 16:755–776.

Koppen, W. (1936). Das geographische system der klimat. Handbuch der klimatologie, 46.

Kurz, C., Thormählen, T., Siedel, H., 2011. Visual Fixation for 3D Video Stabilization. Journal of Virtual Reality and Broadcasting, 8(2):12 p.

Lagabrielle, Y., Goddéris, Y., Donnadieu, Y., Malavieille, J., & Suarez, M. (2009). The tectonic history of Drake Passage and its possible impacts on global climate. Earth and Planetary Science Letters, 279(3-4), 197-211.

Little, T. A., & Jones, A. (1998). Seven million years of strike-slip and related off-fault deformation, northeastern Marlborough fault system, South Island, New Zealand. Tectonics, 17(2), 285-302.

Livermore, R., Nankivell, A., Eagles, G., Morris, P., (2005). Paleogene opening of Drake Passage. Earth Planet. Sci. Lett. 236, 459–470.

Lodolo E., Menichetti M., Tassone A., Sterzai P. (2002). Morphostructure of the central-eastern Tierra del Fuego Island from geological data and remote sensing images. EGS Stephan Mueller Spec Publ Ser 2:1–16.

Lodolo E., Menichetti M., Bartole R., Ben-Avraham Z., Tassone A., Lippai H. (2003). Magallanes-Fagnano continental transform fault (Tierra del Fuego, southernmost South America). Tectonics 22:1076.

Lodolo, E., Lippai, H. F., Tassone, A., Zanolla, C., Menichetti, M., & Hormaechea, J. L. (2007). Gravity map of the isla Grande de Tierra de Fuego, and morphology of Lago Fagnano. Geologica Acta, 5(4), 307-314.

Lomnitz C. (1970). Major earthquakes and tsunamis in Chile during the period 1535 to 1955. Geol Rundsch 59:938–960.

Ludwig W.J., Rabinowitz P.D. (1982). The collision complex of the North Scotia Ridge. J Geophys Res 87:3731–3740.

Meade, B. J., & Hager, B. H. (2005). Block models of crustal motion in southern California constrained by GPS measurements. Journal of Geophysical Research: Solid Earth, 110(B3).

McCalpin, J. P. (Ed.). (2009). Paleoseismology (Vol. 95). Academic press.

McCulloch, R. D., Fogwill, C. J., Sugden, D. E., Bentley, M. J., & Kubik, P. W. (2005). Chronology of the last glaciation in central Strait of Magellan and Bahía Inútil, southernmost South America. Geografiska Annaler: Series A, Physical Geography, 87(2), 289-312.

McGill, S. F., & Sieh, K. (1991). Surficial offsets on the central and eastern Garlock fault associated with prehistoric earthquakes. Journal of Geophysical Research: Solid Earth, 96(B13), 21597-21621.

Mendoza L., Perdomo R., Hormaechea J.L., Del Cogliano D., Fritsche M., Richter A., Dietrich R. (2011). Present-day crustal deformation along the Magallanes-Fagnano Fault System in Tierra del Fuego from repeated GPS observations. Geophys J Int 184:1009–1022.

Mendoza, L., Richter, A., Fritsche, M., Hormaechea, J. L., Perdomo, R., & Dietrich, R. (2015). Block modeling of crustal deformation in Tierra del Fuego from GNSS velocities. Tectonophysics, 651, 58-65.

Menichetti M., Lodolo E., Tassone A. (2008). Structural geology of the Fuegian Andes and Magallanes fold thrust belt—Tierra del Fuego Island. Geologica Acta 6:19–42.

Norris, R. J., & Cooper, A. F. (2001). Late Quaternary slip rates and slip partitioning on the Alpine Fault, New Zealand. Journal of Structural Geology, 23(2-3), 507-520.

Olivero, E. B., & Martinioni, D. R. (1996). Late Albian inoceramid bivalves from the Andes of Tierra del Fuego: Age implications for the closure of the Cretaceous marginal basin. Journal of Paleontology, 70(2), 272-274.

Olivero, E.B., Martinioni, D.R., (2001). A review of the geology of the Argentinian Fuegian Andes. J. South Am. Earth Sci. 14, 175–188.

Olivero, E. B., Malumián, N., & Palamarczuk, S. (2003). Estratigrafía del Cretácico Superior-Paleoceno del área de Bahía Thetis, Andes fueguinos, Argentina: acontecimientos tectónicos y paleobiológicos. Revista geológica de Chile, 30(2), 245-263.

Onorato, M. R., Perucca, L., Coronato, A., Rabassa, J., & López, R. (2016). Seismically-induced soft-sediment deformation structures associated with the Magallanes–Fagnano Fault System (Isla Grande de Tierra del Fuego, Argentina). Sedimentary geology, 344, 135-144.

Pedrera A., Galindo-Zaldívar J., Ruiz-Constán A., Bohoyo F., Torres-Carbonell P., Ruano P., Maestro A, González-Castillo L. (2014). The last major earthquakes along the Magallanes-Fagnano fault system recorded by disturbed trees (Tierra del Fuego, South America). Terra Nova 26:448–453.

Pelayo A., Wiens D. (1989). Seismotectonics and relative plate motions in the Scotia Sea region. J Geophys Res 94:7293–7320.

Perucca L, Alvarado P, Saez M (2015) Neotectonics and seismicity in southern Patagonia. Geol J. doi:10.1002/gj.2649.

Perucca, L. P., & Moreiras, S. M. (2009). Seismic and volcanic hazards in Argentina. Developments in Earth Surface Processes, 13, 267-300.

Pisano Valdés, E. (1977). Fitogeografía de Fuego-Patagonia chilena. I.-Comunidades vegetales entre las latitudes 52 y 56º S. In Anales del Instituto de la Patagonia.

Poblete, F., Roperch, P., Hervé, F., Diraison, M., Espinoza, M., & Arriagada, C. (2014). The curved Magallanes fold and thrust belt: Tectonic insights from a paleomagnetic and anisotropy of magnetic susceptibility study. Tectonics, 33(12), 2526-2551.

Poblete, F., Roperch, P., Arriagada, C., Ruffet, G., de Arellano, C. R., Hervé, F., & Poujol, M. (2016). Late Cretaceous–early Eocene counterclockwise rotation of the Fueguian Andes and evolution of the Patagonia–Antarctic Peninsula system. Tectonophysics, 668, 15-34.

Rabassa, J., Coronato, A., Bujalesky, G., Salemme, M., Roig, C., Meglioli, A., ... & Quattrocchio, M. (2000). Quaternary of Tierra del Fuego, southernmost South America: an updated review. Quaternary International, 68, 217-240.

Rabassa, J., Coronato, A., & Martinez, O. (2011). Late Cenozoic glaciations in Patagonia and Tierra del Fuego: an updated review. Biological Journal of the Linnean Society, 103(2), 316-335.

Rossello E.A. (2005). Kinematics of the Andean sinistral wrenching along the Fagnano-Magallanes Fault Zone (Argentina-Chile Fuegian Foothills). VI International Symposium on Andean Geodynamics, Barcelona, Extended Abstracts, pp 623–626.

Rosello, E. A., Haring, C. E., Suárez, F., Laffitte, G. A., & Nevistic, A. V. (2008). Hydrocarbons and petroleum of Tierra del Fuego, Argentina. Geologica Acta: an international earth science journal, 6(1), 69-83.

Sabbione, N., Connon, G., Hormaechea, J., & Rosa, M. (2007). Estudio de sismicidad en la provincia de Tierra del Fuego, Argentina. Geoacta, 32, 41-50.

Salisbury, J.B., Haddad, D.E., Rockwell, T., Arrowsmith, J R., Madugo, C., Zielke, O., and Scharer, K., (2015). Validation of meter-scale surface faulting offset measurements from high-resolution topographic data: Geosphere, v. 11.

Savage, J. C., & Prescott, W. H. (1978). Asthenosphere readjustment and the earthquake cycle. Journal of Geophysical Research: Solid Earth, 83(B7), 3369-3376.

Schwartz, D. P., & Coppersmith, K. J. (1984). Fault behavior and characteristic earthquakes: Examples from the Wasatch and San Andreas fault zones. Journal of Geophysical Research: Solid Earth, 89(B7), 5681-5698.

Schwartz D.P., Stenner H.D., Costa C., Smalley R., Ellis M., Velasco M.S. (2001). Paleoseismology at the End of the World: Initial observations of the Fagnano fault, Tierra del Fuego. Argentina. Seismol Res Lett 72:265.

SERNAGEOMIN, S. (2003). Mapa Geológico de Chile: versión digital. Servicio Nacional de Geología y Minería, Publicación Geológica Digital, No. 4 CD-Room, versión 1.0, base geológica escala, 1.

Sieh, K. E. (1981). A review of geological evidence for recurrence times of large earthquakes (No. 4, pp. 181-207). Washington, DC: American Geophysical Union.

Smalley R., Kendrick E., Bevis M.G., Dalziel I.W.D., Taylor F., Lauría E., Piana E. (2003). Geodetic determination of relative plate motion and crustal deformation across the Scotia-South America plate boundary in eastern Tierra del Fuego. Geochem Geophys Geosyst 4(9) .

Smalley R., Dalziel I.W.D., Bevis M.G., Kendrick E., Stamps D.S., King E.C., Taylor F.W., Lauría E., Zakrajsek A., Parra H. (2007). Scotia arc kinematics from GPS geodesy. Geophys Res Lett 34: L21308.

Stirling, M. W., Wesnousky, S. G., & Shimazaki, K. (1996). Fault trace complexity, cumulative slip, and the shape of the magnitude-frequency distribution for strike-slip faults: A global survey. Geophysical Journal International, 124(3), 833-868.

Sue, C., & Ghiglione, M. C. (2016). Wrenching tectonism in the Southernmost Andes and the Scotia Sea constrained from fault kinematic and seismotectonic overviews. In Geodynamic Evolution of the Southernmost Andes (pp. 137-171). Springer, Cham.

Tassone, A., Lippai, H., Lodolo, E., Hormaechea, J. L., Ferrer, C., & Connon, G. (2001). Bathymetric survey of Lago Fagnano. Tierra del Fuego Island, Argentina. In XV Congreso Latinoamericano de Geología. Simposio sobre evolución geológica de los Andes. Montevideo, Uruguay.

Tassone, A., Lippai, H., Lodolo, E., Menichetti, M., Comba, A., Hormaechea, J. L., & Vilas, J. F. (2005). A geological and geophysical crustal section across the Magallanes–Fagnano fault in Tierra del Fuego. Journal of South American Earth Sciences, 19(1), 99-109.

Tassone A., Lodolo E., Menichetti M., Yagupsky D., Caffau M., Vilas J.F. (2008). Seismostratigraphic and structural setting of the Malvinas Basin and its southern margin (Tierra del Fuego Atlantic offshore). Geol Acta 6:55–67.

Thomas, C., Livermore, R., & Pollitz, F. (2003). Motion of the Scotia Sea plates. Geophysical Journal International, 155(3), 789-804.

Tong, X., Smith-Konter, B., & Sandwell, D. T. (2014). Is there a discrepancy between geological and geodetic slip rates along the San Andreas Fault System?. Journal of Geophysical Research: Solid Earth, 119(3), 2518-2538.

Torres-Carbonell, P. J., Olivero, E. B., & Dimieri, L. V. (2008). Control en la magnitud de desplazamiento de rumbo del Sistema Transformante Fagnano, Tierra del Fuego, Argentina. Revista geológica de Chile, 35(1), 63-77.

Waldmann, N., Ariztegui, D., Anselmetti, F., Austin Jr, J. A., Dunbar, R. M., Moy, C. M., & Recasens, C. (2008). Seismic stratigraphy of Lago Fagnano sediments (Tierra del Fuego, Argentina)-A potential archive of paleoclimatic change and tectonic activity since the Late Glacial. Geologica Acta, 6(1), 101-110.

Waldmann, N., Ariztegui, D., Anselmetti, F. S., Coronato, A., & Austin Jr, J. A. (2010). Geophysical evidence of multiple glacier advances in Lago Fagnano (54 S), southernmost Patagonia. Quaternary Science Reviews, 29(9-10), 1188-1200.

Waldmann, N., Ariztegui, D., Anselmetti, F. S., Austin Jr, J. A., Moy, C. M., Stern, C., & Dunbar, R. B. (2010). Holocene climatic fluctuations and positioning of the Southern Hemisphere westerlies in Tierra del Fuego (54 S), Patagonia. Journal of Quaternary Science, 25(7), 1063-1075.

Waldmann, N., Anselmetti, F. S., Ariztegui, D., Austin Jr, J. A., Pirouz, M., Moy, C. M., & Dunbar, R. (2011). Holocene mass-wasting events in Lago Fagnano, Tierra del Fuego (54 S): implications for paleoseismicity of the Magallanes-Fagnano transform fault. Basin Research, 23(2), 171-190.

Walcott, R. I. (1978). Present tectonics and late Cenozoic evolution of New Zealand. Geophysical Journal International, 52(1), 137-164.

Wesnousky, S. G. (2006). Predicting the endpoints of earthquake ruptures. Nature, 444(7117), 358.

Winslow M.A. (1982). The structural evolution of the Magallanes basin and neotectonics in the Southernmost Andes. In: Craddrock C (ed) Antarctic geosciences, symposium on Antarctic geology and geophysics. University of Wisconsin Press, Madison, pp 143–154.

Wilson, C. K., Jones, C. H., Molnar, P., Sheehan, A. F., & Boyd, O. S. (2004). Distributed deformation in the lower crust and upper mantle beneath a continental strike-slip fault zone: Marlborough fault system, South Island, New Zealand. Geology, 32(10), 837-840.

Zanolla, C., Lodolo, E., Lippai, H. F., Tassone, A. A., Menichetti, M., Baradello, L., ... & Hormaechea, J. L. (2011). Bathymetric map of lago fagnano (Tierra del Fuego Island).

Zielke, O., Arrowsmith, J. R., Ludwig, L. G., & Akçiz, S. O. (2010). Slip in the 1857 and earlier large earthquakes along the Carrizo Plain, San Andreas fault. Science, 327(5969), 1119-1122.

Zielke, O., Klinger, Y., & Arrowsmith, J. R. (2015). Fault slip and earthquake recurrence along strike-slip faults—Contributions of high-resolution geomorphic data. Tectonophysics, 638, 43-62.

Zúñiga González, J. L. (2016). Generación de modelos tridimensionales a partir de fotogrametría y su aplicación en geología estructural

ANNEXED

Annexed I: Secondary faulting in the MFS area

South of the MFS main fault, the eastern portion of Mount Hope presents a high grade of fragile deformation with different scale N-S to NE-SW faulting noticeable along the road thatgoes along the northwestern shore of Fagnano Lake. I observed. A N-S trending fault was observed inside ~ 5 m width fracture in the southern slope of the ridge cutting the volcanoclastic rocks. A ~100 m width damaged area around this fracture is marked by a high grade of fracturing and a pervasive light-colored hydrothermal alteration. The block east is topographically higher than the block at west and apparently the fault splays in two faults which continue to the north cutting the ridge. Inside of the cave the original volcanoclastic rock has turned totally brecciated and is crossed by abundant quartz veins, at least 3 fault planes are observed according to the presence of slickensides and cemented and uncemented fault rocks. A 10 cm layer of light plastic gouch is founded in a fault plane (2/73), going away in both sides of the plane the fracturing dismisses going from cataclasite to fault breccia. In another fault plane (1/71) left of the above slickensides of 280/30 orientation were observed. Other fault plane at the right were observed 20/74, in a lithified rock, but the graduation of in the degree of fracturing is still perceptible. These fault planes form part of a series of other minor a major structures in a N-S, NE-SW and NW-SE strike conform a damaged area of ~5 km of extension along the southern slope of Mount Hope.

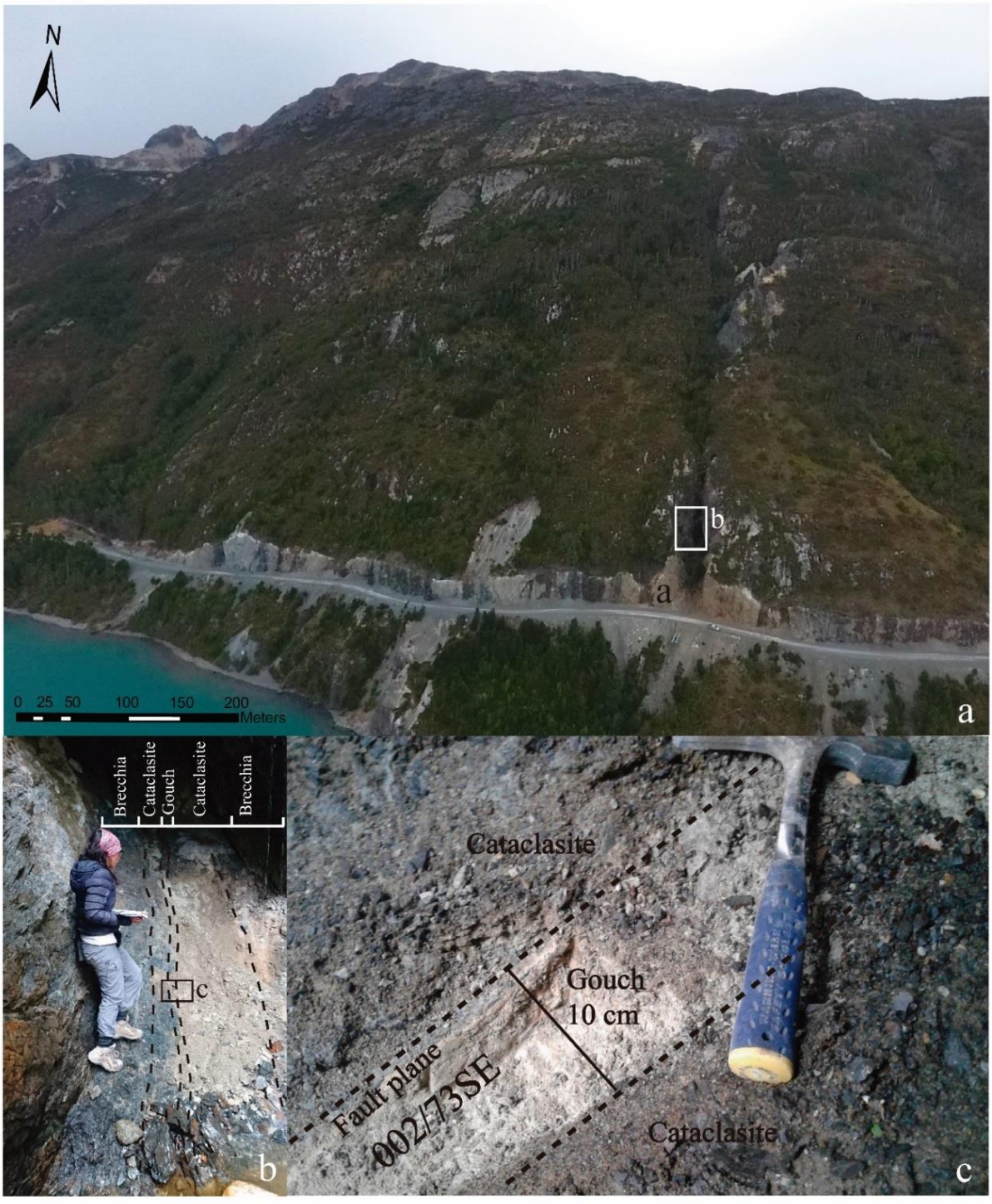

Figure 7.1: Secondary faulting in the MFS in the western Lago Fagnano area, big crack in the southern slope of Mount Hope.

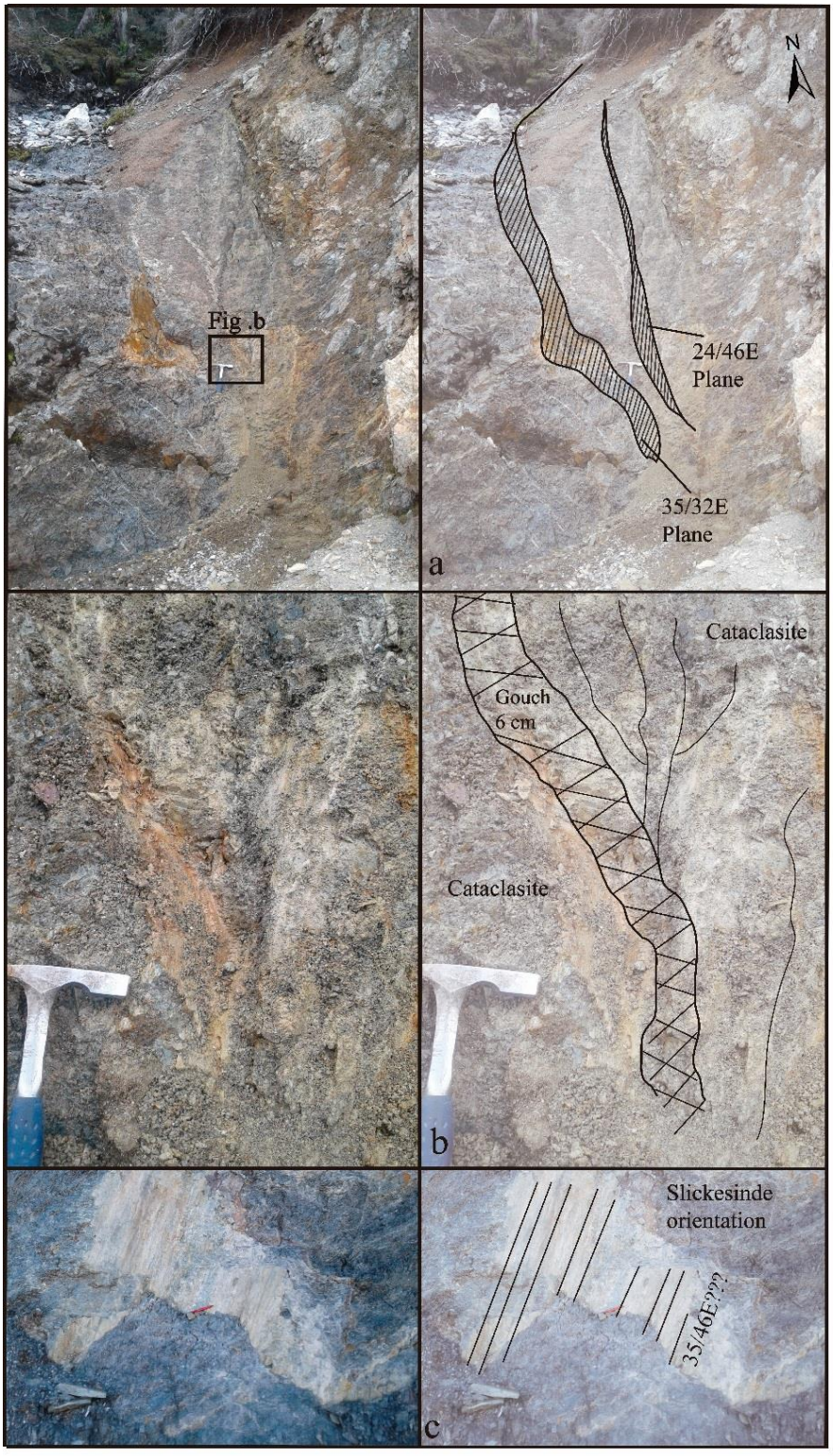

Figure 7.2. Minor scale ~N-S secondary faulting along the southern slope of Mount Hope.

Annexed II: Structure for Motion derived models' details

Table 7.1: SfM models

Model	Number of images	Flying altitude (m)	Ground resolution (cm/pix)	Coverage area (km^2)	Camera stations	Tie points	Camera model	Dem resolution (cm/pixel)	Point density ($points/m^2$)	Focal length (mm)	Pixel size (µm)	XY error (m)	Total error (m)
Caleta María model	213	241	9,2	1,59	213	88,177	FC330	36,8	7,38	3,61	1,56 x 1,56	2,59	3,168
Azopardo valley center model	178	362	14,2	2,2|	178	50,059	FC330	56,7	3,11	3,61	1,56 x 1,56	2,02	4,71
Azopardo valley bridge model (Site 2)	163	288	10,9	1,08	163	59,550	FC330	43,8	5,21	3,61	1,56 x 1,56	2,52	5,612
Hope fault model (Site 1)	202	212	9,3	1,8	212	97,33	FC330	39,4	6,02	3,61	1,56 x 1,56	2,9	5,89
Turbio river segment	313	247	9,45	2,45	310	158,886	FC330	37,8	6,99	3,61	1,56 x 1,56	38	5,118
Lainez river segment (Site 3)	216	265	9,96	1,12	216	148,935	FC330	39,8	6,3	3,61	1,56 x 1,56	2,2	3,47
Turbio river at east model	129	236	0,11	0,53	129	58,8	148,935	36,4	7.54	3,61	1,56 x 1,56	2,53	2,53

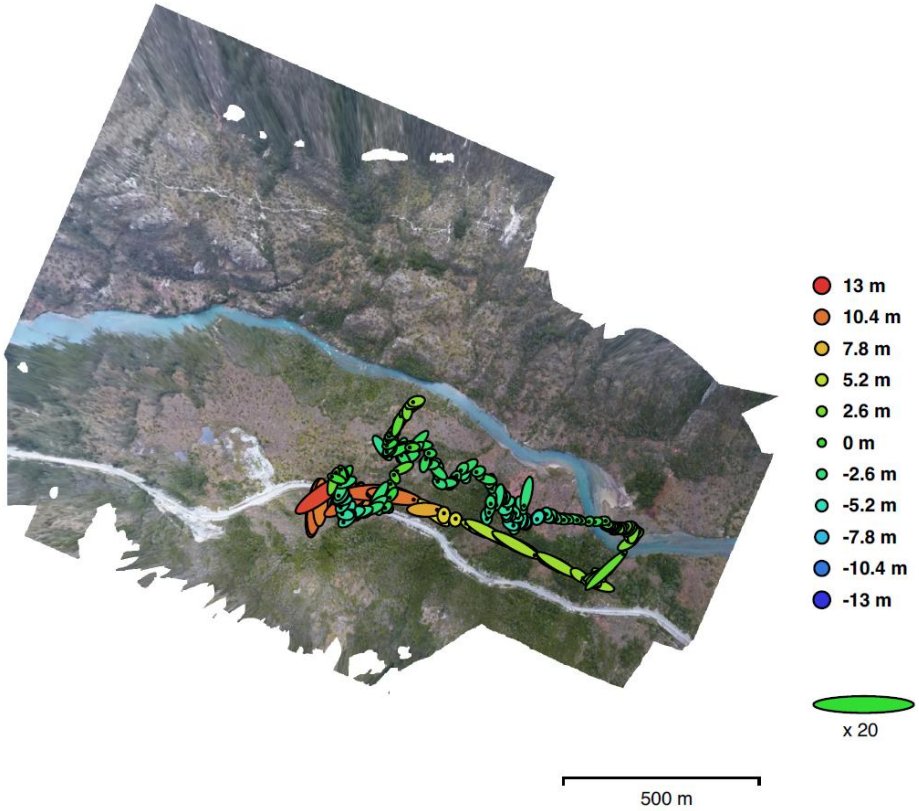

Figure 7.3: Camera locations and error estimates in in the model near Caleta María

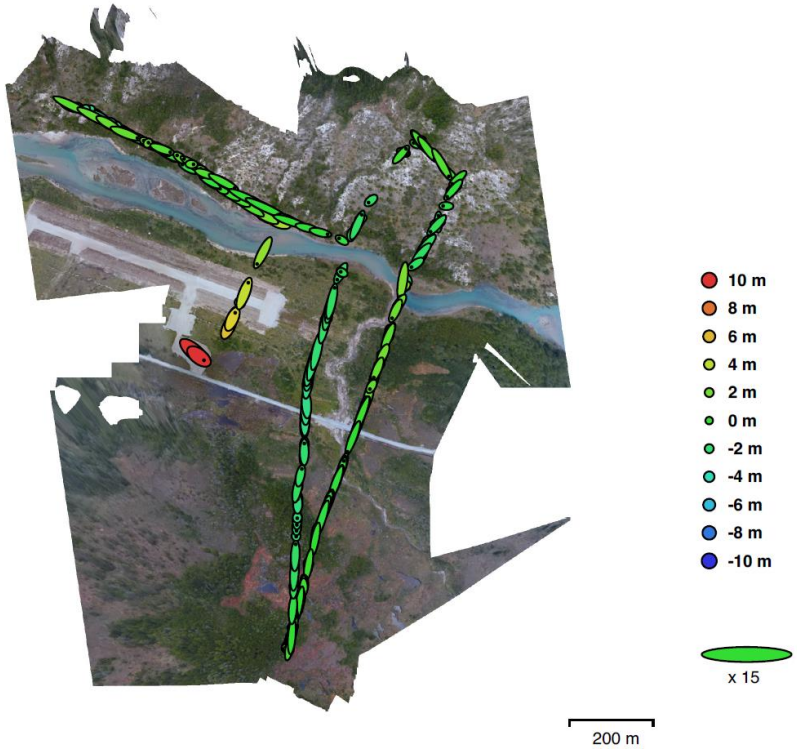

Figure 7.4: Camera locations and error estimates in Azopardo valley in the center model

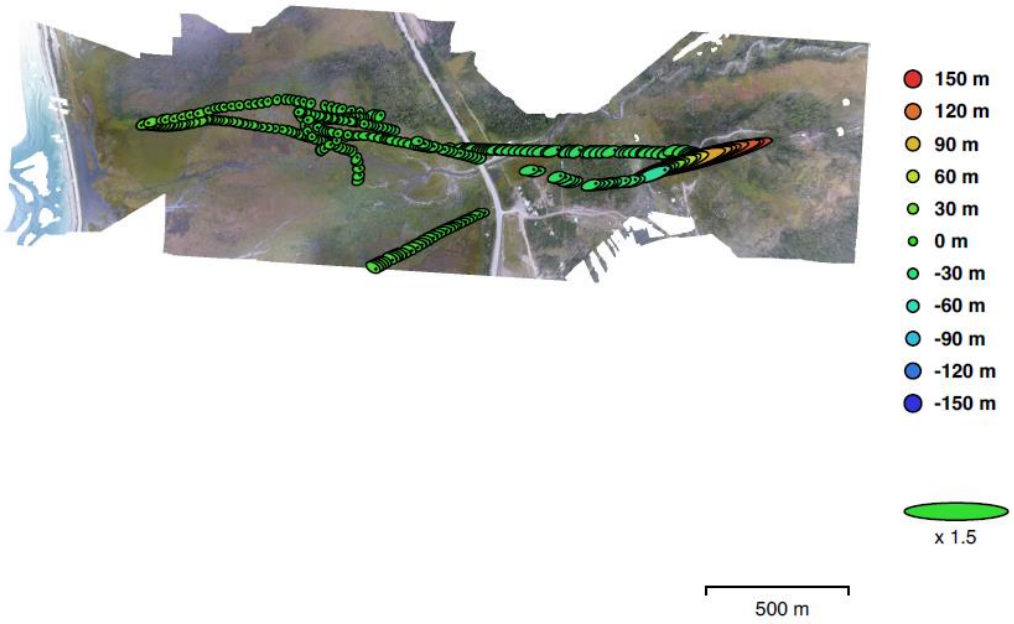

Figure 7.5: Camera locations and error estimates in Rio Turbio segment model

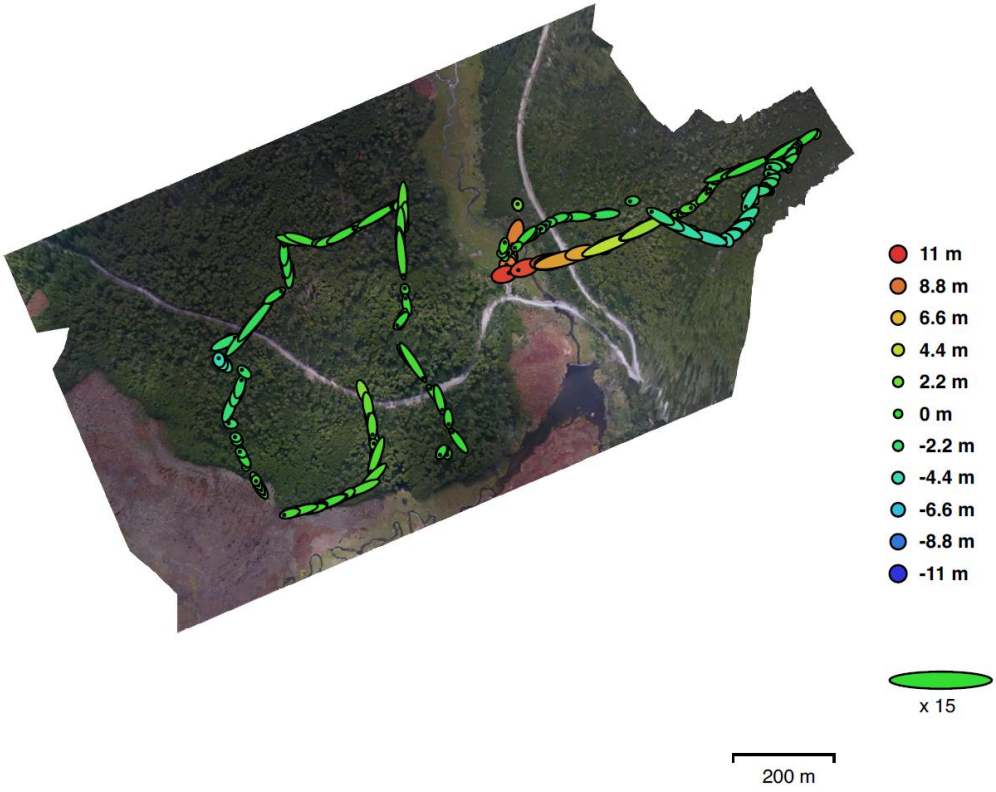

Figure 7.6: Camera locations and error estimates in Lainez river segment model

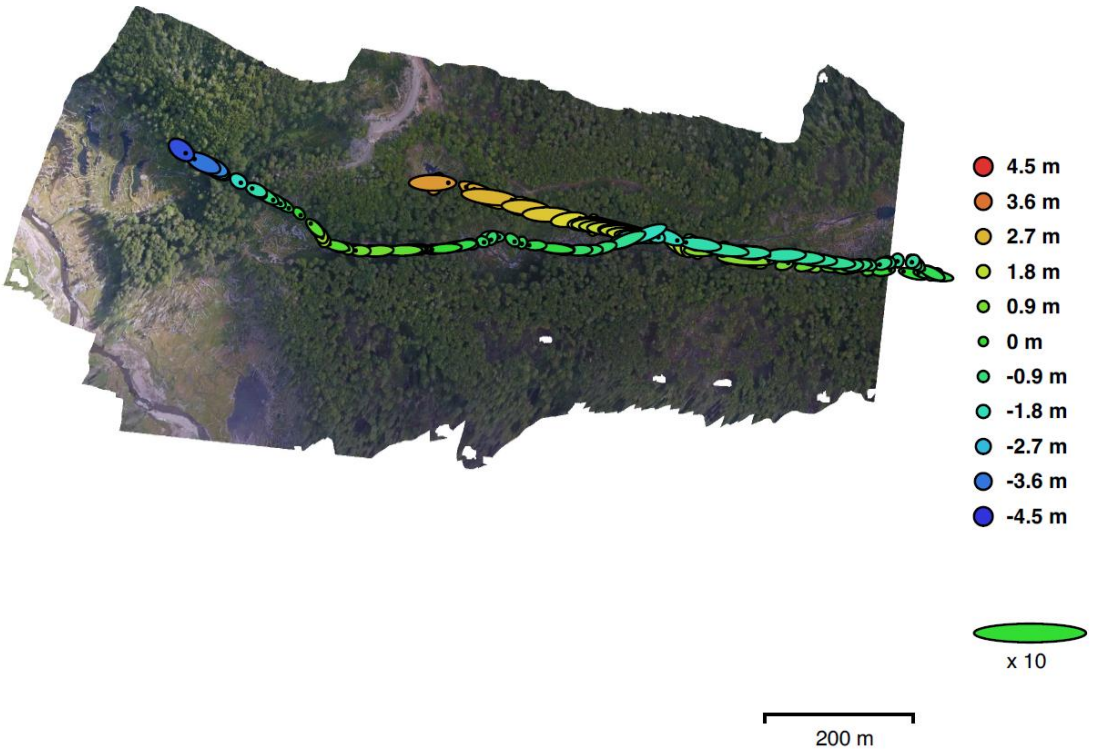

Figure 7.7: Camera locations and error estimates in Turbio river at east model

Annexed III: MFS offsets in ALOSPALSAR 12.5 m DEM

Estimations of geological slip–rates for the MFS trace in Argentina were adittionally made based on satellite imagery and topographic data interpretation (12.5 m/pix resolution). The results fit into these and previous results but are less reliable and have wider ranges due to the difficulties and high amount of uncertainties in the geological markers and pre-deformation geometry estimations. For sites locations see Figure 4.7.

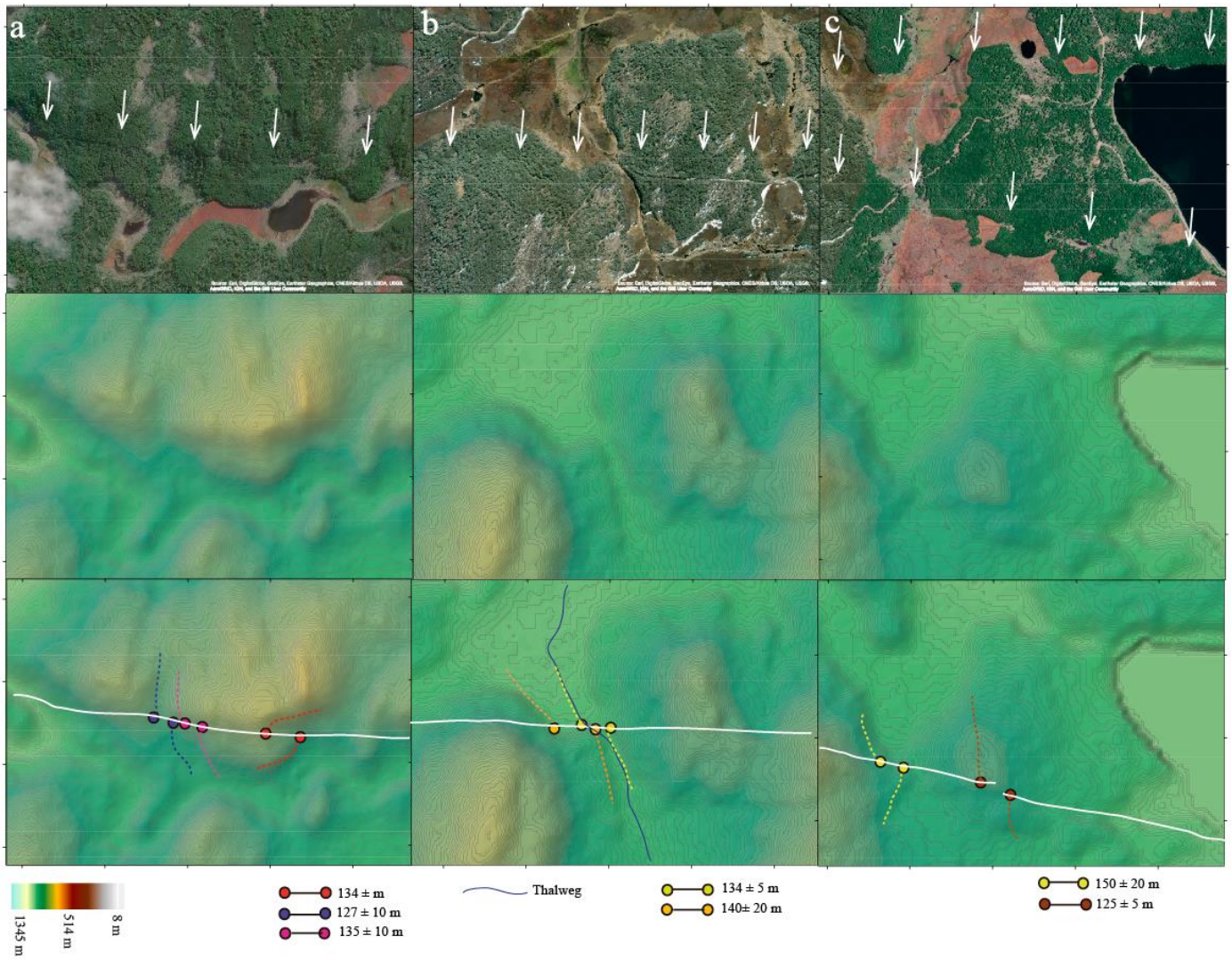

Figure 7.8: Additional MFS offsets in Argentina based on satellite imagery and topographic data (12.5 m/pix resolution) interpretation

Table 7.2 Additional offset measurement synthesis for Argentina segment

	Site a	Site b	Site c
Min offset	127±10	134±10	125±10
Maximum offset	135±10	130±10	150±10
Main offset	131±10	132±10	138± 10
Confidence degree	B	C	C
Age min	13.4 kyr	13.4 kyr	13.4 kyr
Age max	17.8 kyr	17.8 kyr	17.8kyr
Offset range	**6.9 – 10.5 mm/yr**	**6.9- 10.6 mm/yr**	**7.4-11 mm/yr**